

# Determination of Molecular Weights by Light Scattering

Malcolm B. Huglin

Department of Chemistry and Applied Chemistry, University of Salford, Salford M5 4WT,  
England

## Table of Contents

<b>I. Introduction</b>	143
1. Molecular Weight Averages	143
2. Types of Light Scattering	145
<b>II. Theory</b>	146
1. Scattering by Dilute Gases	147
2. Scattering from Polymer Solutions	148
3. Allowance for Non-Ideality	150
4. Allowance for Destructive Interference	151
5. Subsidiary Aspects: Turbidity, Depolarisation, Absorption, Refractive Index Increment	153
6. Brillouin Scattering	156
<b>III. Instrumentation</b>	157
1. Light Scattering Photometers	158
2. Subsidiary Aspects: Clarification, Refractive Index Increment and Calibration	164
3. Brillouin Scattering	171
4. Treatment of Experimental Data	172
<b>IV. Applications to Different Types of Solute</b>	178
1. Low Molecular Weight Liquids	178
2. Simple Compounds and Oligomers	181
3. Polymers	182
4. Ultra-high Molecular Weight Macromolecules	194
<b>V. Multicomponent Systems</b>	197
1. Mixed Solvents	197
2. Polyelectrolytes	203
3. Copolymers and Terpolymers	208
4. Mixtures	219

M. B. Huglin

<b>VI. Concluding Remarks</b> . . . . .	222
1. Comparison of Light Scattering with Other Methods . . . . .	223
2. Errors . . . . .	225
<b>VII. References</b> . . . . .	228

## I. Introduction

The scattering of X-rays, neutrons and visible light is different in origin, since it occurs respectively on free electrons, neutrons and bound electrons. Consequently, what has been termed by Serdyuk and co-workers<sup>1)</sup> the scattering capacity per unit volume of the substance is dictated, in the same order by the electronic density, the scattering length and the refractive index. The joint use of all three types has recently been deployed to quantify the distribution of RNA and protein within the 50S subparticle of *E. coli* ribosomes<sup>2)</sup> as well as to elucidate the structure of synthetic copolymers in solution<sup>3)</sup>. There is, of course, a large difference in the wavelengths appropriate to small angle X-ray scattering and light scattering (LS), but the essential complementarity of both seems conveniently to extend the range accessible to either method alone, and the relevant theoretical expressions can be deduced from the same basic approach<sup>4)</sup>. It is possible, although not yet immediately feasible, that the wavelength range in scattering studies may be extended yet further, when the Synchrotron is fully developed.

LS from solution is an invaluable tool for yielding the dimensions<sup>5, 6)</sup> of the scattering particles and thermodynamic information<sup>7-13)</sup> such as virial coefficients, chemical potentials and excess free energy of mixing. Its main use is to provide the molecular weight<sup>4, 6, 14-16)</sup> of the scattering substance, *i.e.* the solute. If the difference in refractive index between solute and solvent is large enough and with the availability of sufficiently sensitive apparatus there is, in principle, virtually no limit to the range of molecular weight measurable *via* LS. Thus, the molecular weights of diethyl ether<sup>17)</sup> (74) and bacteria<sup>18)</sup> (ca.  $1 \times 10^{11}$ ) have been determined by this means. Nonetheless, for molecular weights below ca.  $2 \times 10^4$  it is probably more convenient to utilise vapour pressure osmometry, although this technique does yield a differently averaged value.

### I. Molecular Weight Averages

If the solute is monodisperse with respect to molecular weight, as in the situation for purified globular proteins for example, then the same value for the molecular weight will be yielded irrespective of the experimental method and its underlying theory. Many synthetic polymers as well as such naturally occurring ones as cellulose, rubber and bacterial dextrans are polydisperse and the experimentally determined molecular weight is an average value. Two of the most important averages are the number average molecular weight  $\bar{M}_n$  and the weight average molecular weight  $\bar{M}_w$ , which are defined as:

$$\bar{M}_n = \frac{\sum_i (n_i M_i)}{\sum_i n_i} \quad (1)$$

$$\bar{M}_w = \frac{\sum_i (n_i M_i^2)}{\sum_i (n_i M_i)} \quad (2)$$

Here the whole solute is considered to comprise  $n_i$  moles of species  $i$  having molecular weight  $M_i$  (the definitions are unaltered if  $n_i$  is considered as the number of

molecules of species  $i$ ). A typical colligative property such as the osmotic pressure  $\Pi$  exerted by the solution is related under ideal conditions to the overall concentration of the solution  $c$  (g/ml) and to the molecular weight  $M$  of the solute by an expression of the form:

$$\Pi \propto c/M \quad (3)$$

The total osmotic pressure is the sum of the osmotic pressure  $\Pi_i$  exerted by each species, viz

$$\Pi = \sum_i \Pi_i \propto \sum_i (c_i/M_i) \quad (4)$$

Denoting mass of species  $i$  by  $g_i$  and using the relation  $n_i = g_i/M_i$  reduces Eq. (1) to

$$\bar{M}_n = \sum g_i / \sum (g_i/M_i) \quad (5)$$

Moreover, the mass in both numerator and denominator of Eq. (5) may be replaced by mass per unit volume, *i.e.* concentration, thus

$$\bar{M}_n = \sum c_i / \sum (c_i/M_i), \text{ whence}$$

$$\sum (c_i/M_i) = \sum c_i / \bar{M}_n = c / \bar{M}_n \quad (6)$$

Combination of Eqs. (4) and (6) shows that the molecular weight yielded by a measurement of osmotic pressure is a number average value:

$$\Pi \propto c / \bar{M}_n \quad (7)$$

As will be demonstrated later, LS can be quantified by an experimental quantity termed the excess Rayleigh ratio between solution and solvent,  $R$ , which is related to the concentration and molecular weight of solute by the following expression valid under ideal conditions:

$$R \propto cM \quad (8)$$

As before, we may write

$$R = \sum R_i \propto \sum (c_i M_i) \quad (9)$$

and Eq. (2) as

$$\bar{M}_w = \sum (g_i M_i) / \sum g_i = \sum (c_i M_i) / \sum c_i \quad (10)$$

$$\therefore \sum (c_i M_i) = \bar{M}_w \sum c_i = c \bar{M}_w \quad (11)$$

Combination of Eqs. (9) and (11) shows that the molecular weight yielded by LS is a weight average quantity, viz

$$R \propto c\bar{M}_w \quad (12)$$

The conventional colligative properties, all of which yield  $\bar{M}_n$ , are depression of freezing point, elevation of boiling point, osmotic pressure and relative lowering of vapour pressure (on which vapour pressure osmometry depends). We have noted that LS yields a different type of molecular weight average and it is commonly considered not to belong to the group of colligative properties. Eisenberg<sup>4)</sup> has pointed out that LS is, in fact, colligative (*i.e.* depends on the number of mols of scattering solute per unit volume) and only appears otherwise since the practical equations are expressed in terms of concentration in mass/volume. Although this is perhaps a semantic point, it is nonetheless correct. Verification can be accomplished by recasting the concentration (mass/volume) in Eqs. (3) and (8) [or equally in Eqs. (7) and (12)] in terms of the number of mols/volume,  $n$ , where  $n = c/M$ . The following results show that  $\Pi$  and  $R$  are both proportional to  $n$ , that is, they are both colligative in nature. LS has the additional characteristic of being also strongly dependent on  $M$ :

$$\Pi \propto n$$

$$R \propto nM^2$$

For ease of notation, the weight average molecular weight  $\bar{M}_w$  will henceforth be written simply as  $M$ . Relative molar mass of a substance is defined<sup>19)</sup> as the ratio of the average mass per molecule of specified isotopic composition of the substance to one twelfth of the mass of an atom of the nuclide  $^{12}\text{C}$ . It is dimensionless. When it is obtained from an experiment involving a known mass of substance or a known concentration (mass/volume) of it in solution, the value obtained is a molar mass or molecular weight expressed in practical units of mass/mol. The customary c.g.s. system employing concentration in gram/vol will yield  $M$  in units of g/mol, whereas the value of  $M$  in units of kg/mol will be a thousand times smaller if the practical concentration are the S.I. one of kg/volume. In this review molecular weights are taken to be in the familiar units of gram/mol.

## 2. Types of Light Scattering

The basics of LS were formulated a considerable time ago by Mie, Zernicke, Prins, Smoluchowski, Rayleigh, Gans and Debye. Scattering by independent particles is usually classified into three types, although there is not complete unanimity about which name should be attributed to each. Here, we shall follow Oster<sup>20)</sup> and refer to them as (a) Rayleigh, (b) Debye and (c) Mie scattering. The class is dictated by two parameters namely the relative refractive index  $\tilde{n}_r$  and the relative size parameter  $D/\lambda$ . The former is the refractive index of the particle relative to that of the surrounding medium, whilst in the latter  $D$  denotes the major dimension of the particle and  $\lambda$  is the wavelength of the light in the scattering medium. Approximate criteria for the classification of LS are given in Table 1.

When unpolarised light of intensity  $I_0$  is incident on a particle, a small fraction of it, of intensity  $i_\theta$ , is scattered at an angle  $\theta$  between the directions of incident

Table 1. Criteria for classification of LS

Type	Refractive Index requirement	Relative size requirement
Rayleigh	$ \tilde{n}_r - 1  \ll 1$	$(D/\lambda) < 1/20$
Debye	$ \tilde{n}_r - 1  \ll 1$	$1 > (D/\lambda) > 1/20$
Mie	$ \tilde{n}_r - 1  \text{ not } \ll 1$	$(D/\lambda) > 1$

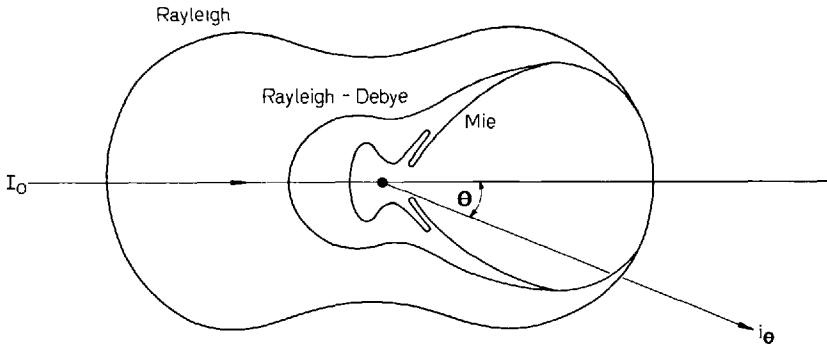


Fig. 1. Polar scattering diagram<sup>21)</sup>: Scattering envelopes according to the three LS theories for particles of increasing size but the same scattering power

beam and observation. The resultant polar scattering diagram<sup>21)</sup> in Fig. 1 illustrates the effect of increasing particle size but the same relative scattering power according to types (a), (b) and (c). For type (a), scattering is symmetrical about 90° (or 270°). For type (b) wherein the particles are larger, interference effects (to be considered more fully later) between parts of the same particle are destructive in the backward direction with the result that scattering is dissymmetrical about 90° (or 270°). Type (c) is much more complex and diffraction patterns begin to appear in the polar scattering diagram. The rigorous Mie theory has been developed for spheres and poses formidable computational problems in order to calculate the intensity of scattered light. We shall be concerned here only with Rayleigh and Debye scattering.

## II. Theory

Many standard texts include sufficient LS theory to render a detailed account unnecessary here. Reference is particularly recommended to treatments by Flory<sup>22)</sup>, Morawetz<sup>23)</sup>, Tanford<sup>24)</sup>, Tsvetkov, Eskin and Frenkel<sup>25)</sup>, Kerker<sup>26)</sup>, and Oster<sup>20)</sup>. Other books<sup>5, 6, 27)</sup> are devoted exclusively to LS from polymer solutions. It will be useful, nonetheless, to summarise the approach<sup>24)</sup> in order to emphasise some significant features of the final result.

## 1. Scattering by Dilute Gases

If the electric field strength of the incident light is  $E_0$ , then the magnitude of the dipole induced in the irradiated material will be directly proportional to  $E_0$  via a proportionality constant termed the polarisability,  $\alpha$ . This dipole acts as a source of new scattered radiation of a different electric field strength  $E_s$ , the magnitude of which depends on the second derivative with respect to time of the dipole moment. The useful experimental quantities are the intensities of scattered ( $i_s$ ) and incident ( $I_0$ ) light. They, in turn, are proportional to  $E_s^2$  and  $E_0^2$  respectively averaged over a vibrational period, that is, from time = 0 to time =  $\lambda_0/\tilde{c}$ , where  $\lambda_0$  is the wavelength of light in vacuo and  $\tilde{c}$  is the velocity of light. One obtains thereby:

$$i_s = 16 \pi^4 \alpha^2 I_0 \sin^2 \theta_1 / \lambda_0^4 r^2 \quad (13)$$

In Eq. (13),  $\theta_1$  is the angle between the dipole axis and the line joining the dipole to the observer. The distance from observer to dipole is  $r$  and, because it is typically ca.  $10^5 - 10^6$  times greater than the size of the dipole itself,  $r$  is effectively the distance between observer and all parts of the dipole. As might be expected *a priori*, the scattering is enhanced by a large incident light intensity and a highly polarisable material. The observation that scattering of sunlight by gas molecules or dust particles imparts a blue (*i.e.* short  $\lambda_0$ ) coloration also leads one to anticipate some form of inverse dependence of scattering intensity on  $\lambda_0$ . The fact that light scattering photometers do not all necessarily exploit this dependence by using very low wavelength sources will be discussed later.

The number of particles per unit volume,  $n$ , as well as  $\alpha$  govern the value of the dielectric constant  $\epsilon$ :

$$\epsilon = 1 + 4 \pi n \alpha \quad (14)$$

Moreover, Maxwell's relationship,  $\epsilon = \tilde{n}^2$  where  $\tilde{n}$  is the refractive index affords

$$\tilde{n}^2 = 1 + 4 \pi n \alpha \quad (15)$$

Changing from number concentration to weight concentration and initial Taylor series expansion of  $\tilde{n}$  give  $\alpha$  as

$$\alpha = M(d\tilde{n}/dc) / 2 \pi \mathcal{N} \quad (16)$$

where  $\mathcal{N}$  is the Avogadro number,  $c$  (mass/volume) is the concentration of particles of molecular weight  $M$  (mass/mol) in the gas, and  $d\tilde{n}/dc$  (volume/mass) is the variation of the refractive index of the dilute gaseous solution with concentration. Hence the mass of a particle is  $M/\mathcal{N} = c/n$  and the intensity of LS from a single particle is, *via* Eqs. (13) and (16):

$$i_s = 4 \pi^2 M^2 I_0 \sin^2 \theta_1 (d\tilde{n}/dc)^2 / \mathcal{N}^2 \lambda_0^4 r^2 \quad (17)$$

A noteworthy feature of this result is the dependence of the scattered light intensity from a single particle on the molecular weight of the particle raised to a power greater than unity. As pointed out by Flory<sup>22)</sup>, if this were not so, the method would not be amenable to the measurement of molecular weight. Experimentally, one determines the scattering per unit volume. Hence there are  $n (=c/M)$  particles per unit volume and multiplying  $i_s$  in Eq. (17) by this number shows that the scattering per unit volume depends directly on  $M$ , viz:

$$i_s = 4 \pi^2 M c I_0 \sin^2 \theta_1 (\tilde{d}\tilde{n}/dc)^2 / \lambda_0^4 r^2 \quad (18)$$

If we were considering a different property such as heat capacity for which the particle makes a contribution directly proportional to its mass raised to the power of unity, the observed value would depend solely on the total quantity of particles in the given volume and would be independent of the number of molecules into which the particles are divided. Measurements of this type of property cannot yield molecular weights. Similarly, for example, an aqueous solution containing 72 g of polyacrylic acid is neutralised by 1000 ml of 1.0 M NaOH and no information regarding the molecular weight of the polymer is afforded, since the titre depends only on the total quantity of acid groups present. Exactly the same titre would be needed to neutralise a solution containing 72 g acrylic acid or even 72 g of a mixture in any proportion of acrylic acid and polyacrylic acid.

With vertically polarised light,  $i_s$  will be independent of angle and  $\sin^2 \theta_1$  will vanish from Eq. (18), because it has a value of unity. For more commonly used unpolarised light it is readily shown that Eq. (18) reduces to:

$$i_\theta = 2 \pi^2 (\tilde{d}\tilde{n}/dc)^2 M c (1 + \cos^2 \theta) / \lambda_0^4 r^2 \quad (19)$$

where the angle of observation  $\theta$  means the angle between the direction of the incident beam and the observed scattered beam of intensity  $i_\theta$  in this direction.

## 2. Scattering from Polymer Solutions

Since the scattering from a single particle is proportional to the square of its molecular weight, macromolecules are especially suitable for study by LS. Moreover, the presence of any smaller molecules makes a relatively minor contribution unlike the situation prevailing in osmotic pressure measurements. In a binary solution of polymer and solvent, scattering from the latter comprises a finite, but small, part of the total and we shall term the difference between scattering from solution and solvent the excess scattering and use the same symbol for it,  $i_\theta$ , as in the preceding Section II. 1.

Assuming in the first instance that the polymer molecules are quite independent, then the situation is analogous to that in the preceding section, except that the scattering molecules (polymer) are now surrounded by solvent molecules of refractive index  $\tilde{n}_0$  instead of by free space of refractive index 1.0. The analogue of Eq. (15) becomes



$$\tilde{n}^2 - \tilde{n}_0^2 = 4 \pi n \alpha \quad (20)$$

and the expression replacing Eq. (19) is

$$i_\theta = 2 \pi^2 \tilde{n}_0^2 (d\tilde{n}/dc)^2 (1 + \cos^2 \theta) M c I_0 / \mathcal{N} \lambda_0^4 r^2 \quad (21)$$

It is convenient to recast this as

$$R_\theta = K M c \quad (22)$$

where

$$R_\theta = i_\theta r^2 (1 + \cos^2 \theta) / I_0 \quad (23)$$

and

$$K = 2 \pi^2 \tilde{n}_0^2 (d\tilde{n}/dc)^2 / \mathcal{N} \lambda_0^4 \quad (24)$$

$$\equiv K' (d\tilde{n}/dc)^2 \quad (25)$$

The total polarisability per unit volume of solute plus solvent has been invoked in Eq. (22) so that the dimensions of the Rayleigh ratio  $R_\theta$  in Eq. (23) are not  $\text{cm}^2$  as it appears, but actually  $\text{cm}^{-1}$ . For pure liquids and polymers of small-moderate molecular weight, scattering at an angle of  $90^\circ$  is used and the Rayleigh ratio in such instances is given simply as

$$R_{90} = i_{90} r^2 / I_0 \quad (26)$$

With unpolarised light in the visible region and at room temperature, the value of  $R_{90}$  for common liquids is usually<sup>26, 28, 29)</sup> in the range  $5 \times 10^{-6} - 50 \times 10^{-6} \text{ cm}^{-1}$ , whilst for polymer solutions in these liquids  $R_{90}$  is much greater, to an extent dependent on the values of  $c$ ,  $M$  and  $d\tilde{n}/dc$ . When dealing with a solution, it is strictly more exact to write the Rayleigh ratio in Eq. (22) as  $\Delta R_\theta$  instead of  $R_\theta$ , since the difference between solution and pure solvent is implied (and is also determined experimentally). Similar imprecise usage of the word "scattering" intended synonymously as "Rayleigh ratio" is also to be noted and accepted. Hence Eq. (22) states that for a solute of a certain molecular weight  $M$ , the scattering increases directly as the weight concentration; for a solute of exceedingly high molecular weight it is only necessary to use very dilute solution to obtain appreciable scattering. Also, for a series of solutes of differing molecular weight but all at the same concentration, the scattering is proportional to  $M$ . In general, the ratio  $c/R_\theta$  for solutions of different concentration should always have the same value, constant  $\times M^{-1}$ , just as for osmotic pressure measurements the ratio  $\Pi/c$  should also always have the same value, constant  $\times \bar{M}_n^{-1}$ . The nature of the constants differs; in the former the constant is  $K^{-1}$ , whilst in the latter it is  $\mathcal{R} T$ , where  $\mathcal{R}$  is the Universal Gas Constant.

### 3. Allowance for Non-Ideality

To obtain a correct form of Eq. (22) allowing for thermodynamic non-ideality of the solution, fluctuation theory originally developed by Einstein, Zernicke, Smoluchowski and Debye has been adapted to polymer solutions.

The solution is regarded as comprising arbitrarily chosen volume elements  $\delta V$  which

(a) are very small relative to the wavelength of light in the medium  $\lambda$  ( $\lambda = \lambda_0/\tilde{n} \approx \lambda_0/\tilde{n}_0$  for dilute solution) and

(b) contain a small number of polymer molecules and a large number of solvent molecules.

Fluctuations in refractive index occur within a volume element and arise from variations in density and concentration. The former are responsible for scattering by the solvent and may be ignored in the present context since solution and solvent scatterings are subtracted. Regarding the dissolved polymer, it is only necessary, therefore, to consider scattering caused by local fluctuations in concentration.

The concentration  $c$  of the solution may be written as

$$c = c' + \delta c \quad (27)$$

where  $c'$  is the fluctuating concentration over the whole solution and  $\delta c$  is the (positive or negative) magnitude of the small concentration fluctuation.

Correspondingly, the actual polarisability  $\alpha$  of a volume element at any instant of time is

$$\alpha = \alpha' + \delta \alpha \quad (28)$$

where  $\alpha'$  is the average polarisability of a volume element and  $\delta \alpha$  is the contribution due to the concentration fluctuation  $\delta c$ . Since  $\delta V$  is the volume of one volume element, there are  $1/\delta V$  volume elements per unit volume and Eq. (13) yields eventually for the scattered intensity per unit volume:

$$i_s = 16 \pi^4 \sin^2 \theta_1 I_0 \langle (\delta \alpha)^2 \rangle / \lambda_0^4 r^2 \delta V \quad (29)$$

where  $\langle (\delta \alpha)^2 \rangle$  is the time average of  $(\delta \alpha)^2$  for a single volume element or, equivalently, the average value at any instant for a large number of volume elements. At constant pressure  $p$  and temperature  $T$ :

$$\delta \alpha = \left( \frac{\partial \alpha}{\partial c} \right)_{T,p} \cdot \delta c \quad (30)$$

The quantity  $(\partial \alpha / \partial c)_{T,p}$  is obtained from Eq. (20) using  $n = 1/\delta V$ , whence Eq. (29) reduces to the following expression after conversion to conditions of unpolarised light:

$$i_\theta = 2 \pi^2 \tilde{n}^2 (d\tilde{n}/dc)^2 (1 + \cos^2 \theta) I_0 \langle (\delta c)^2 \rangle / \lambda_0^4 r^2 \quad (31)$$

Fluctuation theory gives Eq. (32), which is converted to Eq. (33) *via* thermodynamic transpositions and approximation of partial molar volume of solvent to its molar volume  $V_1$ :

$$\langle(\delta c)^2\rangle = k T / \left( \frac{\partial^2 G}{\partial c^2} \right)_{T,p} \quad (32)$$

$$= -k T / \left( \frac{\delta V}{c V_1} \right) \left( \frac{\partial \mu_1}{\partial c} \right)_{T,p} \quad (33)$$

Here,  $k$  is the Boltzmann constant ( $= \mathcal{R} / \nu$ );  $G$  is the Gibbs free energy of the whole solution and  $\mu_1$  is the chemical potential of the solvent in solution. Moreover,

$$\left( \frac{\partial \mu_1}{\partial c} \right)_{T,p} = -V_1 \left( \frac{\partial \Pi}{\partial c} \right)_T \quad (34)$$

and the concentration dependence of osmotic pressure  $\Pi$  for a non-ideal solution is a virial expansion involving coefficients  $A_2$  and  $A_3$ . This expansion enables  $\partial \Pi / \partial c$  to be formulated so that Eqs. (31), (33) and (34) yield

$$i_\theta = \frac{2 \pi^2 \tilde{n}_0^2 (d\tilde{n}/dc)^2 I_0 (1 + \cos^2 \theta) c}{\mathcal{R}^2 \lambda_0^4 (1 + 2 A_2 c + 3 A_3 c^2 + \dots)} \quad (35)$$

For most practical purposes the influence of the third virial coefficient  $A_3$  is slight in dilute solution so that the following form of Eq. (35) is adequate

$$Kc/R_\theta = 1/M + 2 A_2 c \quad (36)$$

As the second virial coefficient of non-ideality,  $A_2$ , is generally finite, the molecular weight is given by

$$M = 1 / \lim_{c \rightarrow 0} (Kc/R_\theta) \quad (37)$$

#### 4. Allowance for Destructive Interference

In the Rayleigh scattering just outlined the relative size parameter was small. Table 1 indicates that a rough criterion of this is that the major dimension of the scattering particle should not exceed ca.  $\lambda/20$ . For example, for a dilute aqueous solution of the particles irradiated with green mercury light the upper limit of the dimension would be given as

$$\lambda/20 = (\lambda_0/\tilde{n})/20 \approx (\lambda_0/\tilde{n}_0)/20 = (546/1.33)/20 \approx 200 \text{ \AA}$$

Debye scattering deals with the situation wherein the relative size parameter is large. Since the root mean square radius of gyration of the particle,  $\langle s^2 \rangle^{1/2}$ , is a

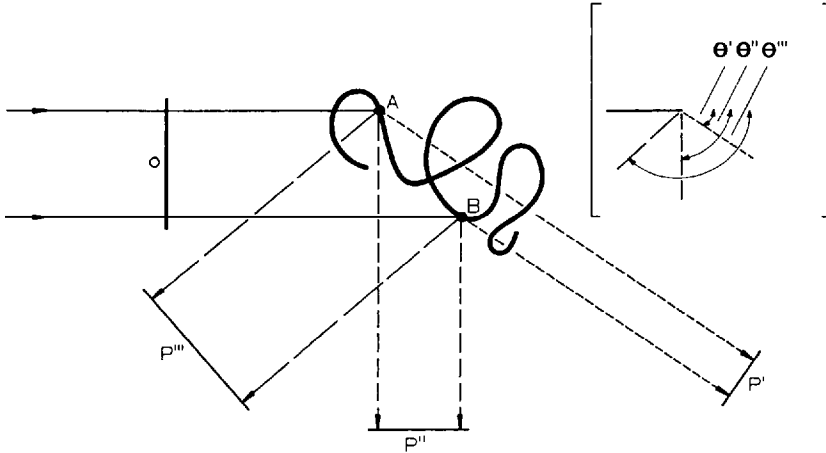


Fig. 2. Destructive interference for a particle having a large relative size parameter

dimension independent of the precise shape, the size parameter is conveniently expressed as  $(s^2)^{1/2}/\lambda$ . If the dimensions of the particle begin to approach  $\lambda$  in magnitude, light scattered from different regions of the large particle reaches the observer with different phases. Consequently, the value of  $i_\theta$  is reduced due to interference and the measured scattered light intensity is less than it should be.

Figure 2 illustrates the incident light reaching a reference plane in phase and being scattered subsequently from two different points A and B of the large particle. Perpendicular planes P', P'' and P''' are drawn in the scattered beam for three scattering angles  $\theta' < \theta'' < \theta'''$ . Considering the last of these, for example, the path length between O and P''' via A is smaller than the corresponding length via B so that the scattered light from A reaches the observer out of phase with the light scattered from B. A similar situation obtains for scattering at the two other angles, but the effect is less pronounced the smaller the angle. At a viewing angle of zero the scattered light intensity is not weakened at all by interference. The particle scattering factor  $P(\theta)$ , which is a function of both relative size parameter and angle of observation, describes the angular dependence of LS from a large particle. It is defined as<sup>30)</sup>

$$P(\theta) = \frac{\text{Scattered intensity for the large particle}}{\text{Scattered intensity in absence of interference}} = \frac{R_\theta}{R_0} \quad (38)$$

where  $R_0$  signifies the Rayleigh ratio for a viewing angle of zero and  $P(\theta)$  varies in magnitude according to the angle.  $P(\theta) = 1$  only when  $\theta = 0$ . It may be shown that with small particles  $P(\theta) = 1$ , because there is no reduction in LS intensity at  $\theta > 0$ . For large particles considered here,  $P(\theta)$  serves as a correction factor in Eq. (36), the amended form of which is now

$$Kc/R_\theta = (1/M)[1/P(\theta)] + 2 A_2c \quad (39)$$

For low values of  $\theta$  the truncated expansion of  $P(\theta)$  yields

$$Kc/R_\theta = (1/M)[1 + (\tilde{\mu}^2/3) \langle s^2 \rangle] + 2 A_2 c \quad (40)$$

where

$$\tilde{\mu} \equiv (4 \pi/\lambda) \sin(\theta/2) \quad (41)$$

The two types of correction thus give the molecular weight as

$$M = 1/\lim_{\substack{c \rightarrow 0 \\ \theta \rightarrow 0}}(Kc/R_\theta) \quad (42)$$

A full treatment of particle scattering functions has been written by Kratochvíl<sup>30)</sup> and the modes of effecting the limits indicated in Eqs. (37) and (42) will be described in a later Section (III.4).

An alternative<sup>31)</sup>, but less frequently used, formulation is to regard the scattering factor as a function of the whole parameter  $\tilde{\mu}$  instead of merely  $\theta$ . Appropriate changes of subscript then render the relevant variables as  $P(\tilde{\mu})$ ,  $R_{\tilde{\mu}}$  and  $K_{\tilde{\mu}}$ .

### 5. Subsidiary Aspects: Turbidity, Depolarisation, Absorption, Refractive Index Increment

By analogy with absorption spectroscopy we may identify an extinction coefficient due to scattering with the turbidity  $\tau$  which is defined as:

$$\tau = (1/l) \ln(I_0/I_t) \quad (43)$$

$I_t$  is the intensity of light transmitted by a sample of path length  $l$ . It can be shown that  $\tau = (16 \pi/3) R_\theta$  so that Eqs. (22) and (40) may be expressed with  $\tau$  in place of  $R_\theta$  and an optical constant  $H (= 16 \pi K/3)$  in place of  $K$ . Although  $\tau$  is usually too small to be measured as such directly, some experimental results are often reported in the form of  $Hc/\tau$  even though  $Kc/R_\theta$  is the measured quantity.

So far the scattering particle has been assumed to be optically isotropic. For anisotropic particles the direction of the electric field associated with the incident light may not coincide with the induced movement of the electron cloud. Consequently, the light scattered at  $90^\circ$  is not plane polarised perpendicular to the plane of the incident beam and the direction of observation; it exhibits a weak component in the horizontal direction. The ratio of the horizontally to vertically polarised components of the unpolarised incident beam (known as the depolarisation ratio  $\rho_u$ , although polarisation ratio might be a better term) will, therefore, not be zero. The general expression for  $\rho_u$  involves the three principal polarisabilities of the scattering molecules and, from the form of this expression,  $\rho_u$  attains a maximum value of 0.5 for long rod-shaped particles in which one of the polarisabilities is much larger than the other two. Values of  $\rho_u$  range from  $10^{-3}$  for the rare gases to 0.10 for gaseous carbon disulphide and from 0.01 to 0.05 for low molecular weight organic molecules in the gaseous state<sup>23)</sup>. A depolarisation ratio can refer to any specified scattering

angle  $\theta$  (see Casassa and Berry<sup>32</sup>), but most commonly relates to  $90^\circ$ . The intensity of light scattered at  $90^\circ$  from anisotropic molecules is increased over the value predicted on the basis of isotropy by the Cabannes factor. For unpolarised (u) incident light at an angle  $90^\circ$  the Cabannes factor  $f_c^u$  is given by

$$f_c^u = (6 + 6 \rho_u)/(6 - 7 \rho_u) \quad (44)$$

where:

$$\rho_u = \frac{H_u(\text{solution}) - H_u(\text{solvent})}{V_u(\text{solution}) - V_u(\text{solvent})}$$

$H_u(\text{solution})$  and  $H_u(\text{solvent})$  are the readings using a horizontal analyser, whilst  $V_u(\text{solution})$  and  $V_u(\text{solvent})$  are the corresponding data with a vertical analyser. When using vertically (v) polarised incident light the Cabannes factor  $f_c^v$  is given by

$$f_c^v = (3 + 3 \rho_v)/(3 - 4 \rho_v) \quad (45)$$

where the depolarisation ratio  $\rho_v$  is obtained as

$$\rho_v = \frac{H_v(\text{solution}) - H_v(\text{solvent})}{V_v(\text{solution}) - V_v(\text{solvent})}$$

$H_v(\text{solution})$  and  $H_v(\text{solvent})$  are the readings using a horizontal component analyser whilst  $V_v(\text{solution})$  and  $V_v(\text{solvent})$  are the corresponding data with a vertical analyser.

The expressions for scattered light intensity (and Rayleigh ratio) must be corrected by dividing by the appropriate Cabannes factor. Effectively this is equivalent to replacing the optical constant  $K$  as defined in Eq. (24) by  $Kf_c^u$  and by  $2 Kf_c^v$  for unpolarised and vertically polarised incident light respectively.

For solutions of high polymers the Cabannes correction is close to unity, although the occurrence of stereoregularity can present a notable exception. The necessity to apply the factor to oligomers will be apparent from Fig. 3 where a value of  $f_c^u = 1$  is only attained for polyethylene oxides<sup>33</sup> of  $M > \text{ca. } 10^4$ . In a later section (IV.1) it is shown how LS can be used to measure  $M$  for a low molecular weight simple solute. In such circumstances it is imperative to employ the isotropic Rayleigh ratio. Thus, the measured  $R_{90}$  for pure benzene ( $\lambda_0 = 546 \text{ nm}$  and  $T = 25^\circ \text{C}$ ) is  $16.3 \times 10^{-6} \text{ cm}^{-1}$  and the measured value of  $\rho_u$  is 0.42, whence from Eq. (44),  $f_c^u = 2.78$ . Hence the isotropic Rayleigh ratio is  $16.3 \times 10^{-6}/2.78 = 5.85 \times 10^{-6} \text{ cm}^{-1}$ . A marked concentration dependence of  $f_c$  is often observed for simple compounds or oligomers<sup>34, 35</sup>) and in such circumstances the limiting value at infinite dilution is employed in the LS equation by some workers. In common with Maron and Lou<sup>36</sup>) the author is inclined to believe it more theoretically sound to use the separate different  $f_c$  values for each concentration.

Stabilisers introduced to suppress degradation of polymers at elevated temperature can introduce errors due to their absorption or fluorescence. Absorbing groups are frequently active in the UV region. In general, neither absorption nor fluorescence

poses a serious problem within the range  $\lambda_0 = 400\text{--}600$  nm used for most LS experiments. Since it is the excess scattering which is measured, fluorescence from solvent need not be corrected for, unless the solute has a quenching action on it. Brice *et al.*<sup>37)</sup> have described a procedure for correcting for fluorescence from solute which has proved adequate in many instances. Alternatively, special filters may be inserted into the nosepiece of the LS photometer, which transmit a negligible amount of fluorescence.

When a polymer absorbs very strongly in the visible region, near IR incident radiation is used. In a very coloured solution the scattered intensity is reduced by a factor  $\exp(-\epsilon\ell)$  where  $\epsilon$  is the absorption coefficient of the solvent. Hence  $i_\theta$  must be multiplied by  $\exp(+\epsilon\ell)$  in order to obtain the true scattered intensity undiminished by absorption effects. For small values of  $\epsilon\ell$ , the quantity  $\exp(\epsilon\ell)$  approximates well to  $(1 + \epsilon\ell)$  so that Eq. (42) becomes<sup>38)</sup>.

$$M = 1/\lim_{\substack{c \rightarrow 0 \\ \theta = 0}} [Kc/R_\theta (1 + \epsilon\ell)] \quad (46)$$

An example is provided by the work of Valtasaari<sup>39)</sup> on solutions of cellulose in the coloured complex solvent FeTNa, which necessitates this correction even though the transmittance maximum of this solvent lies conveniently at  $\lambda_0 = 546$  nm. In the absence of an absorption correction the molecular weight obtained will be lower than its true value.

An important characteristic of a solution with regard to its LS is the specific refractive index increment  $\tilde{dn}/dc$  (frequently denoted also by the symbol  $\nu$ ). As will

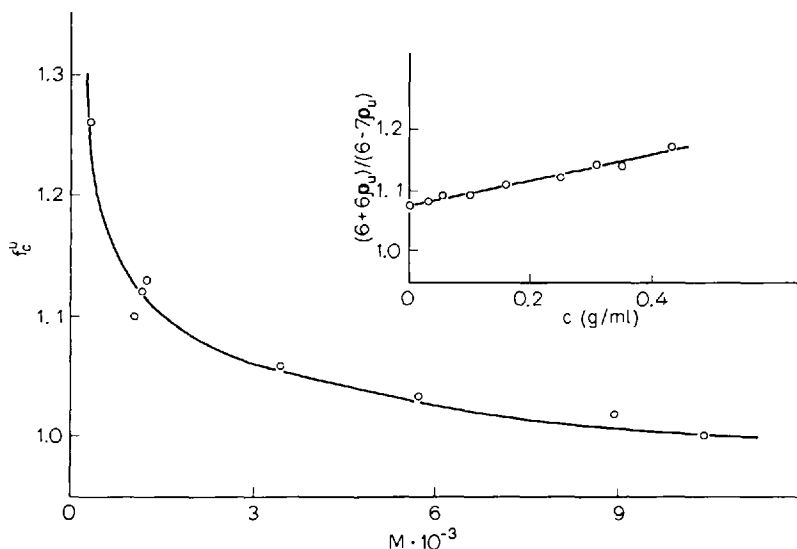


Fig. 3. Cabannes factor as a function of molecular weight for solutions of polyethylene glycol in methanol<sup>33)</sup> at  $T = 25^\circ\text{C}$  and  $\lambda_0 = 546$  nm. [Inset - refer to Section IV.2: Dependence of Cabannes factor on concentration for solutions indicated in Fig. 5]

be apparent from Eq. (19), the scattered intensity is proportional to the square of this quantity. The difference between the refractive indices of solution and solvent is measured by either differential refractometry or interferometry<sup>40</sup>. Separate absolute measurement of each refractive index is insufficiently accurate. The quantity  $(\tilde{n} - \tilde{n}_0)/c$  sometimes exhibits a concentration dependence and extrapolation yields the value appropriate to the expressions in which it is used:

$$\nu \equiv \frac{d\tilde{n}}{dc} = \lim_{c \rightarrow 0} (\tilde{n} - \tilde{n}_0)/c \quad (47)$$

For a given solute,  $\nu$  depends on  $\tilde{n}_0$ ,  $\lambda_0$  and  $T$ , the last two of these being maintained constant. For a molecular weight determination one attempts to select a solvent affording the largest value of  $|d\tilde{n}/dc|$  (since the value can be positive or negative). The value of  $d\tilde{n}/dc$  is constant for a given polymer – solvent pair and independent of  $M$  except for oligomers, in which case  $d\tilde{n}/dc$  only attains constancy above a certain molecular weight<sup>35</sup>, as illustrated in Fig. 4.

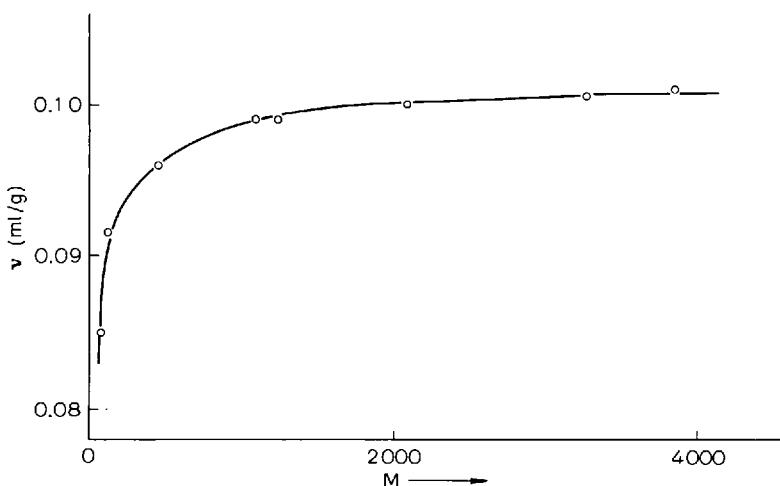


Fig. 4. Dependence of  $\nu$  on molecular weight for polypropylene glycol<sup>35</sup> in acetone at 25 °C

## 6. Brillouin Scattering

An alternative to the common device of determining relative intensities is a study of the fine structure of the scattered beam. This entails resolving the spectrum of scattered light into its three peaks, viz. a central peak and two side ones. The need is thus obviated to refer to  $I_0$  or, according to the apparatus, the scattering power of a standard calibration material. The method is used mainly for determining diffusion constants and thermodynamic properties of liquids.

In the Brillouin scattering method the side peaks serve as references and a measurement of the ratio of the intensity of the central peak to the sum of intensities



of the side peaks,  $J$ , is related to  $M$  in a manner analogous to  $R_\theta$  for the total isotropic LS. Under thermodynamically ideal conditions, the expression (48) is the analogue of Eq. (22), viz.<sup>41)</sup>

$$K_1 K_2 c / (J - J_0) = 1/M \quad (48)$$

whilst allowance for non-ideality [cf. Eq. (36)] gives:

$$K_1 K_2 c / (J - J_0) = 1/M + 2 A_2 c + \dots \quad (49)$$

Here  $J_0$  is the value of  $J$  for the pure solvent. The constant  $K_1$  ( $\text{cm}^3 \text{ gm}^{-2} \text{ mol}$ ) is defined as

$$K_1 = (C_p / \mathcal{R} T^2) [d\tilde{n}/dc] / (d\tilde{n}/dT)^2 \quad (50)$$

where the heat capacity at constant pressure  $C_p$  relates to  $1 \text{ cm}^3$  of solvent. Because of the presence of  $d\tilde{n}/dT$ , the value of  $K_1$  is affected by both solute and solvent. On the other hand, the constant  $K_2$  depends only on the solvent. For a relaxing solvent,  $K_2 = J_0$ , but for a non-relaxing one,  $K_2 < J_0$  viz

$$K_2 = (J_0 + 1) [(C_p/C_v) - 1] / (C_p/C_v)(1 + f) \quad (51)$$

$$\text{where, } f = [2b/(1 - b)] + (C_p/C_v)b^2/(1 - b)^2 \quad (52)$$

$$b = 1 + \beta_T (d\tilde{n}/dT) / \tilde{\alpha} (d\tilde{n}/dp) \quad (53)$$

Here,  $C_v$  is the heat capacity of solvent at constant volume;  $\tilde{\alpha}$  ( $\text{deg}^{-1}$ ) is its coefficient of thermal expansion;  $\beta_T$  ( $\text{cm}^2 \text{ dyne}^{-1}$ ) is the coefficient of isothermal compressibility. From Eq. (49) it is seen that the molecular weight of solute is simply:

$$M = 1/\lim_{c \rightarrow 0} [K_1 K_2 c / (J - J_0)] \quad (54)$$

### III. Instrumentation

In recent years much information has accrued from the study of LS under the influence of external factors<sup>6, 42)</sup> such as applied electric field, applied pressure, hydrodynamic flow etc. Pulse induced critical scattering has also been developed to investigate in an elegant manner phase equilibria and changes in polymer solutions. These refinements are not, however, germane to the objective of molecular weight determination, for which the fundamental instrumental requisites are<sup>32, 43)</sup>

- (a) stable light source to provide a collimated beam on the sample,
- (b) optical components for detecting scattered light,
- (c) a cell assembly for solution and solvent, which allows for passage of incident and scattered light – preferably with temperature control,

(d) electrical and electronic components, comprising a circuit for operation of light source, photomultipliers in the monitor and scattering detector and some form of instrumentation (*e.g.* galvanometer) to provide a read out.

As well as requirements (a) – (d), most (but not all) photometers include the facility for measuring polarisation and altering the wavelength by means of filters. Neutral transmittance filters can be inserted to reduce  $I_0$  by a known amount so as to render the reading comparable in magnitude with that of the much smaller quantity,  $i_\theta$ . The scattered intensity may be decreased similarly under warranted conditions *e.g.* phase separation studies at temperatures approaching the critical separation point. The range of  $\lambda_0$  available from a single source is not exceptionally wide. The following sources and wavelengths have been used: Hg lamp 365, 436, 546 and 578 nm; Ar ion laser 476, 480, 514 and 533 nm; Kr ion laser 531, 547 and 568 nm; He-Cd laser 442 nm; He-Ne laser 633 and 1080 nm; Nd-YAG laser 1064 nm. A quantum doubling substance in conjunction with a laser halves the wavelength; *e.g.* barium sodium niobate with an IR nyodinium laser gives  $\lambda_0 = 532$  nm.

Only light from within the scattering volume should impinge on the receiving phototube, and the incident beam should be correspondingly large enough. Concomitantly, the beam must be sufficiently narrow that measurements at small angle can be made without picking up the transmitted beam (which eventually falls on the light trap). A useful criterion of good resolution is that the volume viewed by the receiver should vary directly as  $1/\sin \theta$ , which condition is generally found to hold to within better than 1% in well aligned instruments. Effectively, the product of  $\sin \theta$  and the galvanometer or recorder deflection  $G_\theta$  should remain constant at all angles. An example<sup>44)</sup> is provided in Fig. 5.

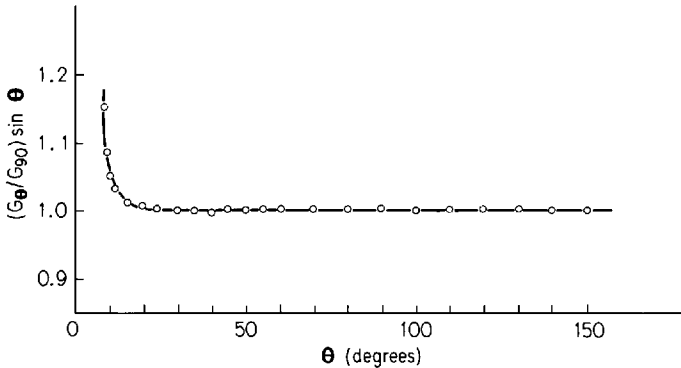


Fig. 5. Angular variation of scattering from benzene ( $T = 30^\circ \text{C}$ ,  $\lambda_0 = 436 \text{ nm}$ ) measured on the LS photometer LS-2 of Utiyama and Tsunashima<sup>44)</sup>.  $G_\theta$  and  $G_{90}$  denote the recorder deflections at angles  $\theta^\circ$  and  $90^\circ$  respectively

### 1. Light Scattering Photometers

Critical reviews of LS photometers, especially those which are commercially available, have been made recently enough to render all but the main points and recent develop-

ments unnecessary here. The main instruments are (a) Brice-Phoenix (U.S.A.), (b) Shimadzu-Seisakasho (Japan), (c) Sofica (France), (d) Aminco (U.S.A.), (e) Polymer Consultants (U.K.). Instrument (e), known also as the Peaker photometer, is manufactured now only to special order by A. D. Whitehead, Ardleigh, Colchester, U.K. and must be regarded as obsolescent. It has been reported recently<sup>16)</sup> that instrument (d) is unlikely to remain long in production.

If the geometry is precisely defined, as in photometer (d), there is no need for a calibration standard.  $R_{90}$  is proportional to  $G_{90}/G_0$  where  $G_{90}$  and  $G_0$  are the photocurrent readings at  $90^\circ$  and  $0^\circ$ , the known constant of proportionality involving the size of the slits and the photocell nosepiece and their distance apart. No temperature control is provided. Correction factors and calibration procedures for instrument (a) have been covered over the years by Kratochvil and co-workers<sup>45, 46)</sup>. In particular, reflection effects constitute important corrections with this instrument. When they are made, the results agree to within 3% of those obtained on an apparatus [photometer (c)] which is virtually free from such effects. A modification of photometer (a) by Roche and Tanner<sup>47)</sup> enables the intensity of scattered light to be measured free from reflection effects, over an extended angular range of  $30^\circ$ – $150^\circ$  and with a higher resolution than is possible with the unmodified model. A resolution of  $0.02^\circ$  has been achieved by Aughey and Baum<sup>48)</sup> in their modified low-angle Brice-Phoenix photometer, which is now available from the same manufacturers who supply the unmodified instrument. Details have been described by Livesey and Billmeyer<sup>49)</sup>, and more recently, by Levine *et al.*<sup>50)</sup>. The latter report on its use within the range  $2^\circ$ – $35^\circ$ .

The Shimadzu is a basically similar instrument to photometer (a), but has much superior facilities for temperature control. The low angle PG-21 instrument, superseded subsequently by an improved version LS-2 are both modifications of the Shimadzu by Utiyama *et al.*<sup>44, 51)</sup>. In the later version the temperature stability within  $5^\circ$ – $100^\circ\text{C}$  is probably the best available in any instrument, and this photometer is capable of allowing routine measurements at angles down to  $9^\circ$ .

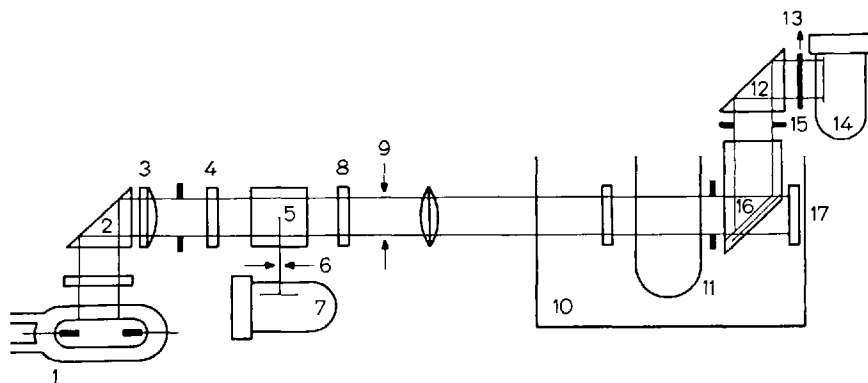


Fig. 6. The Sofica LS photometer: 1 – Hg Pump cooled by high pressure water, 2 – total reflection prism, 3 – achromatic condensing lens, 4 – wavelength filters, 5 – glass diffuser, 6 – iris diaphragm, 7 – reference photomultiplier, 8 – polariser, 9 – variable slit, 10 – constant temperature vat, 11 – entrance slit, 12 – total reflection prism, 13 – manual shutter, 14 – photomultiplier, 15 – exit slit, 16 – air blade total reflection prism, 17 – light trap

The Sofica (Fig. 6), which is of a more radical design than instruments (a) and (e), is unique in that the sample cell and observation prism are immersed in a bath (normally containing toluene for  $T \gtrsim$  ca.  $70^\circ\text{C}$ ; mesitylene can be used for temperatures up to ca.  $120^\circ\text{C}$ ), that not only serves as a thermostat, but also eliminates unwanted refraction and reflection effects. For all the photometers, the detector is a photomultiplier tube rotatable to the desired angle either manually or, in instrument (c), by a motor. The newer, so-called automatic, version of instrument (c) (Fica 50) probably offers the widest versatility of commercial non-absolute photometers. The temperature range is from  $-10^\circ\text{C}$  to  $300^\circ\text{C}$  with a stability of  $0.1^\circ\text{C}$ . The lowest angle of measurement is claimed to be  $15^\circ$  (instead of  $30^\circ$ ), although this is still insufficient for the instrument to qualify as a low angle LS photometer. A high degree of sophistication is provided, particularly with regard to extended range of wavelengths ( $\lambda_0 = 365, 436, 546$  and  $578$  nm), dilution, subtraction of solution and solvent readings, repetitive calculations and print-out.

Serious errors are inevitable, if extrapolations to  $\theta = 0^\circ$  are made from data obtained for insufficiently low angles. Commenting on the feasibility of accurate measurements in the  $6^\circ - 10^\circ$  range, Levine *et al.*<sup>50)</sup> quote the views of other workers as "unlikely"<sup>52)</sup>, "unfeasible"<sup>53)</sup>, "impractical"<sup>54)</sup> or "impossible"<sup>55)</sup>. Nevertheless, these quoted workers and others<sup>56, 57)</sup> stressed the need for very low angle data to supplement those obtained fairly readily at  $\theta = 30^\circ - 150^\circ$ ; a need especially critical for measuring the molecular weights of biopolymers of high  $M$ . Some low angle instruments have been constructed, but two recent commercial ones merit particular mention.

The Bleeker small angle LS photometer<sup>58)</sup> comprises a primary beam section, a sample chamber and a rotatable detection system, the first and last parts being provided with diaphragms and filter holders. The scattered light can be detected with an accuracy of better than  $0^\circ 2'$  within the range  $0^\circ 30' - 130^\circ$ . The detector is a photomultiplier tube intercepting a very small angle for higher angular resolution. Modulation of the primary beam by means of a built-in chopper can be effected for very low LS intensities. The source is a 100 W high pressure Hg lamp with neutral density filters. For its primary intended use a planparallel solid sample is contained between glass slides in a holder. For solutions and gels, special cuvettes are available which have planparallel walls, the separation of which is adjustable so as to alter the thickness of sample, that is, volume of solution. The Rayleigh ratio is obtained without a secondary scattering standard, because the geometry is such that energies rather than intensities are measured. If Eq. (23) is written so that the relevant symbols imply intensities rather than intensities per unit volume, then

$$R_\theta = i_\theta r^2 / I_0 V \quad (55)$$

where  $V$  is the scattering volume. In the focal plane of lens L2 (Fig. 7) before the photomultiplier, two pinholes are mounted. Using the one of large diameter at  $\theta = 0^\circ$ , all the primary beam is collected onto the photocathode. Hence the incident intensity is:

$$I_0 = \epsilon_0 / A \quad (56)$$

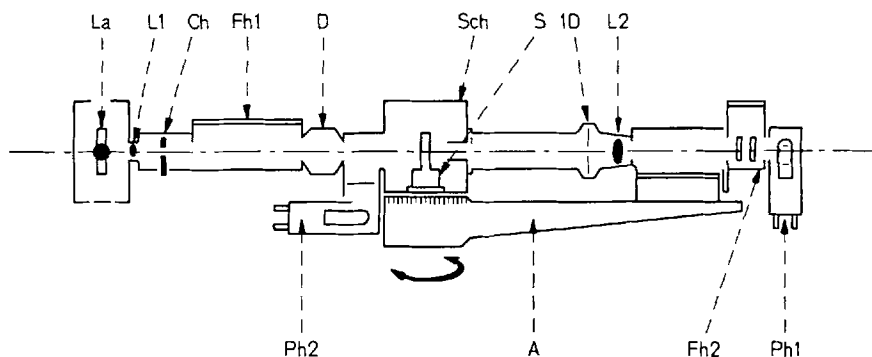


Fig. 7. The Bleeker small angle LS photometer<sup>58</sup>): La – light source, L1 condenser lens, Ch – chopper disc, Fh1 – filter holder, D – iris diaphragm and interchangeable pinholes of various sizes, Sch – sample chamber, S – sample holder, ID – iris diaphragm, L2 – receiver lens, Ph2 – detector photomultiplier, A – measuring arm, Fh 2 – filter holder, Ph1 - detector photomultiplier

where  $\epsilon_0$  is the energy measured at  $\theta = 0^\circ$  and A is the cross-sectional area of the primary beam. For scattering at  $\theta \neq 0^\circ$ , the pinhole of smaller diameter is used to increase the angular resolution. In this case, therefore, the scattered energy is measured over an area  $\pi r^2 \tan^2 \gamma$  (where  $\gamma$  = radius of smaller pinhole used/focal length of lens L2). Hence if  $\epsilon_\theta$  is the scattered light energy, the scattered intensity is

$$i_\theta = \epsilon_\theta / \pi r^2 \tan^2 \gamma \quad (57)$$

Since the scattering volume is given by  $V = A\ell$ , where  $\ell$  is the thickness of sample, Eq. (56) and (57) in conjunction with Eq. (55) yield

$$R_\theta = \frac{\epsilon_\theta r^2 A}{\epsilon_0 \pi r^2 A \ell \tan^2 \gamma} = \left( \frac{\epsilon_\theta}{\epsilon_0} \right) \left( \frac{1}{\pi \ell \tan^2 \gamma} \right) = \left( \frac{G_\theta}{G_0} \right) \left( \frac{1}{\pi \ell \tan^2 \gamma} \right) \quad (58)$$

where the ratio  $\epsilon_\theta/\epsilon_0$  has been replaced by the measured ratio  $G_\theta/G_0$  of photocurrents. The cuvette is not ideally suitable for dilution *in situ* to obtain solutions of different concentration, but the angular range and the realisation of absolute Rayleigh ratios render this a potentially very attractive photometer meriting wider use than is so far apparent from the literature.

The newest addition is the expensive Chromatix KMX-6 low angle LS photometer (Fig. 8). This also yields absolute values of  $R_\theta$  *via* two measurements, viz. (a) a reading of the photomultiplier signal  $G_\theta$  from the sample at an angle  $\theta$  and (b) a reading of the signal  $G_0$  caused by the illuminating beam transmitted through the sample. Since the former is much weaker than the latter, attenuators are inserted when measuring  $G_0$  so that  $G_0$  may be obtained as a signal reading that is ca. 25% of the full-scale reading of  $G_\theta$  for the same setting of amplifier gain and photomultiplier voltage. The final expression for the Rayleigh ratio is

$$R_\theta = (G_\theta/G_0)/(q/\sigma\ell) \quad (59)$$

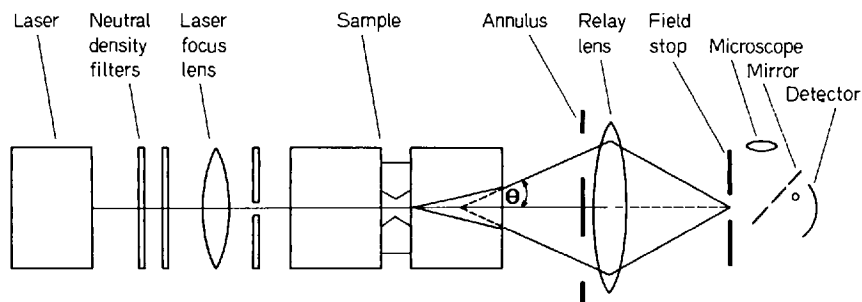


Fig. 8. Schematic of the Chromatix KMX-6 low angle laser LS photometer<sup>59)</sup>

The factor  $(q/\sigma\ell)$  may be obtained from independent optical and geometrical measurements, since  $q$  is the transmittance of the attenuator used for the incident beam,  $\sigma$  is the solid angle of detection of scattered light and  $\ell$  is the thickness of sample.

The philosophy of design of this instrument is founded on the limitations imposed by conventional light sources such as a Hg lamp, which requires good collimation to allow resolution of the scattering signal as a function of angle. This obstacle is normally met by a collimated beam of large cross-sectional area, which in turn demands consideration as two further problems viz (a) limitation of angular resolution by the change in scattering angle across the scattering volume as seen by the detection aperture and (b) high probability of dust or other contaminant being in the relatively large scattering volume. A laser beam permits a very large power output to be transmitted through a very small cross-sectional area, while maintaining a small angle of divergence. However, early applications of lasers to LS concentrated on their high power output without due recognition of the significance of spatial aspects. Such sources were thus incorporated with optical systems that were geared for use with Hg lamps, without regard to optics more appropriate to a laser.

The radically different approach in the Chromatix instrument is to implement a low power (3 mW) He-Ne laser ( $\lambda_0 = 633$  nm) so that its spatial characteristics enable scattering to be measured at angles below  $2^\circ$  and with an illuminated sample diameter of only ca. 100 microns; this alleviates the power angular resolution. Furthermore, there is only a very slight probability of adventitious dust particles being present within the small illuminated area. The small sample volume (ca. 0.15 ml), also, is of importance when the quantity of available polymer is strictly limited on economic or other grounds. Fluorescence absorption is unlikely for most substances at the wavelength in question and, despite the dependence of  $i_\theta$  on  $\lambda_0^{-4}$ , a signal to noise ratio of better than 100 is claimed even from such a weakly scattering liquid as water. The high sensitivity affords sufficient scattering even for very dilute solutions. In general, as intimated by Utiyama, a LS photometer should possess a sensitivity such that the Rayleigh ratio of the most dilute solution used is at least twice that of the pure solvent alone, that is, the excess scattering should not be less than the scattering of the solvent. A nomogram<sup>59)</sup> (Fig. 9), relating to the Chromatix instrument, shows the lowest concentration  $c_{\min}$  (g/ml) at which the excess  $R_\theta$  equals the Rayleigh ratio of water, as a function of  $M$  for aqueous solutions of several biologically important macromolecules. Because this is a low angle photometer, ( $\theta$  from  $7^\circ$  down to  $2^\circ$ ), obtaining and

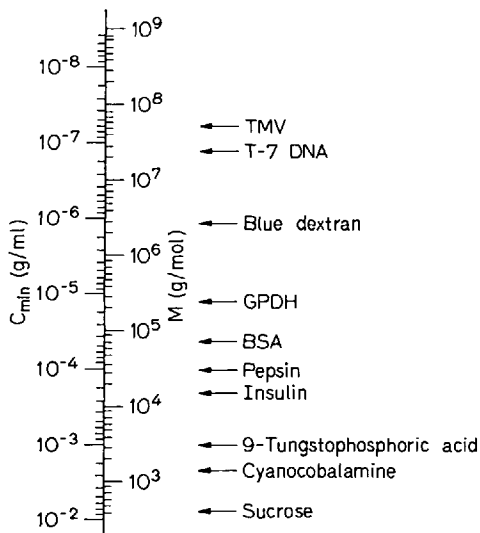


Fig. 9. Nomogram for Chromatix photometer<sup>59)</sup> showing the minimum concentration at which the excess Rayleigh ratio of aqueous solutions of polymers of different molecular weight equals the Rayleigh ratio of pure water

manipulating data for molecular weight determination is greatly simplified. Readings of  $R_\theta$  at a low angle of, say,  $4^\circ$  may be taken effectively to be the same as  $R_\theta$  at  $\theta = 0^\circ$ . Hence extrapolation to zero angle is unnecessary and Eq. (39) reduces to Eq. (36), requiring only extrapolation to infinite dilution.

For solutes of exceptionally high molecular weight there has been a discernible move towards conducting LS experiments in the near IR region ( $\lambda_0 \approx 1000$  nm), which effectively reduces the relative size parameter  $\langle s^2 \rangle^{1/2} / \lambda$ , even though  $\langle s^2 \rangle^{1/2}$  itself is very large for such materials. The associated problems of absorption and

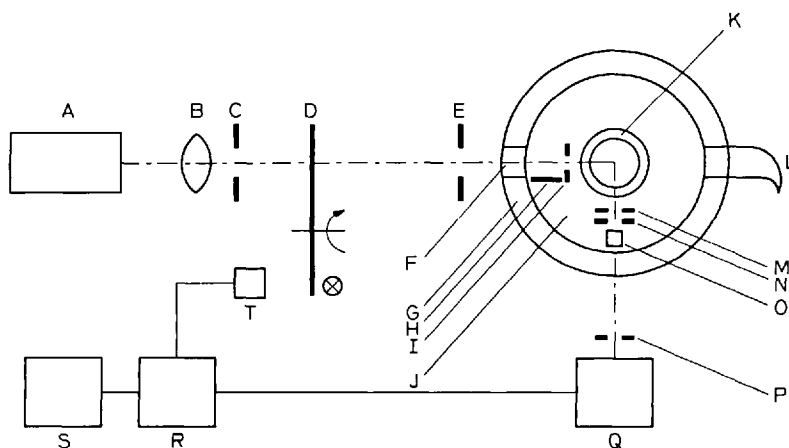


Fig. 10. LS photometer<sup>60)</sup> for use at  $\lambda_0 = 1086$  nm: A - laser, B - lens, C - shutter, D - rotating chopper, E - shutter, F - entrance window, G - thermostat vessel, H - metal shield, I - shutter, J - thermostat liquid, K - cylindrical LS cuvette, L - light trap, M - shutter, N - shutter, O - prism, P - shutter, Q - photomultiplier, R - amplifier, S - x-t recorder

calibration have been discussed by Meyerhoff<sup>60)</sup> and Jennings<sup>18)</sup>, the instrument constructed by Meyerhoff and Burmeister<sup>60)</sup> being illustrated schematically in Fig. 10. Modification<sup>18)</sup> of an existing commercial instrument for use with a Nd YAG laser ( $\lambda_0 = 1060$  nm) is shown in Fig. 11. It is clear from Eqs. (40) and (41) that, for a given sample, data extrapolated to infinite dilution will require a much smaller subsequent extrapolation to  $\tilde{\mu}^2 = 0$  (that is, to a value of  $1/M$ ) for, say,  $\lambda_0 = 1086$  nm than for  $\lambda_0 = 436$  nm. Examples will be provided later and it will be demonstrated also that in certain circumstances the LS behaviour falls outside the Rayleigh-Debye region unless the relative size parameter is reduced by using light of large wavelength.

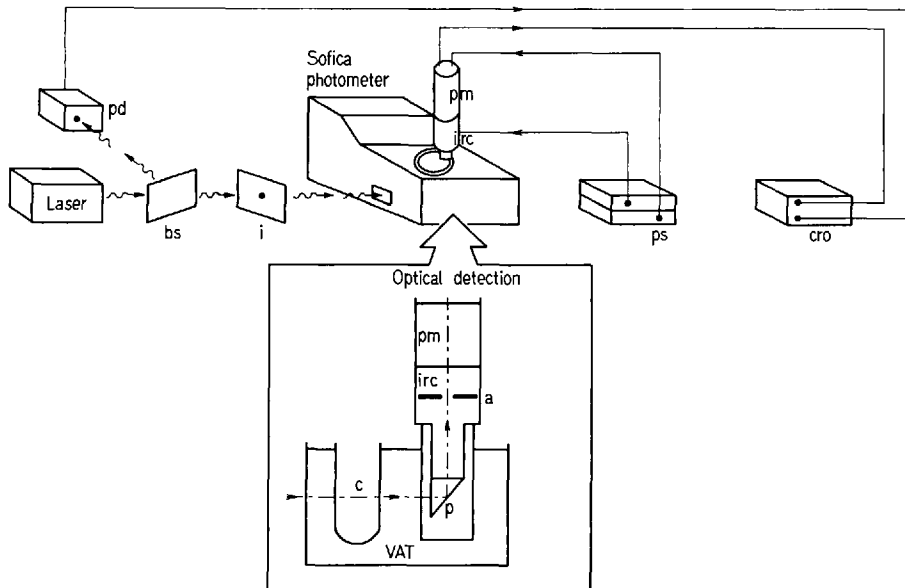


Fig. 11. Modification<sup>18)</sup> of Sofica photometer for use at  $\lambda_0 = 1060$  nm: pd – monitoring photodiode, bs – beam splitter, i – iris, pm – photomultiplier, irc – infrared converter, ps – power supplies, cro – cathode ray oscilloscope, a – aperture, p – reflecting prism, c – cell

## 2. Subsidiary Aspects: Clarification, Refractive Index Increment and Calibration

An indispensable requirement for reliable LS data is the freedom of the medium from extraneous matter such as dust particles. Clarification procedures have been reviewed<sup>51)</sup> and consist of (a) centrifugation followed by careful removal of the upper clarified portion and/or (b) filtration; through ultrafine filters. Contamination during transference in (a) can be overcome by using the LS cell as centrifuge tube; the dust therein remains held at the bottom for the duration of the LS readings. For aqueous solutions, which are notoriously difficult to clarify, the addition of salt is often found effective in bringing down the dust. Electrostatic attraction of dust particles by organic droplets appears to be the underlying cause of the effectiveness of a rather



specific expedient due to Bernadi<sup>62</sup>). Aqueous nucleic acid solution is emulsified by shaking with a binary organic mixture which, after gravity separation and centrifugation, yields a highly clarified aqueous solution. Filters are selected on the basis of their chemical resistance to the solvent used as well as their efficiency, viz. pore size. 0.1  $\mu\text{m}$  Polycarbonate filters (Nuclepore Corporation, U.S.A.) have been reported<sup>50</sup> to produce markedly clearer solutions at faster flow rates than the more commonly used cellulose ester filters (Millipore Corporation) of the same nominal pore size. The special problems associated with solutions of native DNA have been discussed. A useful microfiltration apparatus, which prevents re-introduction of dust into filtered solution through contact with laboratory air, has been described by Levine *et al.*<sup>50</sup>, and is shown in Fig. 12. The liquid is placed in the upper chamber and the lid closed. Filtration into the LS cell and recycling back into the upper chamber are carried out and repeated several times by manipulation of the stopcocks. Finally the filled cell is sealed and placed in the LS photometer. A rather similar device has been reported by Casassa and Berry<sup>32</sup>).

As indicated, the specific refractive index increment is best measured by differential refractometry or interferometry. Experimental procedures as well as tabulated values of  $\tilde{dn}/dc$  for many systems have been presented elsewhere<sup>40, 63</sup>). The relevant wavelength and temperature are those used for LS. The value of  $\lambda_0$  is invariably 436 or 546 nm, but with the advent of laser LS, values of  $\tilde{dn}/dc$  at other wavelengths are required. These can be estimated with good reliability using a Cauchy type of dispersion ( $\tilde{dn}/dc \propto 1/\lambda_0^2$ ). For example the values of  $\tilde{dn}/dc$  for aqueous solutions of the bacterium T-ferrioxidans at 18 °C are 0.159, 0.141 and 0.125 ml/gm at  $\lambda_0 = 488, 633$  and 1060 nm respectively<sup>64</sup>).

Modifications of existing differential refractometers have been made for precise evaluation of  $\tilde{dn}/dc$  at high  $\lambda_0$ , which has been particularly necessary where values at other wavelengths are not known. The apparatus of Jennings *et al.*<sup>64</sup>) is based on the immersed prism technique of Debye (also used in the commercial Shimadzu-

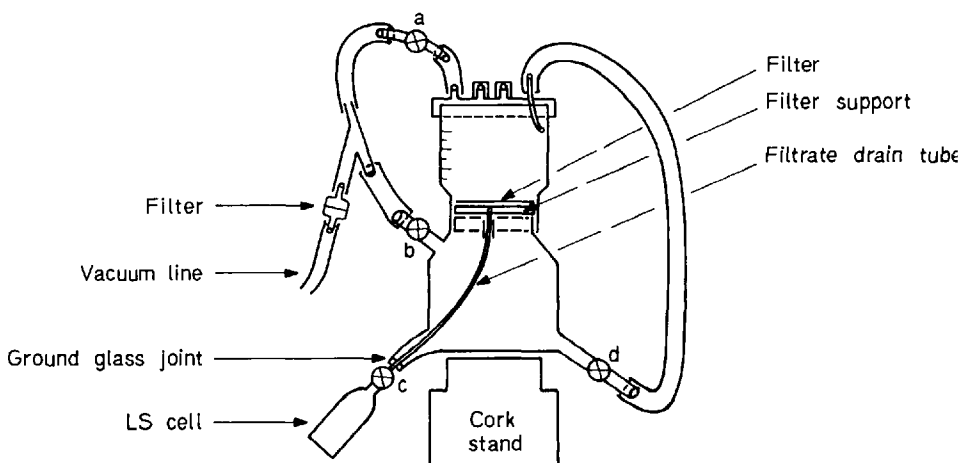


Fig. 12. Microfiltration apparatus<sup>50</sup>): a, b, c and d denote respectively the upper vacuum stopcock, the lower vacuum stopcock, the cell stopcock and the recycling stopcock

Seisakusho differential refractometer). For a solution of known concentration, the difference in refractive index,  $(\tilde{n} - \tilde{n}_0)$ , between the liquid in the prism and that in the solvent bath causes refraction of the light beam, which is observed as a displacement  $\delta$  of the image at a distance  $d$  from the prism centre. The overall sensitivity depends on the precision of measuring  $\delta$  and the refractive index difference is given by

$$\tilde{n} - \tilde{n}_0 = \delta / 2d \tan(\gamma/2) \quad (60)$$

where  $\gamma$  is the angle of the prism, that is, the angle subtended by the sides through which the light beam is transmitted. Advantages of the laser beam used include (a) high intensity, which is especially critical for systems such as bacterial suspensions that strongly attenuate the beam because of their intense scattering power. This is probably the reason for the dearth of experimental  $d\tilde{n}/dc$  values for such systems at visible wavelengths, (b) the low divergence and high penetrability of the beam enable emergent light to be projected over a large distance  $d$ , thereby yielding a higher value of  $\delta$ .

The instrument of Meyerhoff<sup>60)</sup> (Fig. 13) is based on the differential refractometer of Bodmann. It measures an image displacement which is proportional to  $(\tilde{n} - \tilde{n}_0)$  via an instrumental calibration constant the value of which must be established by means of standard solutions of known  $(\tilde{n} - \tilde{n}_0)$ . Values of the latter quantity have been collated for several aqueous salt solutions, but relate mainly to  $\lambda_0 = 436, 546$  and  $589$  nm. Calibration at  $\lambda_0 = 1086$  nm and  $T = 20^\circ\text{C}$  may be effected with aqueous KCl for which  $d\tilde{n}/dc$  (at  $c = 0$ ) has a reported<sup>65)</sup> value of  $0.1351$  ml/g. This datum and other useful data relative to the increasingly used (laser source) wavelengths are assembled in Table 2.

As will be seen later (Section V.1), meaningful molecular weights in multicomponent systems can be determined, if the specific refractive index increment appertains to conditions of constant chemical potential of low molecular weight solvents (instead of at constant composition). Practically, this can be realised by dialysing the solution against the mixed solvent and then measuring the specific refractive index increment of the dialysed solution. The theory and practice have been reviewed<sup>4, 14, 15, 72)</sup>.

There is little doubt that the disagreement among many reported molecular weights can be attributed in some measure to uncertainty in calibration procedures and/or failure to effect calibration in conjunction with associated corrections. Reference is recommended to full discussions by Utiyama<sup>29)</sup>, Kratochvil<sup>73)</sup> and Casassa,

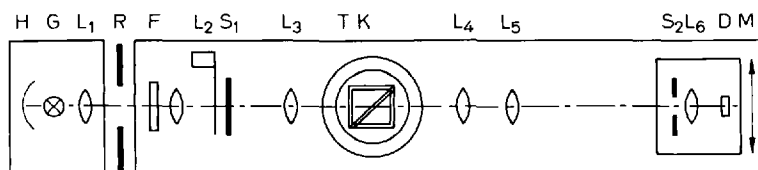


Fig. 13. Differential refractometer<sup>60)</sup> for use at  $\lambda_0 = 1086$  nm: H – hollow mirror, G – incandescent halogen lamp, L<sub>1</sub> – L<sub>6</sub> – lenses, R – heat reflector, F – interference filter, S<sub>1</sub> – S<sub>2</sub> – slits, T – heating mantle, K – differential cell, D – silicon photocell, M – micrometer thread

## Determination of Molecular Weights by Light Scattering

 Table 2. Refractometric and LS data at less common wavelengths  $\lambda_0$ 

System	Quantity	Value	$\lambda_0$ (nm)	Temp (°C)	Ref.
Acetone	$\tilde{n}_0$	1.3574	633	23	66)
Benzene	$\tilde{n}_0$	1.4971	633	23	66)
Carbon disulphide	$\tilde{n}_0$	1.6207	633	23	66)
Carbon tetrachloride	$\tilde{n}_0$	1.4582	633	23	66)
Chloroform	$\tilde{n}_0$	1.4444	633	23	66)
Cyclohexane	$\tilde{n}_0$	1.4254	633	23	66)
Methanol	$\tilde{n}_0$	1.3274	633	23	66)
Methyl ethyl ketone	$\tilde{n}_0$	1.3773	633	23	66)
Toluene	$\tilde{n}_0$	1.4921	633	23	66)
Water	$\tilde{n}_0$	1.3324	633	23	66)
Water	$\tilde{n}_0$	1.324	1060	25	67)
Bacterium <i>S. marcescens</i> in water	$d\tilde{n}/dc$ (ml/g)	0.175	488	18	64)
Bacterium <i>S. marcescens</i> in water	$d\tilde{n}/dc$ (ml/g)	0.158	1060	18	64)
Bacterium <i>E. coli</i> in water	$d\tilde{n}/dc$ (ml/g)	0.152	1060	18	64)
Bacterium <i>T. ferrooxidans</i> in water	$d\tilde{n}/dc$ (ml/g)	0.125	1060	18	64)
Bacterium <i>T. ferrooxidans</i> in water	$d\tilde{n}/dc$ (ml/g)	0.159	488	18	64)
Bovine plasma albumen in water	$d\tilde{n}/dc$ (ml/g)	0.192	488	18	64)
Bovine plasma albumen in water	$d\tilde{n}/dc$ (ml/g)	0.181	1060	18	64)
$\beta$ -Lactoglobulin in water	$d\tilde{n}/dc$ (ml/g)	0.171	1060	18	64)
$\beta$ -Lactoglobulin in water	$d\tilde{n}/dc$ (ml/g)	0.184	488	18	64)
Tobacco mosaic virus in water	$d\tilde{n}/dc$ (ml/g)	0.181	488	18	64)
DNA in water	$d\tilde{n}/dc$ (ml/g)	0.183	488	18	64)
Sucrose in water	$d\tilde{n}/dc$ (ml/g)	0.144	488	18	64)
Cellulose trinitrate in acetone	$d\tilde{n}/dc$ (ml/g)	0.0982	1086	25	60)
Polystyrene in benzene	$d\tilde{n}/dc$ (ml/g)	0.102	633	25	41)
Polystyrene in benzene	$d\tilde{n}/dc$ (ml/g)	0.1021	644	20	68)
Polystyrene in toluene	$d\tilde{n}/dc$ (ml/g)	0.1060	644	20	68)
Polystyrene in toluene	$d\tilde{n}/dc$ (ml/g)	0.1065	633	25	41)
Polystyrene in toluene	$d\tilde{n}/dc$ (ml/g)	0.1051	1086	25	60)
Polystyrene in toluene	$d\tilde{n}/dc$ (ml/g)	0.1034	1086	20	60)
Polystyrene in dimethyl formamide	$d\tilde{n}/dc$ (ml/g)	0.1064	644	20	68)
Polystyrene in methyl ethyl ketone	$d\tilde{n}/dc$ (ml/g)	0.2110	644	20	68)
Polybenzyl acrylate in methyl ethyl ketone	$d\tilde{n}/dc$ (ml/g)	0.1623	644	20	68)
Polyethyl acrylate in methyl ethyl ketone	$d\tilde{n}/dc$ (ml/g)	0.0852	644	25	68)
Polymethyl acrylate in methyl ethyl ketone	$d\tilde{n}/dc$ (ml/g)	0.0915	644	20	68)
Polymethyl methacrylate in methyl ethyl ketone	$d\tilde{n}/dc$ (ml/g)	0.1102	644	20	68)
Polymethyl methacrylate in acetone	$d\tilde{n}/dc$ (ml/g)	0.1276	644	20	68)
Polyvinyl bromide in tetrahydrofuran	$d\tilde{n}/dc$ (ml/g)	0.112	644	-	69)

Table 2. (continued)

System	Quantity	Value	$\lambda_0(\text{nm})$	Temp ( $^{\circ}\text{C}$ )	Ref.
KCl in water	$\tilde{dn}/dc(\text{ml/g})$	0.1351	1086	20	65)
$\text{NH}_4\text{NO}_3$ in water	$\tilde{dn}/dc(\text{g/g})$	0.1239	633	—	66)
NaCl in water	$\tilde{dn}/dc(\text{g/g})$	0.1766	633	—	66)
KCl in water	$\tilde{dn}/dc(\text{g/g})$	0.1371	633	—	66)
Carbon disulphide	$\rho_u$	0.653	633	23	66)
Carbon disulphide	$\rho_u$	0.632–0.669	633	23	70)
Toluene	$\rho_u$	0.491	633	23	66)
Toluene	$\rho_u$	0.506–0.528	633	23	70)
Benzene	$\rho_u$	0.419	633	23	66)
Benzene	$\rho_u$	0.438–0.453	633	23	70)
Chloroform	$\rho_u$	0.211	633	23	66)
Chloroform	$\rho_u$	0.204	633	23	70)
Carbon tetrachloride	$\rho_u$	0.036	633	23	66)
Carbon tetrachloride	$\rho_u$	0.031–0.099	633	23	70)
Cyclohexane	$\rho_u$	0.046	633	23	66)
Cyclohexane	$\rho_u$	0.059	633	23	70)
Acetone	$\rho_u$	0.155	633	23	66)
Acetone	$\rho_u$	0.226	633	23	70)
Methanol	$\rho_u$	0.049	633	23	66)
Methanol	$\rho_u$	0.050	633	23	70)
Carbon disulphide	$\rho_v$	0.485	633	23	66)
Carbon tetrachloride	$\rho_v$	0.0184	633	23	66)
Chloroform	$\rho_v$	0.118	633	23	66)
Cyclohexane	$\rho_v$	0.0235	633	23	66)
Benzene	$\rho_v$	0.265	633	23	66)
Toluene	$\rho_v$	0.325	633	23	66)
Acetone	$\rho_v$	0.084	633	23	66)
Methyl ethyl ketone	$\rho_v$	0.077	633	23	66)
Methanol	$\rho_v$	0.025	633	23	66)
Water	$\rho_v$	0.025	633	23	66)
Benzene	$10^6 \times R_{90}(\text{cm}^{-1})$	8.765	633	23	71)
Toluene	$10^6 \times R_{90}(\text{cm}^{-1})$	10.31	633	23	71)
Methanol	$10^6 \times R_{90}(\text{cm}^{-1})$	1.349	633	23	71)
Water	$10^6 \times R_{90}(\text{cm}^{-1})$	0.490	633	23	71)

and Berry<sup>32)</sup>; illustrations involving several modes of calibration have been provided by Levine *et al.*<sup>50)</sup> and by Jennings and Plummer<sup>74)</sup>. The latter workers appear to have been the first to have conducted a completely reliable calibration of a LS photometer on the basis of Mie theory for solutions of large monodisperse latices. Calibration involving calculation from the geometry of the apparatus is generally complex and is rarely used now. In general for non-absolute photometers the purpose of the necessary calibration is to relate instrument response (such as a galvanometer reading  $G_{90}$  at an angle  $90^{\circ}$ ) to the actual Rayleigh ratio. The three major modes are (a) comparison of  $G_{90}$  for a standard substance with the known value of  $R_{90}$  for that substance (b) comparison of  $G_{90}$  from a colloidal suspension of small spheres with the turbidity  $\tau$  determined by subsidiary photometric transmission measurements, (c) use of a polymer of accurately known  $M$ , and comparing the known value of  $1/M$

with the result of extrapolating  $Kc/G_\theta$  to infinite dilution and zero concentration.

Provided the standard is stable, free from fluorescence and exhibits sufficient scattering, method (a) is the simplest and most frequently used. Benzene has long been employed for this purpose, although there was a controversy for many years regarding its true  $R_{90}$  values at  $\lambda_0 = 436$  and  $546$  nm; two schools of thought subscribed to values which differed between them by about 40%. Today, the situation has been resolved in favour of the higher values and, indeed, when adopting them for calibration, one obtains the same value of  $M$  as that found by an absolute technique<sup>41)</sup> not requiring any calibration. The most recent values<sup>75)</sup> of  $R_{90}$  ( $\text{cm}^{-1}$ ) and  $\rho_u$  for benzene as a function of temperature  $T$  ( $^\circ\text{C}$ ) and at  $\lambda_0 = 436$  nm are:

$$R_{90} = 10^{-6} (45.4 + 0.109 T)$$

$$\rho_u = 0.486 - 0.00148 T$$

It is convenient to employ a secondary standard of known Rayleigh ratio relative to that of the primary standard. Thus a solid cylindrical rod of flint glass (manufactured by Schott and Gen, Mainz, W. Germany) is recommended for use with the Sofica photometer and the value of the ratio of the relative scatterings  $r_{bg}$  of benzene to glass is quoted;  $r_{bg}$  has a value of the order of unity. The relation between the true Rayleigh ratio  $R_{90}$  and the observed galvanometer reading  $G_{90}$  for the solution in question is

$$R_{90} = [G_{90}/r_{bg} G_{90}(\text{glass})] R_{90}(\text{benzene}) [\tilde{n}/\tilde{n}(\text{benzene})]^2 \quad (61)$$

In Eq. (61),  $G_{90}(\text{glass})$  is the galvo reading for the glass standard and the product  $r_{bg} G_{90}(\text{glass})$  denotes the reading which would have been obtained, if benzene itself had been used instead of glass. The final factor in Eq. (61) is the "refractive index squared" correction of Hermans and Levinson<sup>76)</sup> which is unity only if the refractive index of the substance studied,  $\tilde{n}$ , is the same as that of the primary calibrant,  $\tilde{n}$  (benzene). Although this correction for the different refracting powers is very frequently used, results of Jennings and Plummer<sup>74)</sup> in Table 3 suggest that the true form of the correction might be some intermediate function between "refractive index" and "refractive index squared". In fact, within experimental error, the factor seems to be simply  $\tilde{n}/\tilde{n}(\text{water})$  for these data involving calibration with aqueous solutions.

Since the scattering due to dust is negligible relative to the very large scattering from colloidal suspensions, procedure (b) is inherently attractive. Using the definition of turbidity  $\tau$  and the interrelation between  $\tau$  and  $R_{90}$ , the calibration constant  $\Phi$  of the instrument is given by

$$(c/G_{90})_{c=0}/(c/\tau)_{c=0} = \Phi(16\pi/3) \exp(\tau\ell) \quad (62)$$

Hence  $c$  (g/ml) is the concentration of colloidal suspension;  $G_{90}$  is the reading on the LS photometer at  $\theta = 90^\circ$ ,  $\ell$  is the path length, which equals the cell diameter when using a cylindrical cell;  $\tau$  is the turbidity obtained from measurements of optical density. Table 4 gives the results of calibrating a Sofica instrument with colloidal

Table 3. Molecular weight  $M$  of a monodisperse polystyrene fraction in solvents of different refractive index  $\tilde{n}_0$ ; role of refractive index correction factor<sup>74)</sup>

Solvent	$\tilde{n}_0$	Apparent $M^1)$	$M^2)$ using correction in $\tilde{n}_0^2$	Correction in $\tilde{n}_0$
Benzene	1.50	51300	65300	57800
Dioxan	1.42	54200	61900	57900
Methyl ethyl ketone	1.38	55400	60100	57500

<sup>1)</sup> Obtained from LS readings and average value of calibration constant  $\Phi$  for the wavelength used (546 nm).

<sup>2)</sup> Obtained from LS readings, average value of  $\Phi$  and invoking correction factor.

Table 4. Calibration constants obtained with colloidal silicas and with Mie particles<sup>74)</sup>

	$\Phi \times 10^5$ ( $\text{cm}^{-1}$ ) at $\lambda_0 = 436$ nm	at $\lambda_0 = 546$ nm
Ludox HS (colloidal silica)	48.0	14.6
Syton 2X (colloidal silica)	47.0	14.7
Polystyrene latex (Mie particles)	47.5	15.2

silica as well as with a larger Mie scatterer. Excellent accord is evident among the values of  $\Phi$  obtained. For subsequent use in an actual molecular weight determination, the value of  $\Phi$  must be multiplied (as indicated in Table 3) by the appropriate refractive index correction. Tomato bushy stunt virus, in aqueous solution is such an intense scatterer that its optical density (and hence  $\tau$ ) is measurable. It is rarely used, since it is a far less accessible material than Ludox (E. I. du Pont de Nemours) or Syton 2X (Monsanto Chemicals Ltd).

Just as analysis of pure urea gives two amino groups and one carbonyl group per molecule and a calculated molecular weight of 60, so also is the exact number and identity of amino acid residues in a protein molecule often known. Thus, irrespective of the accuracy of a molecular weight measurement, the molecular weight of intact un-ionised human haemoglobin must of necessity be exactly 64458 (including four haeme groups)<sup>32)</sup>. Appealing as the use of such a material for procedure (c) is, the increasing current availability of highly monodisperse synthetic polymer makes these latter substances the preferred choice today. In comparison with method (a), more work is entailed when using polymer solutions as calibrants, since effectively one has to conduct an entire LS experiment at different angles and different concentrations of standard polymer in order to obtain the calibration constant. Similar considerations apply to silicotungstic acid which is of lower molecular weight but which has been

recommended and shown suitable as calibration standard for several types of LS photometer. In solution it is a Rayleigh scatterer and allows measurements free from the complication of dissymmetry. The formula is  $\text{SiO}_2 \cdot 12 \text{WO}_3 \cdot 26 \text{H}_2\text{O}$  and  $M = 3311$ . In aqueous salt solution, the dissolved molecule is  $\text{H}_4\text{SiW}_{12}\text{O}_{40}$  and  $M = 2879$ . These solutions develop colour on contact with metal, and only glass and plastic cells and filtration apparatus must be used<sup>50</sup>.

Some Rayleigh ratios at less common wavelengths have been assembled with cognate refractometric data in Table 2.

### 3. Brillouin Scattering

The whole field of Brillouin scattering spectroscopy is a rapidly developing one with regard to instrumentation. For the present purpose it will suffice to reproduce schematically a device which has been used to measure molecular weights<sup>41, 77</sup>. In Fig. 14 the source is a low power (10 mW) He-Ne laser and the sample is contained in a standard Brice-Phoenix square turbidity cell. The scattered light is analysed with a piezoelectrically driven scanning Fabry-Perot interferometer (Fig. 15). Typical spectra<sup>77</sup> for pure solvent and solution of known concentration are shown in Fig. 16. Occasional spikes in the traces are due to the presence of dust particles passing through the incident light beam.

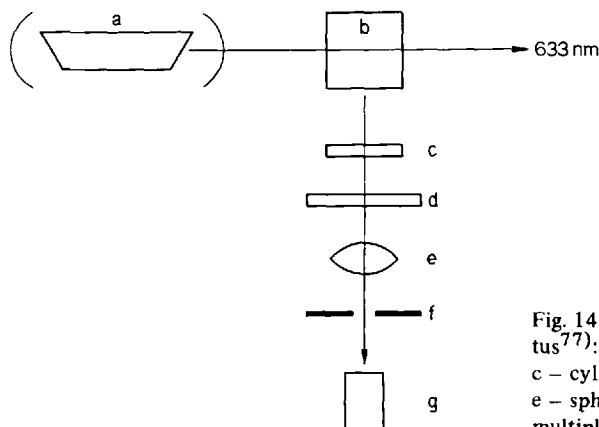


Fig. 14. Schematic of Brillouin LS apparatus<sup>77</sup>: a – He – Ne laser, b – square cell, c – cylindrical lens, d – interferometer, e – spherical lens, f – pinhole, g – photo-multiplier

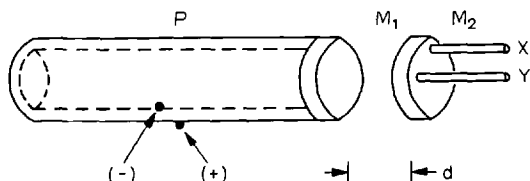


Fig. 15. Simplified diagram of scanning Fabry – Perot interferometer<sup>77</sup> showing piezoelectric ceramic tube (P), multilayer dielectric mirrors ( $M_1$ ,  $M_2$ ), micrometer adjustment for parallelism (X, Y). Mirror spacing (d) is adjustable

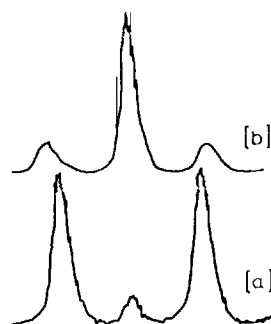


Fig. 16. Brillouin LS spectra<sup>77)</sup> at 25 °C for (a) pure water and (b) solution of 300 g of glycerol/kg of water

#### 4. Treatment of Experimental Data

LS data necessitate extrapolation to infinite dilution. The clarification procedure may well introduce a small change (usually, an increase) in concentration from the initially known one. The values of  $c$  should therefore be determined on the clarified solution by an appropriate analytical procedure such as spectrophotometry for solutions of DNA using the known phosphorous extinction coefficient, acid-base titration for solution of polyacrylic acid or by evaporating an aliquot to dryness. When high vacuum conditions are obligatory not only for preparing the polymer, but also for dissolving and diluting it and making LS measurements, there is less freedom of choice and spectrophotometry is normally used. Extrapolation to  $c = 0$  is facilitated if  $A_2$  [cf. Eq. (36)] is small as obtains in a poor solvent or is zero under conditions of thermodynamic ideality. The latter state is often realised at a temperature different from ambient. If this should be an elevated temperature, filtration rather than centrifugation is the normal mode of clarification. The temperature in some polymer-solvent systems is below ambient as illustrated in Fig. 17 where a large value of  $A_2$  obtains in the good solvent<sup>78)</sup>, methyl ethyl ketone at 30 °C, whereas the extrapolation to  $c = 0$  presents no uncertainty at all under the ideal condition<sup>78)</sup> prevailing in ethyl lactate at 11.7 °C. In principle, only a single LS measurement on one solution suffices to yield  $M$  in such a system provided that the data at different angles have been extrapolated to  $\theta = 0$ .

For large particles, Eq. (40) may be treated *via* different methods the most popular of which is the Zimm plot. Essentially, all the data are displayed on a grid which yields on appropriate extrapolations, two lines representing (a) the dependence of  $(Kc/R_\theta)_{\theta=0}$  on concentration and (b) the dependence of  $(Kc/R_\theta)_{c=0}$  on angle. The common intercept of these lines is  $1/M$ . The abscissa in the Zimm plot is  $k_1 \sin^2(\theta/2) + k_2 c$  where a value of unity is normally (but not necessarily) assigned to the arbitrary constant  $k_1$  and the other constant  $k_2$  is also selected rather arbitrarily so as to afford the most convenient spread of data points on the graph. For the two extrapolated lines (a) and (b), the abscissa become  $k_2 c$  and  $k_1 \sin^2(\theta/2)$  respectively. Methods of obtaining an optimum value of  $k_2$  have been proposed<sup>79)</sup>. Frequently, an involuted Zimm plot can be unravelled<sup>80)</sup> by assigning a negative value to  $k_2$  (Fig. 18).



Determination of Molecular Weights by Light Scattering

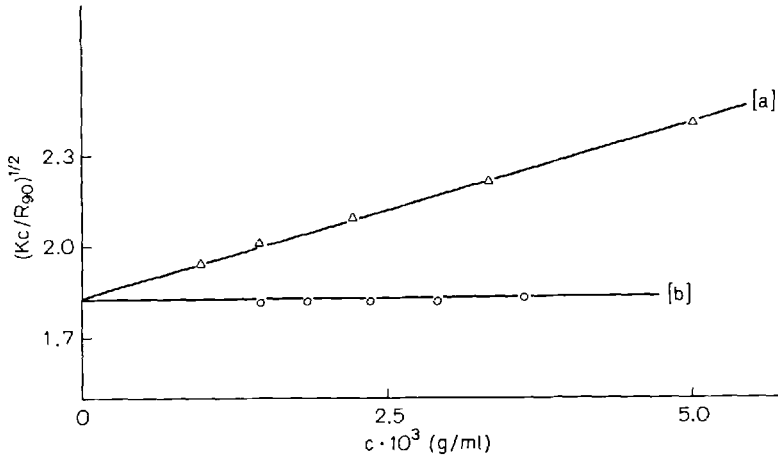


Fig. 17. Square root plot of  $90^\circ$  LS for a solution of low molecular weight polyphenyl acrylate<sup>78</sup> in (a) methyl ethyl ketone at  $30^\circ\text{C}$  (non ideal conditions) and (b) ethyl lactate at  $11.7^\circ\text{C}$  (thermodynamically ideal conditions). The value of  $K$  is different for plots (a) and (b)

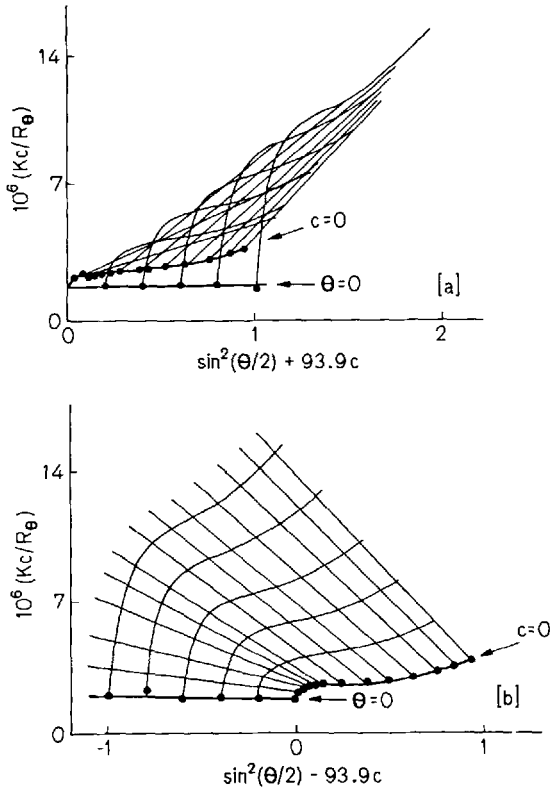


Fig. 18. Use of a negative value for the plotting constant  $k_2$  for solutions of amylose<sup>80</sup> in dimethyl sulphoxide: (a)  $k_2 = +93.9$ , (b)  $k_2 = -93.9$ . The primary data points have been omitted for clarity

An exactly equivalent and equally acceptable alternative to the variable  $\sin^2(\theta/2)$  is the parameter  $\tilde{\mu}^2$ , which is identical to [constant  $\times \sin^2(\theta/2)$ ] for an experiment involving light of one fixed wavelength<sup>31)</sup>. It is convenient to omit the optical constant  $K$  from the plots. Hence the ordinate becomes simply  $c/R_\theta$  and the molecular weight is given by  $M = 1/K$  (intercept). For reasons outlined elsewhere<sup>32)</sup>, the author is inclined to the belief that the Zimm grid offers few advantages in real terms, and that it is preferable to construct separate plots for the concentration dependence of  $c/R_\theta$  at each fixed angle and for the angular dependence of  $c/R_\theta$  at each fixed concentration. One important factor militating against the indiscriminate use of the Zimm plot is that the angle and concentration scales cannot be selected simultaneously so as to give the optimum separation of data points for accurate extrapolations of both dependences.

Square root plots proposed by Berry<sup>81)</sup> are often more linear than the conventional ones and hence allow an easier extrapolation. Thus, at zero angle

$$(c/R_\theta)_{\theta=0}^{1/2} = (1/MK)^{1/2}(1 + MA_2c) \quad (63)$$

and the resultant intercept at  $c = 0$ , when the left-hand-side of Eq. (63) is plotted against  $c$ , yields:

$$M = 1/K(\text{intercept})^2$$

At zero concentration:

$$(c/R_\theta)_{c=0}^{1/2} = (1/MK)^{1/2} [1 + (8\pi^2/3\lambda^2)\langle s^2 \rangle \sin^2(\theta/2)] \quad (64)$$

and the resultant intercept at  $\theta = 0$ , similarly yields the molecular weight, when the left-hand-side of Eq. (64) is plotted versus  $\sin^2(\theta/2)$ :

$$M = 1/K(\text{intercept})^2$$

The procedure is outlined schematically in Fig. 19. Such plots can usually be constructed without difficulty, but there are theoretical reasons why they need not necessarily be parallel when the heterogeneity of the sample is high.

The dissymmetry method is useful especially if the instrument does not afford facilities for a wide angular scan of scattered intensities. For large particles the scattering envelope is not symmetrical and, as already indicated in Fig. 1, the forward scatter is larger than that in the backward direction. Hence the dissymmetry  $Z_d$  is greater than unity, where

$$Z_d = R_{45}/R_{135} = P(45)/P(135) = G_{45}/G_{135} \quad (65)$$

Here the symbols  $R$ ,  $P$  and  $G$  denote respectively the Rayleigh ratio, particle scattering function and instrument scattering reading. It is possible to take other angles such as  $60^\circ$  and  $120^\circ$ , which are also symmetrical about  $90^\circ$ . However, the angles  $45^\circ$  and  $135^\circ$  are most frequently selected, and the widely used Brice-Phoenix photo-

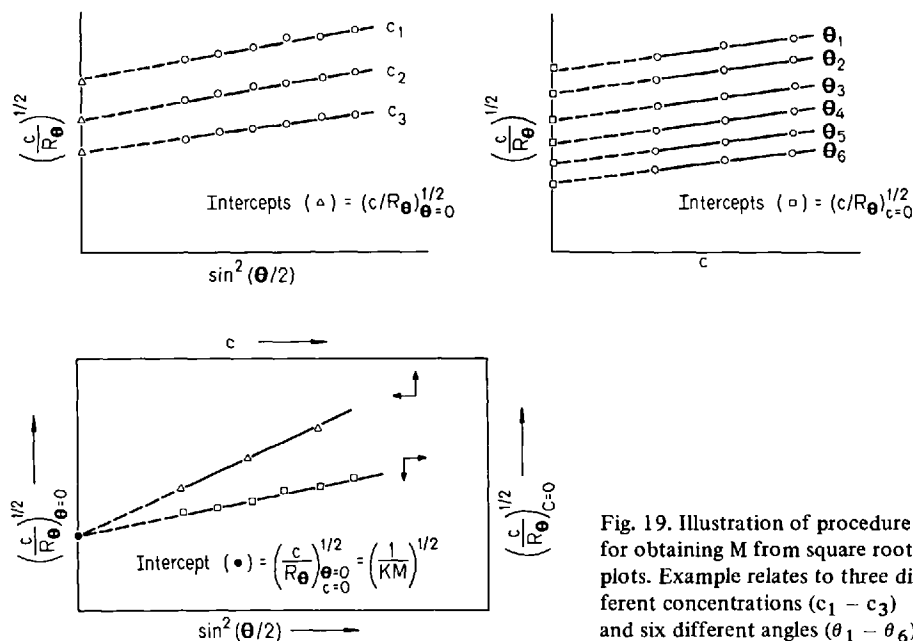


Fig. 19. Illustration of procedure for obtaining  $M$  from square root plots. Example relates to three different concentrations ( $c_1 - c_3$ ) and six different angles ( $\theta_1 - \theta_6$ )

meter is equipped with a special semi-octagonal cell for measuring specifically at these angles. The appropriate dissymmetry is the one relating to infinite dilution, which is termed the intrinsic dissymmetry,  $[Z_d]$ . The dependence of  $Z_d$  on  $c$  is not linear, but the variation of  $1/(Z_d - 1)$  on  $c$  is normally sufficiently linear to allow extrapolation to  $c = 0$  and thereby obtain the value of  $[Z_d]$  from the intercept in such a plot, thus<sup>30)</sup>:

$$[Z_d] = 1 + 1/(\text{intercept}) \quad (66)$$

For readings at  $90^\circ$  only:

$$Kc/R_{90} = (1/M)[1/P(90)] + 2 A_2 c \quad (67)$$

and neglect of the particle scattering function, that is assumption that  $P(90)$  is unity, gives only an apparent molecular weight  $M^*$

$$\lim_{c \rightarrow 0} (Kc/R_{90}) = 1/M^* \quad (68)$$

The correction is effected by assigning the appropriate value of  $1/P(90)$ , which may be found from tables<sup>30)</sup> wherein it is correlated with  $[Z_d]$ .

When this is done, the molecular weight corrected for dissymmetry,  $M_d$ , is given by

$$M_d = 1/P(90)/\lim_{c \rightarrow 0} (Kc/R_{90}) \quad (69)$$

Table 5. Approximate values of  $[Z_d]$  and  $1/P(90)$  for different particle shapes

Coil [ $Z_d$ ]	$P^{-1}(90)$	Rod [ $Z_d$ ]	$P^{-1}(90)$	Sphere [ $Z_d$ ]	$P^{-1}(90)$	Disc [ $Z_d$ ]	$P^{-1}(90)$
1.02	1.02	1.02	1.01	1.02	1.01	1.02	1.01
1.12	1.09	1.13	1.09	1.12	1.08	1.13	1.09
1.21	1.15	1.22	1.15	1.20	1.14	1.20	1.14
1.31	1.22	1.33	1.24	1.32	1.21	1.31	1.21
1.62	1.46	1.62	1.48	1.62	1.39	1.62	1.41
2.03	1.81	2.04	2.01	2.00	1.60	2.07	1.69
3.05	2.99	—	—	3.02	2.09	2.99	2.25
4.01	4.99	—	—	3.91	2.44	4.00	2.93

Some selected and approximate values of  $[Z_d]$  and  $1/P(90)$  are quoted as illustration in Table 5. A wider range of exact values is available in tabulated and graphical form in the literature<sup>30</sup>. Inspection of Table 5 shows that the corrected molecular weight is ca. 8% greater than the uncorrected one, when  $[Z_d] \approx 1.1$ , and this applies irrespective of particle shape. In fact it is unnecessary to know the shape for intrinsic dissymmetries up to ca. 1.3, but thereafter such a knowledge is required in order to select  $1/P(90)$  from the measured  $[Z_d]$ .

Tables of this sort are valid for Gaussian coils only. In thermodynamically good solvents the Gaussian behaviour of chain molecules is perturbed by what is called the "excluded volume effect"<sup>30</sup>. The  $P(\theta)$  function depends on the distribution of mass within the particle and this, in turn, is changed if the volume effect is operative. A useful parameter for quantifying the effect is  $\tilde{\epsilon}$ , which is defined as

$$\tilde{\epsilon} = (2\tilde{\nu} - 1)/3 \quad (70)$$

where  $\tilde{\nu}$  is the exponent in the Mark-Houwink equation relating the intrinsic viscosity of the polymer in the particular solvent (the same solvent as used in LS) to the molecular weight. In an ideal solvent  $\tilde{\nu} = 0.50$  and  $\tilde{\epsilon} = 0$ . The magnitude of  $\tilde{\epsilon}$  increases with the goodness of the solvent, since under these conditions  $\tilde{\nu} > 0.50$  and hence  $\tilde{\epsilon} > 0$ .

The methods are illustrated in Fig. 20 where the data<sup>78</sup> refer to a sample of poly(phenyl acrylate) in methyl ethyl ketone at  $\lambda_0 = 436$  nm and  $T = 30^\circ\text{C}$ . Plots (a) and (b) utilise a full angular scan; their common intercept in conjunction with the optical constant  $K$  yield a molecular weight of  $1.09 \times 10^6$ . A lower molecular weight of  $M^* = 0.746 \times 10^6$  is given by the intercept of plot (c) which invokes only data for  $90^\circ$  scattering. The intercept of plot (d) yields an intrinsic dissymmetry of 1.62. Reference to Table 5 for this value of  $[Z_d]$  gives a corresponding value of 1.46 for  $1/P(90)$  assuming a random coil configuration in solution; hence the molecular weight,  $M_d$ , corrected for dissymmetry is  $0.746 \times 10^6 \times 1.46 = 1.09 \times 10^6$ . The value of  $\tilde{\nu}$  for this system has been found<sup>78</sup> to be 0.72 and hence  $\tilde{\epsilon} = 0.15$ . Tables<sup>30</sup>, not reproduced here, relate  $[Z_d]$  to a relative size parameter  $\langle h^2 \rangle_d^{1/2}/\lambda$ , where  $\langle h^2 \rangle$  is the mean square end-to-end distance of a coil and equals  $6\langle s^2 \rangle$ ; the subscript d indicates

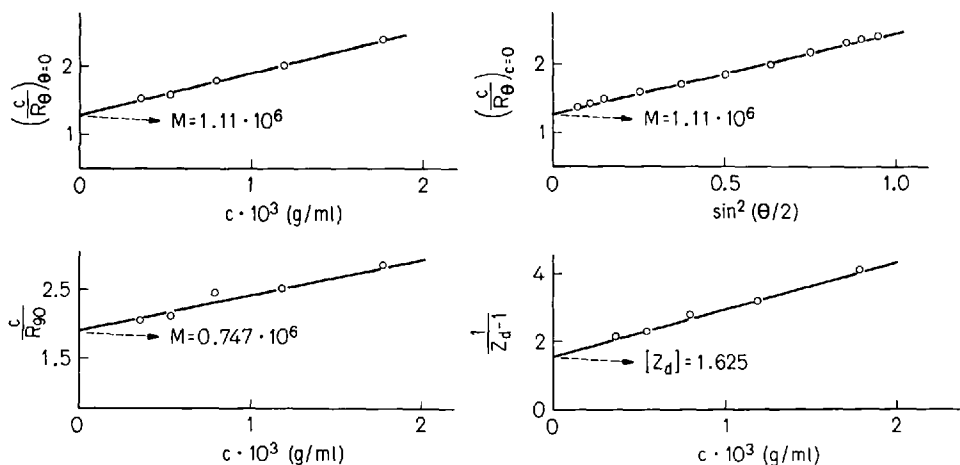


Fig. 20. Determination of  $M$  for high molecular weight polyphenyl acrylate<sup>78</sup>) in methyl ethyl ketone ( $T = 30^\circ\text{C}$ ,  $\lambda_0 = 436\text{ nm}$ ): upper curves – full angular scan, lower curves –  $90^\circ$  scattering and estimation of intrinsic dissymmetry

dissymmetry. For a value of  $[Z_d] = 1.62$ , these tables give  $\langle h^2 \rangle_d / \lambda = 0.30$ . Interpolating to a curve for  $\tilde{\epsilon} = 0.15$  in Fig. 21, yields  $M/M_d = 1.01$  for the value of  $\langle h^2 \rangle_d / \lambda$  in question. Hence the final molecular weight corrected for the excluded volume effect is 1.01 times greater than the molecular weight corrected for dissymmetry, that is,  $M = 1.10 \times 10^6$ . Consequently, the dissymmetry correction is quite sufficient in this example, but for very large molecules in thermodynamically good solvents ( $\langle h^2 \rangle_d / \lambda$  and  $\tilde{\epsilon}$  both large), the implementation of the additional excluded volume correction can be important.

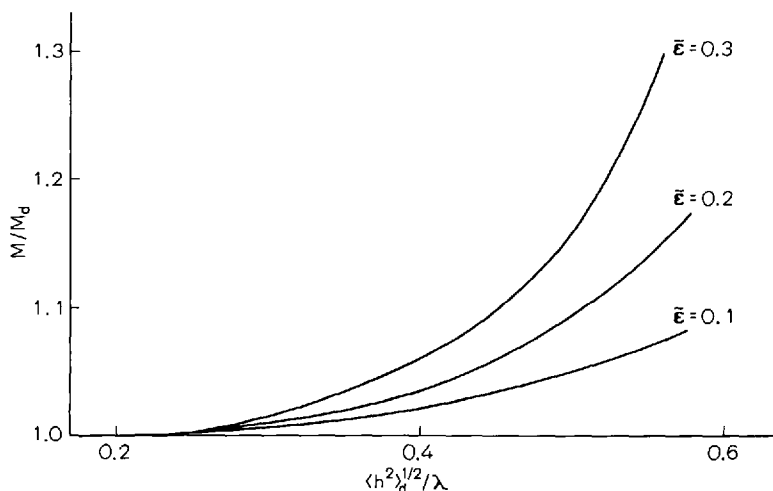


Fig. 21. Ratio between the correct molecular weight ( $M$ ) and that calculated from dissymmetry ( $M_d$ ), as a function of the root mean square end-to-end distance calculated from dissymmetry ( $\langle h^2 \rangle_d^{1/2}$ ) for different values of  $\tilde{\epsilon}$  (30)

Much of the tedium of deriving  $M$  from LS data has been removed by computer programming. This consists in the first instance of converting raw experimental data (e.g. galvanometer readings, neutral filter factor, angles, concentrations etc.) into values of  $Kc/R_\theta$  or  $[\sin^2/\theta/2) + k_2c]$ , which can be plotted. Additionally, these can then be treated by computer least squares analysis to yield  $M$  directly, without the necessity to plot the results. A programme<sup>82)</sup> geared to the Brice-Phoenix instrument was among the first to be used successfully; this was adapted later<sup>83)</sup> for use with the Sofica instrument. Most important programmes have been listed and discussed<sup>79)</sup>. More recent ones include those of Bryce<sup>84)</sup> and of Miller and Stepto<sup>85)</sup>.

#### IV. Applications to Different Types of Solute

General simplified outlines have been covered in the preceding sections. In practice there are several complicating features not readily assimilated into a general treatment. Among these may be included charge effects and multicomponent systems. Here we shall illustrate and discuss some applications of LS to the determination of molecular weights and introduce any additional theory where relevant to the system under consideration. In the first instance it will prove convenient to classify the applications according to the approximate order of molecular weight of the solute.

##### 1. Low Molecular Weight Liquids

LS measurements on binary liquid mixtures have been directed primarily as a means of obtaining fundamental thermodynamic information such as chemical potentials and the excess mixing functions. Although molecular weights could in fact be derived from some published data, this has largely not been done by the authors, since such an exercise on substances of known molecular weight would have been subsidiary to the main purpose of their studies.

One of the most elegant LS studies on liquid mixtures is that of Sicotte and Rinfret<sup>17)</sup> and it will be instructive to summarise their approach solely with regard to that aspect which is concerned with molecular weight determination. Liquid 1 will be considered as solvent and liquid 2 (of ostensibly unknown molecular weight  $M_2$ ) as solute. The Rayleigh ratios implied are the isotropic ones, which are obtained for liquid 1 as well as for solutions (subscript 12) *via* the measured Cabannes factors [Eqs. (44) and (45)].

For pure liquid 1 the Rayleigh ratio  $R_d$  arises from density fluctuations in accord with Einstein theory:

$$R_d = (\pi^2 k T \beta_1 / 2 \lambda_0^4) [(1/\beta_1)(\partial \tilde{n}_1^2 / \partial p)_T]^2 \quad (71)$$

Here,  $\beta_1$  (instead of the more cumbersome notation  $\beta_{T1}$ ) is used for the coefficient of isothermal compressibility of liquid 1. The presence of the second liquid gives rise

to an additional scattering due to concentration fluctuations,  $R_c$ . As seen earlier [cf. Eq. (36)], this is related to  $M_2$  as follows:

$$R_c = Kc_2 / [(1/M_2) + 2A_2c_2] \quad (72)$$

The  $90^\circ$  Rayleigh ratio of the mixture,  $R_{12}$ , is normally considered as the sum of the two constituent sources of scattering, viz:

$$R_{12} = R_d + R_c \quad (73)$$

If the density fluctuation of a dilute solution of liquid 2 in solvent 1 is identified with the Rayleigh ratio of pure solvent, then  $R_d \equiv R_1$ , from which  $R_c = R_{12} - R_1$ . Hence, using Eq. (72) in the customary manner one obtains  $1/M_2$  as the intercept at  $c_2 = 0$  in a plot of  $Kc_2/R_c$  versus  $c_2$ . An example of such a plot<sup>17)</sup> appears in Fig. 22(a) for carbon disulphide in carbon tetrachloride at  $25^\circ\text{C}$  and  $\lambda_0 = 546\text{ nm}$ . The intercept yields  $M_2 = 125$ , compared with the true value of 76. An absolute error of 49 in the molecular weight is, of course, quite negligible for macromolecules in solution. In this connection, it has been estimated that the normal Eq. (72) is unlikely to introduce an error of more than 100 in  $M_2$  provided there is a sufficiently large optical constant  $K$ . In the present instance, the error is extremely large and arises from the assumption that the density fluctuation is a constant characteristic of the solvent and is independent of concentration, that is, of the presence of liquid 2.

Bullough<sup>86)</sup> has proposed that:

$$R_{12} = R_d(1 + Y) + R_c \quad (74)$$

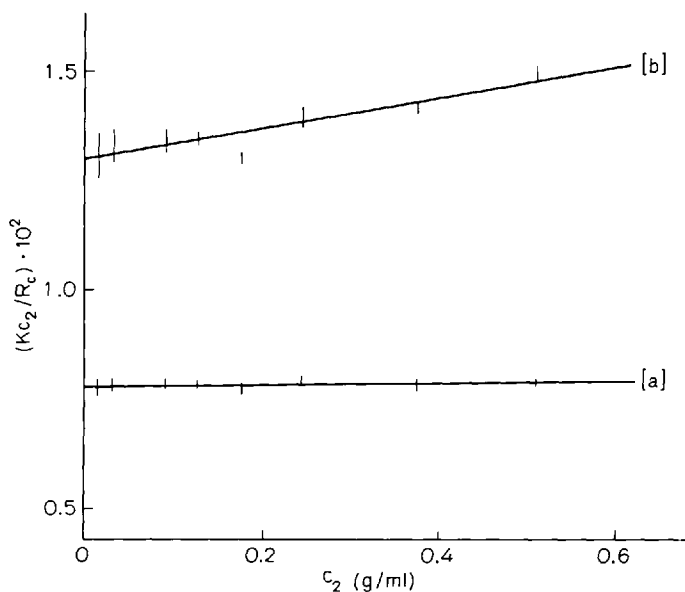


Fig. 22. LS plots for  $\text{CS}_2$  in benzene<sup>17)</sup> according to (a) – Eq. (72) and (b) – Eq. (76)

where

$$Y \equiv 2(\partial \tilde{n}_{12}^2 / \partial c_2)_{p,T} / (1/\beta_{12})(\partial \tilde{n}_{12}^2 / \partial p)_{c,T} \quad (75)$$

Hence the amended form of Eq. (72), which allows for the effect of concentration on the density fluctuation, is:

$$Kc_2/[R_{12} - R_d(1 + Y)] = 1/M_2 + 2 A_2 c_2 \quad (76)$$

Use of Eq. (76) requires determinations of the isotropic Rayleigh ratio for mixtures of various concentrations  $c_2$ . The density fluctuation  $R_d$  differs slightly for each solution and is determined from the following expression [Eq. (77)], which is obtained by comparing the forms of Eq. (71) for pure liquid 1 and a mixture, and in which  $R_1$  denotes the isotropic Rayleigh ratio for pure liquid 1:

$$R_d = \left( \frac{\beta_1}{\beta_{12}} \right) \left[ \left( \frac{\partial \tilde{n}_{12}^2}{\partial p} \right)_{c,T} \right]^2 / \left[ \left( \frac{\partial \tilde{n}_{12}^2}{\partial p} \right)_T \right]^2 \quad (77)$$

Evaluations of  $R_d$  and  $Y$  necessitate a knowledge of certain physical properties of the two liquids and the mixtures. The variation of refractive index with concentration is measured readily by refractometry, if  $|\tilde{n}_1 - \tilde{n}_2|$  is large. The coefficient of isothermal compressibility of a mixture  $\beta_{12}$  requires specialised equipment. Alternatively, it can be determined from the heat capacity and the coefficient of isentropic compressibility<sup>87, 88</sup>, the latter being yielded from velocity of sound data<sup>88</sup>. However, provided  $\beta_1$  and  $\beta_2$  for the pure compounds are known,  $\beta_{12}$  is evaluated most conveniently on the basis of additivity, thus:

$$\beta_{12} = (1/V_{12})(X_1 V_1 \beta_1 + X_2 V_2 \beta_2) \quad (78)$$

where  $V$  and  $X$  denote molar volume and mole fraction respectively. The variation of refractive index with pressure has been measured by some workers, but this also requires specialised apparatus. This requirement can be by-passed by an indirect evaluation *via* the following relationships which are quoted in general terms without any specific identifying subscripts:

$$\rho \left( \frac{\partial \epsilon}{\partial p} \right)_T = \frac{1}{\beta} \left( \frac{\partial \epsilon}{\partial p} \right)_T = \frac{2 \tilde{n}^2}{\beta} \left( \frac{\partial \tilde{n}^2}{\partial p} \right) \quad (\text{since } \epsilon = \tilde{n}^2) \quad (79)$$

Among the semi-empirical relationships available for the quantity  $\rho(\partial \epsilon / \partial p)_T$  (where  $\rho$  denotes density), that due to Eykmann appears<sup>7</sup> to be among the most accurate, viz

$$\rho \left( \frac{\partial \epsilon}{\partial p} \right)_T = 2 \tilde{n}^2 (\tilde{n}^2 - 1)(\tilde{n} + 0.4) / (\tilde{n}^2 + 0.8 \tilde{n} + 1) \quad (80)$$



Using this approach the left-hand-side of Eq. (76) may be evaluated and plotted versus  $c_2$  in the normal way to obtain  $M_2$  [see Fig. 22(b)]. The resultant molecular weight of 77 for carbon disulphide is only ca. 1% greater than the true value.

## 2. Simple Compounds and Oligomers

For solutes which are not macromolecules the requirements for a successful determination of  $M$  are (a) higher concentrations than for polymer solutions, (b) selection of solvent yielding a large value of  $\nu$  and (c) essential implementation of corrective depolarisation factor. Since  $\nu$  changes with  $M$  for low molecular weight polymers, it must consequently be measured separately for each sample if the molecular weight is suspected to be low. Similarly the depolarisation factor  $\rho_u$  (or  $\rho_v$  for vertically polarised light) is dependent on both concentration and molecular weight, as was illustrated in Fig. 3. For propylene glycol in acetone at 25 °C the Cabannes factor is 1.35 at infinite dilution for vertically polarised incident light, and the molecular weight obtained from LS neglecting this factor would therefore be too high by 35% in relation to the true corrected  $M$ . Highly purified samples of simple compounds of known formula have been employed to test the sensitivity of LS photometers. Table 6 demonstrates that, in most studies, remarkably good agreement is possible between the measured and known molecular weights.

Table 6. Molecular weights by LS for pure simple low molecular weight compounds

Substance	$M$ by LS	Theoretical	Ref.
Propylene glycol	67	74	35)
Dipropylene glycol	125	134	35)
Diphenyl	160	154	35)
Dibenzyl	184, 186	182	91)
Dibenzyl	184, 181, 186, 195	182	92)
Methylated poly-oligophenylene	174	182	89)
Glucose	189	190	90)
Methylated poly-oligophenylene	250	273	89)
Sucrose	244	342	90)
Sucrose	332, 344	342	36)
Methylated poly-oligophenylene	360	363	89)
Methylated poly-oligophenylene	458	453	89)
Methylated poly-oligophenylene	543	543	89)
Raffinose	571	594	90)
Sucrose octa-acetate	660, 677	678	92)
Sucrose octa-acetate	690	678	93)
Sucrose octa-acetate	674, 740	678	94)
Methylated poly-oligophenylene	720	723	89)
Tristearin	860	891	35)
Pentaerythritol tetrastearate	1280	1202	35)

The same essential requirements are needed also for measurements on oligomers, which are low molecular species of polymers ( $M < \text{ca. } 10^4$ ). LS has been used to measure  $M$  for oligomers of the following: methylated polyphenylenes<sup>89</sup>), nylon 66<sup>95</sup>), polyethylene glycol<sup>96</sup>), poly- $\alpha$ -methyl styrene<sup>97</sup>), polystyrene<sup>91</sup>), polyheptamethylene urea<sup>98</sup>), polyoctadecyl vinyl ether<sup>99</sup>), polypropylene glycol<sup>35</sup>), poly(trimethyl)hexamethylene urea<sup>98</sup>), polyvinyl pyrrolidone<sup>100</sup>) and polydimethyl siloxane<sup>101</sup>). Data for the first of these are included in Table 6, since their theoretical molecular weights are known from the mode of synthesis.

In general the true value of  $M$  for an oligomer as a basis for comparison is rarely known. However, demonstration of internal consistency and use of a method additional to LS can provide supporting evidence. Thus, for a sample of polyvinyl pyrrolidone, LS gives  $M = 7150, 7400, 7500$  and  $7250$  from measurements in water at  $\lambda_0 = 436 \text{ nm}$ , in water at  $\lambda_0 = 546 \text{ nm}$ , in chloroform at  $\lambda_0 = 436 \text{ nm}$  and in chloroform at  $\lambda_0 = 546 \text{ nm}$  respectively<sup>102</sup>). For a sample of poly- $\alpha$ -methyl styrene<sup>97</sup>), LS and sedimentation equilibrium yield  $M = 1450 \pm 28$  and  $1450 \pm 10$  respectively, as opposed to a value of  $\bar{M}_n = 1310 \pm 50$  afforded by VPO. If the value of  $\bar{M}_n$  is assumed to be subject to very low error for this low molecular weight polymer prepared by anionic polymerisation, then one would anticipate a low degree of polydispersity, giving a value of  $M$  which is ca. 5% greater than that of  $\bar{M}_n$  (it is actually 11% greater, probably due to the fact that techniques for producing very monodisperse samples by anionic polymerisation had not quite attained their present level of sophistication).

### 3. Polymers

Molecular weights of both synthetic and naturally occurring polymers have been obtained by LS almost as a routine measurement. For reasons which are not wholly evident but which probably have historical and medical connotations, sedimentation in the ultracentrifuge seems to be somewhat preferred by workers in the field of biopolymers, although this technique offers no advantages over LS. Indeed LS can frequently provide additional information and is less time consuming.

Polymer samples of known  $M$  and  $\bar{M}_n$ , usually highly monodisperse in nature, are becoming increasingly available commercially as standards. They include polystyrene, poly- $\alpha$ -styrene, polyethylene, polymethyl methacrylate, polyisoprene (95% *cis*) and polytetrahydrofuran. The last of these offers a considerable improvement on polystyrene with regard to monodispersity in the low molecular weight region. Polymer fractions of known polydispersity ( $M/\bar{M}_n$ ) are also available, for example polyvinyl chloride, polyethylene and polyphenylene oxide. The quoted value of  $M$  for standards represents the mean of a large number of experimental determinations, usually by LS. Some LS plots for a N.B.S. polystyrene standard (No 705) are shown in Fig. 23; they relate to two recent techniques, viz Brillouin spectroscopy and fixed low angle LS on the Chromatix instrument. The resultant values of  $M$  together with other values obtained for this sample are assembled in Table 7.

Several anomalies in the LS determinations of molecular weight have been attributed to the presence of a stable supramolecular structure, which can persist even in thermodynamically good solvents<sup>104</sup>). Examples have been reported for solutions of

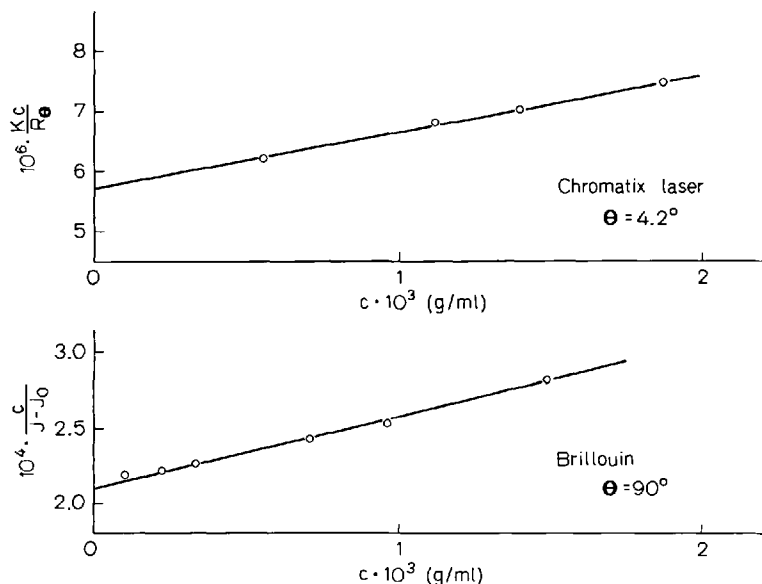


Fig. 23. Determination of  $M$  for polystyrene (N.B.S. sample No. 705) by Chromatix low angle scattering<sup>66</sup> at  $\theta = 4.2^\circ$  and by Brillouin scattering<sup>41</sup> at  $\theta = 90^\circ$

Table 7. Weight average molecular weight of a standard polystyrene sample (N.B.S. 705) by different methods

Solvent	Method	$M \times 10^{-5}$	Ref.
Cyclohexane	LS	1.79	Datum supplied with sample by N.B.S.
Cyclohexane	Sedimentation	1.90	Datum supplied with the sample by N.B.S.
Benzene	LS	1.76	103)
Benzene	Brillouin scattering	1.73	41)
Toluene	Brillouin scattering	1.73	41)
Toluene	Low angle (Chromatix) LS	1.78	66)

polyacrylonitrile, polyethylene, polyvinyl alcohol, methyl cellulose, natural rubber and, most frequently, polyvinyl chloride. The microgel, often present in unfractionated species as well as in high molecular weight fractions, manifests itself by abnormally large LS at low angles. The resultant curvature in the plot of  $(Kc/R_\theta)_{c=0}$  versus  $\sin^2(\theta/2)$  renders an extrapolation to zero angle either impossible or one fraught with uncertainty. Examples in Fig. 24 relate to a copolymer prepared by grafting with  $\gamma$ -irradiation to different doses<sup>105</sup>). The lightly grafted copolymer is normal in behaviour displaying a fairly constant value of  $(Kc/R_\theta)_{c=0}$  and small dimensions, whereas more highly grafted species of incompatible constituents induces microgel formation. The downward curvature becomes very pronounced and extra-

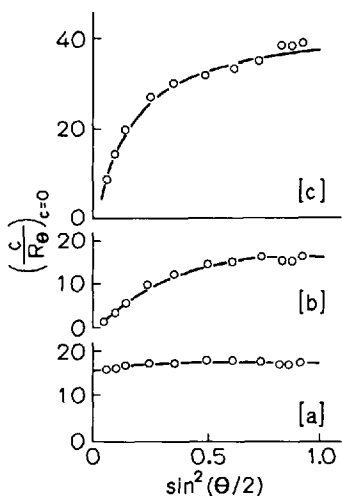


Fig. 24. LS at zero concentration for solutions of nylon-6/acrylic acid copolymers prepared by radiation grafting<sup>105</sup>. The degrees of grafting are (a) 0.038, (b) 0.056, (c) 0.123

polation, if possible, would indicate astronomically high molecular weights. A treatment based on a model system has been put forward by Altgelt and Schulz<sup>106</sup> for rubber microgel and for polyvinyl chloride Kratochvíl<sup>107</sup> proposed a model having a scattering pattern identical with that of the system studied. This model is a two-component one comprising a large weight fraction of small (cf.  $\lambda$ ) particles and a small proportion by weight of very large particles. The overall scattering function was expressed in terms of the constituent ones and the approximation was made that  $P(\theta) \approx 1$  for the small molecularly dissolved particles displaying normal behaviour. The curvature of experimental points at low angles accords well with the angular dependence for the suggested model. Moreover, it is often just feasible<sup>30, 108</sup> to obtain the value of  $M$  by extrapolation from readings relating to moderate-high angles (Fig. 25). Aggregation at normal temperatures may be evidenced by LS and disruption of this by heating<sup>109</sup> (Fig. 26) frequently restores the plot to its normal form. In Fig. 25 the polymer is a rather low molecular weight sample of polyvinyl chloride for which the value of  $(Kc/R_\theta)$  would be expected to remain rather constant. It is seen that this only obtains after heating.

In certain systems the radiation envelope demonstrates that the polymer is not perfectly and molecularly dissolved, and the downward curvature can only be eliminated by very extended dissolution times and/or heating. As noted, this can be adequate, but the scattering envelope may then develop its normal form at the expense of uniformly decreased scattering, which indicates the result of molecular breakdown by hydrolysis, for example. These effects for solutions of nylon-6<sup>110</sup> are illustrated in Fig. 27. In fact it has been shown that molecular dissolution without aggregation, hydrolysis or polyelectrolyte behaviour (see Section V.2) can only be accomplished by the use of a mixed solvent comprising lithium chloride, water and 2,2',3,3' tetrafluoropropanol<sup>111</sup>. In such a system the value of  $M$  for nylons is yielded readily and without ambiguity by LS. A very recent, and hence less commonly appreciated, effect is that of possible cryogenic degradation of polymers in solution<sup>112, 113</sup>. For example, polystyrene ( $M = 7.3 \times 10^6$ ) in *p*-xylene is reduced in molecular weight to  $2.3 \times 10^6$

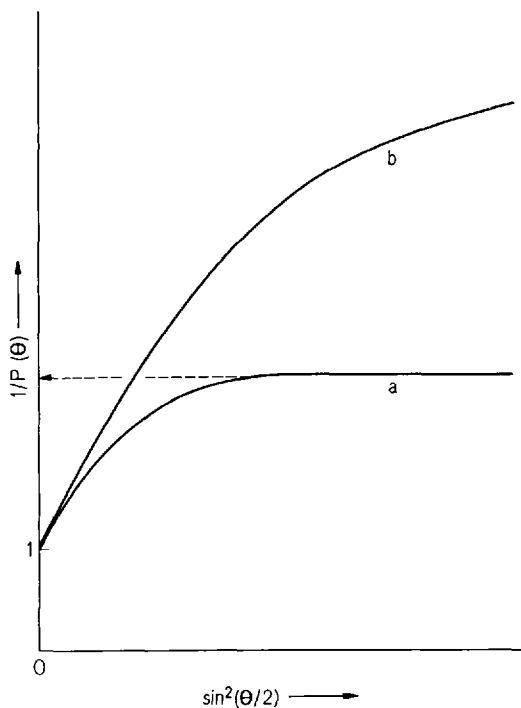


Fig. 25. Typical forms of reciprocal particle scattering functions for systems containing supermolecular structure<sup>30, 108</sup>: (a) small individual macromolecules and a small amount of supermolecular structure sometimes allowing extrapolation to unity (and hence  $I/M$ ) from moderate – high  $\theta$ , as indicated, (b) large individual macromolecules or small individual macromolecules but high content of supermolecular structure

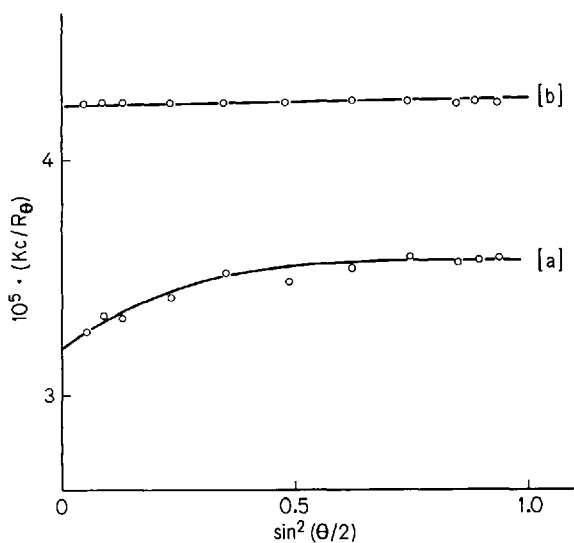


Fig. 26. LS plots for polyvinyl chloride ( $M = 28 \times 10^3$ ) at a concentration  $c = 5 \times 10^{-3}$  g/ml in cyclohexanone, (a) before heating, (b) after heating. The sample loses dissymmetry on heating<sup>109</sup>

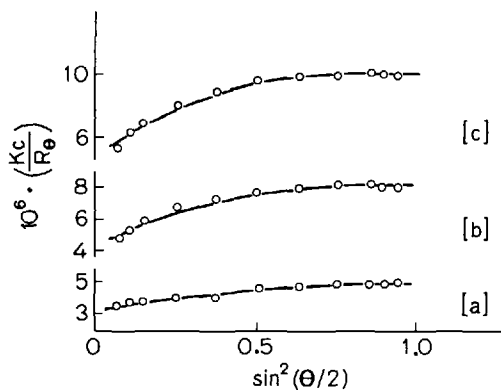


Fig. 27. LS plot for nylon-6 at a concentration  $c = 4 \times 10^{-3}$  g/ml in 90% formic acid containing 1.0 M KCl: (a) without heating, (b) 7 hr. at  $70^\circ\text{C}$ , (c) 12 hr. at  $70^\circ\text{C}$ . Intensity of LS decreases on heating<sup>110)</sup>

after a large number of freezing cycles. This effect is not noted if the initial molecular weight of the polymer is smaller ( $< 2 \times 10^6$ ).

Upward curvature at low angles (that is, decreased scattering) has been observed for solutions of polyvinyl carbanilate<sup>114)</sup> (Fig. 28). This was interpreted as being due to interparticle scattering emanating from ordering of the solution, which is broken down at high temperature. According to measurements at high temperature and in other solvents, the abnormal data at room temperature can yield the correct molecular weight, if extrapolation is conducted on data for high angles only.

Multimerisation as an intermolecular process is accompanied by a change in particle mass and the process can thus be studied *via* the concentration dependence

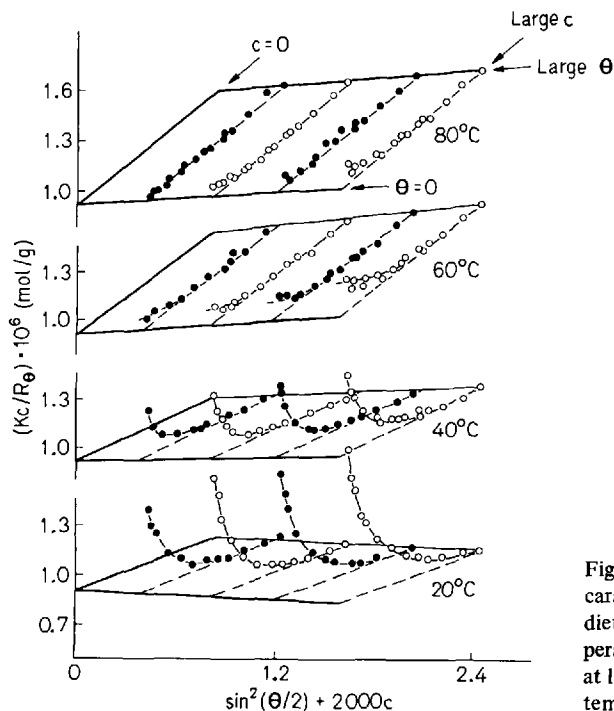


Fig. 28. Zimm plots for polyvinylcarbanilate ( $M = 1.1 \times 10^6$ ) in diethyl ketone at different temperatures. The upward curvature at low angles is absent only at high temperature<sup>114)</sup>

of the apparent molecular weight<sup>115</sup>). An apparent molecular weight in this context is the molecular weight calculated from experimental data at final concentrations using an equation valid for infinite dilution only. The helical aggregation in dioxan of poly- $\gamma$ -benzyl-L-glutamate has thus been elucidated by LS<sup>116</sup>). The various types of aggregation which may be studied by LS have been classified and reviewed in great detail by Elias<sup>115</sup>). The work of Sund and Markau<sup>117</sup>) places a greater emphasis on biopolymers.

In certain instances the value of  $M$  may be required for a polymer which is not accessible in the sense that isolation and dissolution prior to LS measurements would either not be possible or would alter the nature of the polymer. Two examples may be quoted:

Polyimides are thermally stable, heterocyclic aromatic materials of desirable engineering properties. They are, however, insoluble. A typical mode of preparation<sup>118, 119</sup>) is given in Fig. 29 where reactants (a) as well as the polyamic acid or pyrnone prepolymers (b) are maintained in solution.

Ring closure without change in chain length occurs in the stage (b)  $\rightarrow$  (c). LS is conducted directly on solution (b) as formed and the value of  $M$  may be identified with the desired molecular weight of (c) making a small corrective allowance for the elements of water involved in the cyclisation stage. Due to fluorescence and absorption it is often necessary to operate at  $\lambda_0 = 633 \text{ nm}$  (red laser) for such solutions.

Anionic polymerisation of hydrocarbon monomers is initiated by lithium butyl to produce a living polymer the association number of which in solution is required to elucidate the kinetics. When the living polymer (for example polystyryl lithium) is terminated, the polystyrene can be isolated and a solution then made to determine its molecular weight,  $M$ . If the living polymer is associated in solution, the ratio of its

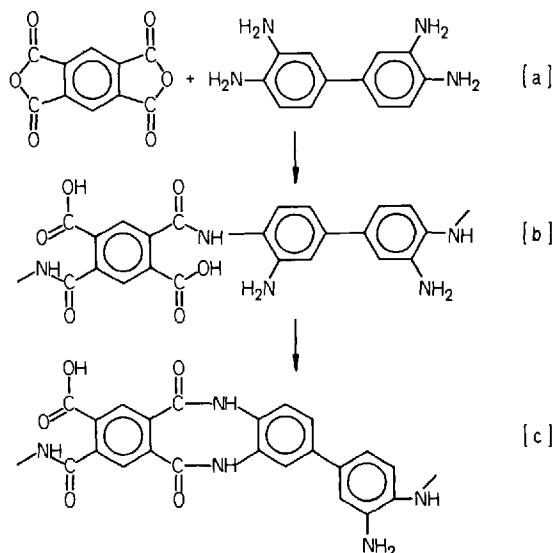


Fig. 29. Preparation of insoluble cyclised polyimide (c) from soluble reactants (a) and soluble intermediate (b). LS is measured directly on solution (b), containing polymer of the same chain length as that of the polyimide<sup>118, 119</sup>)

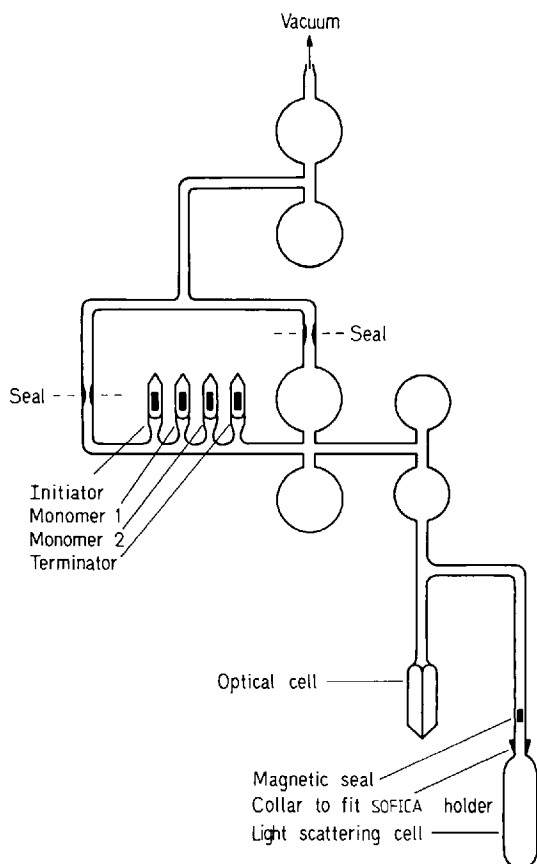


Fig. 30. Apparatus for purifying and manipulating reactants under high vacuum in order to prepare solutions of block copolymers via anionic polymerisation. Concentrations are determined spectrophotometrically in the optical cell and LS is measured on the solution in the Sofica cell<sup>120)</sup>

molecular weight to  $M$  gives the association number. The preparation, LS measurements and estimation of concentrations necessitate high vacuum conditions as indicated in the apparatus of Worsfold and Bywater<sup>120)</sup> (Fig. 30). In addition to the difficult experimental technique involved there is also a problem regarding the determination of molecular weights for some of these systems by LS. For polystyryl lithium (PS-Li) the use of cyclohexane as solvent at 35 °C constitutes thermodynamically ideal conditions so that  $A_2 = 0$  and the molecular weight is obtained readily by extrapolation according to Eq. (36). With the same solvent and temperature for solutions of polyisoprenyl lithium (PI-Li) and polybutadienyl lithium (PBD-Li), however, extrapolation is uncertain due to the presence of finite virial coefficients since the conditions are no longer thermodynamically ideal. In fact there are no thermodynamically ideal solvents for these polymers, which are suitable media for anionic polymerisation also. The problem was overcome by adding a little isoprene or butadiene to the living polymer PS-Li. From the standpoint of associative capacity the products are characteristic of PI and PBD. Moreover since they comprise predominantly PS, they behave thermodynamically as this polymer, that is,  $A_2 = 0$  in cyclohexane at 35 °C and their molecular weights are obtained readily. By this means an association number of 4 has been found for PI-Li and for PBD-Li; the value for PS-Li is 2.



Table 8. Survey of existing complex solvents for cellulose<sup>1 2 2)</sup>

Solvent	Formula	Designation	Characteristics
Cuprammonium hydroxide	$[\text{Cu}(\text{NH}_3)_4](\text{OH})_2$	Cuoxam	Good solvating properties, extensive oxidative degradation <sup>1)</sup> , rather unstable, clear, coloured (blue)
Cupriethylene diamine hydroxide	$[\text{Cu}(\text{en})_2](\text{OH})_2$	Cuen and CED	Good solvating properties, extensive oxidative degradation, rather unstable on storage, clear, coloured (blue)
Tri-ethylene diamine Cobalt hydroxide	$[\text{Co}(\text{en})_3](\text{OH})_2$	Cooxen	Good solvating properties, extensive oxidative degradation, coloured (claret)
Tri-ethylene diamine nickel hydroxide	$[\text{Ni}(\text{en})_3](\text{OH})_2$	Nioxen	Good solvating properties, extensive oxidative degradation, coloured (violet)
Iron - tartaric acid - sodium complex solution	$[(\text{C}_4\text{H}_3\text{O}_6)_3\text{Fe}]\text{Na}_6$	EWNN	Good solvating properties, extremely high salt concentration, slight oxidative degradation, coloured (green)
Tri-ethylene diamine zinc hydroxide	$[\text{Zn}(\text{en})_3](\text{OH})_2$	Zincoxen	Questionable solvating power, stable only at low temperatures, slight oxidative degradation, colourless
Tri-ethylene diamine cadmium hydroxide	$[\text{Cd}(\text{en})_3](\text{OH})_2$	Cadoxen and Cden <sup>3)</sup>	Good solvating properties, slight oxidative degradation, clear, stable and colourless

<sup>1)</sup> Degradation characteristics of the various solvents taken from Ref. 1 2 3).

<sup>2)</sup> (en) denotes ethylenediamine.

<sup>3)</sup> Proposed as a further abbreviation of cadoxen, analogous to Cuen.

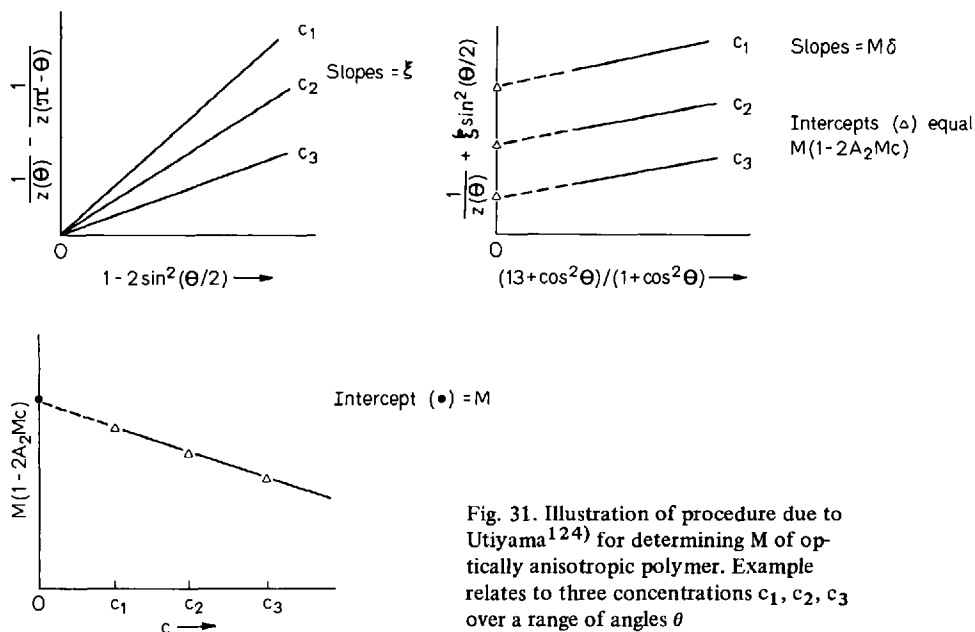


Fig. 31. Illustration of procedure due to Utiyama<sup>124)</sup> for determining  $M$  of optically anisotropic polymer. Example relates to three concentrations  $c_1, c_2, c_3$  over a range of angles  $\theta$

Table 9. LS results for fractions of isotactic polystyrene in chlorobenzene.  $M^*$  denotes apparent molecular weight obtained directly,  $\delta$  is the anisotropy parameter and  $M$  is the molecular weight obtained after correcting for anisotropy *via* the method of Utiyama<sup>124)</sup>

Fraction No	$M^* \times 10^{-5}$	$\delta \times 10^3$	$M \times 10^{-5}$
F-2	4.63	1.78	4.03
F-3	5.99	3.13	5.75
F-4	4.13	53.3	3.41
F-5	2.29	8.34	2.18

The inherently limited solubility of certain (but fortunately, few) polymers poses problems with regard to measurements of both LS and  $\nu$ . Thus, poly-L-lactic acid is soluble at room temperature in only a few liquids such as chloroform, m-cresol and dichloroacetic acid, but the values of  $\nu$  are very small. Limited solubility in bromobenzene is exhibited at temperatures above 50 °C and LS has been conducted at 85 °C to determine molecular weights<sup>121)</sup>. However, even under these conditions, the solubility does not exceed 0.8 g/dl and the moderately acceptable magnitude of  $\nu$  ( $= -0.06$  ml/g) is subject to a quoted error of  $\pm 0.002$  ml/g resulting in a possible error of ca.  $\pm 7\%$  in  $M$  even before any LS measurements. There are no simple solvents for cellulose and the complex ones usually employed are coloured and/or unstable. The most satisfactory one for LS has been found<sup>122)</sup> to be Cadoxen (see Table 8). Mixed solvents (Section V.1) frequently offer the only satisfactory means of achieving solubility and the phenomenon of co-solvency is beginning to be investigated

more fully. Thus a polymer may dissolve in a binary mixture both components of which are individually non-solvents.

Anisotropy in polymer solutions is rather rare, but, where it occurs, the effect on the derived molecular weight can be large enough to warrant appropriate corrections. The procedures have been developed by Utiyama<sup>124)</sup> and by Utiyama and Kurata<sup>125)</sup>. Without a polariser or analyser the normal reciprocal scattering function  $Kc/R_\theta$  can be measured. It is denoted by  $Z(\theta)$  the form of which contains an anisotropy parameter  $\delta$  which is a function of the number of optically anisotropic elements and the principal polarisabilities in the chain:

$$1/Z(\theta) = M(1 - 2 A_2Mc) - \xi \sin^2(\theta/2) + M\delta (13 + \cos^2\theta)/(1 + \cos^2\theta) \quad (81)$$

where<sup>a)</sup>

$$\xi \equiv M\tilde{\mu}^2 \langle s^2 \rangle (1 - 4 A_2Mc)/3 \sin^2(\theta/2) \quad (82)$$

Formulation of the corresponding expression in terms of the angle  $(180 - \theta)$  and subtraction from Eq. (81) yields

$$1/Z(\theta) - 1/Z(180 - \theta) = \xi [1 - \sin^2(\theta/2)] \quad (83)$$

Hence for each concentration, separate plots of the left-hand-side of Eq. (83) give lines of slope equal to  $\xi$ . From Eq. (82) it is evident that the slope decreases with increase in  $c$ . Insertion of the values of  $\xi$  thereby derived into Eq. (81) and re-arrangement yield

$$1/Z(\theta) + \xi \sin^2(\theta/2) = M(1 - 2 A_2Mc) + M\delta (13 + \cos^2\theta)/(1 + \cos^2\theta) \quad (84)$$

Since the left-hand-side of Eq. (84) is now known for each concentration, it may be plotted versus  $(13 + \cos^2\theta)/(1 + \cos^2\theta)$  to yield lines of intercept equal to  $M(1 - 2 A_2Mc)$  and slope equal to  $M\delta$ . When these intercepts and now plotted against concentration, the resultant intercept at infinite dilution is  $M$ . Because  $M$  has been evaluated, the magnitude of  $\delta$  is also known. These procedures are outlined schematically in Fig. 31. In Table 9 are assembled some data of Utiyama<sup>124)</sup> for solutions of isotactic polystyrene in chlorobenzene. For samples having finite values of  $\delta$ , the discrepancy between the true corrected molecular weight and the uncorrected one (termed "apparent" in this context) can be quite considerable, amounting to 24% for one sample. Another procedure due to Utiyama<sup>124)</sup> may be referred to. This consists of using polarised incident light to evaluate  $\delta$ .

The feasibility of obtaining not only  $M$  but also  $\bar{M}_n$  from a single set of LS measurements is an inherently attractive proposition. The procedure is based on the

<sup>a)</sup> The symbols  $\xi$ ,  $\xi_1$ ,  $\xi'$  and  $\xi''$  appear in this article as abbreviations for complex expressions. The exact forms of these expressions are mostly omitted, but may be found in the appropriate quoted references. It should be stressed, however, that these abbreviations have totally different connotations in different parts of the text.

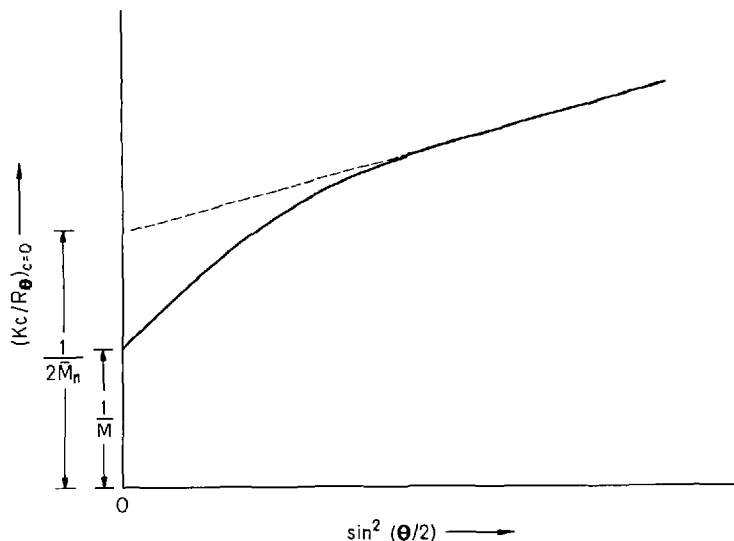


Fig. 32. Molecular weights obtainable in principle from the angular dependence of LS by linear Gaussian coils

asymptotic (rather than initial) behaviour of the particle scattering function  $P(\theta)$  at infinite dilution, which yields finally:

$$\lim_{c \rightarrow 0} (Kc/R_\theta) = (1/2 \bar{M}_n)(1 + \langle s^2 \rangle_n \tilde{\mu}^2) \quad (85)$$

For a fixed wavelength the variable  $\tilde{\mu}^2$  is equivalent to  $\sin^2(\theta/2)$  and hence at high angles the left-hand-side of Eq. (85) should be a linear function of  $\sin^2(\theta/2)$ , yielding an intercept of  $1/2 \bar{M}_n$  at zero angle. The non-asymptotic region, that is, the initial linear part at lower angles yields an intercept of  $1/M$  as previously noted. Figure 32 illustrates the mode of obtaining  $M$  and  $\bar{M}_n$  in principle. This analysis may be applied only if two prerequisites are fulfilled: (a) all the dissolved polymer molecules are linear Gaussian coils and (b) the dimensions of the molecules are such that for all of them it is possible to measure the initial and the asymptotic regions. Benoit *et al.*<sup>126)</sup> showed for molecules of small-moderate dimensions the asymptotic region is not attainable within the normal angular range of  $\theta = 30^\circ - 150^\circ$ . Moreover, if the dimensions are exceedingly high, the entire experimentally accessible set of data lies in the asymptotic region and it is the initial region which is beyond reach. The procedures and precautions necessary when interpreting the asymptotic behaviour of  $1/P(\theta)$  have been discussed by Kratochvíl<sup>30)</sup>.

For solutes comprising thin rod-like molecules the analysis of Holtzer<sup>127)</sup> for the asymptotic reciprocal scattering function yields:

$$\lim_{c \rightarrow 0} (Kc/R_\theta) = (2/\pi^2 \bar{M}_n) [1 + (\pi \bar{L}_n/2) \tilde{\mu}] \quad (86)$$

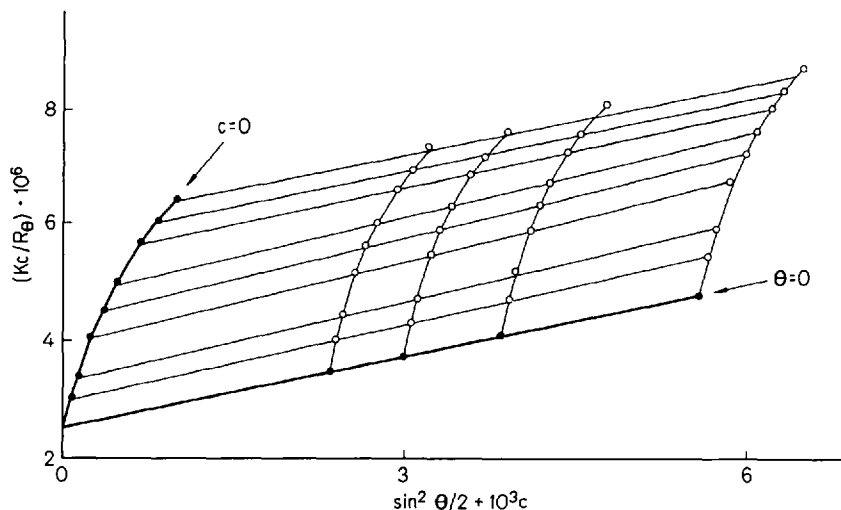


Fig. 33. Zimm plot<sup>128)</sup> for a sample of poly- $\gamma$ -benzyl-L-glutamate in dimethyl formamide at 25 °C

where  $\bar{L}_n$  is the number average length of the rod. We note here that the variable is  $\mu$  and hence the left-hand-side of Eq. (86) should be a linear function of  $\sin(\theta/2)$  and not of  $\sin^2(\theta/2)$ . The intercept at zero angle should yield  $2/\pi^2 \bar{M}_n$ . The synthetic polypeptide poly- $\gamma$ -benzyl-L-glutamate (PBLG) adopts a random coil configuration in dichloroacetic acid, but is helical or rod-like in many solvents such as dimethyl formamide and chloroform. In Fig. 33 the conventional Zimm diagram is shown for

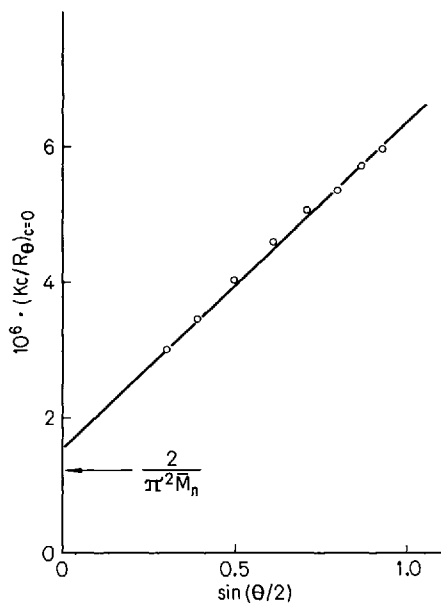


Fig. 34. Plot<sup>128)</sup> according to Eq. (86) for sample in Fig. 33

a PBLG sample in dimethyl formamide<sup>128</sup>). The initial region of the angular dependence is linear and its intercept is identical with that of the extrapolated line for  $\theta = 0$ . The resultant value of  $M$  is  $4.1 \times 10^5$ . However, the curvature of  $(Kc/R_\theta)_{c=0}$  versus  $\sin^2(\theta/2)$  is evident at high angles. The plot<sup>128</sup>) according to Eq. (86) is shown in Fig. 34 and from the intercept a value of  $1.40 \times 10^5$  is derived for  $\bar{M}_n$ . This agrees reasonably with the value of  $1.62 \times 10^5$  obtained by direct osmotic pressure measurements on the sample.

On the other hand, Cassassa and Berry<sup>32, 129</sup>) conclude from their LS measurements on rod-like fibrinogen in solution that Eq. (86) is followed very well, but the intercept is extremely small or effectively zero. A rather trivial change in the model can be shown to produce a theoretical intercept of zero. Accordingly, they consider that the asymptotic scattering data reveal nothing about  $\bar{M}_n$  but do give information from the slope on the ratio  $\bar{L}_n/\bar{M}_n$ .

In this brief survey on molecular weights of polymers emphasis has been laid on abnormal behaviour and difficulties, which do not of course constitute the norm.

#### 4. Ultra-high Molecular Weight Macromolecules

Provided the specific refractive index increment is large, solutions of ultra-high molecular weight polymers ( $M > \text{ca. } 3 \times 10^6$ ) do not necessitate that the highest

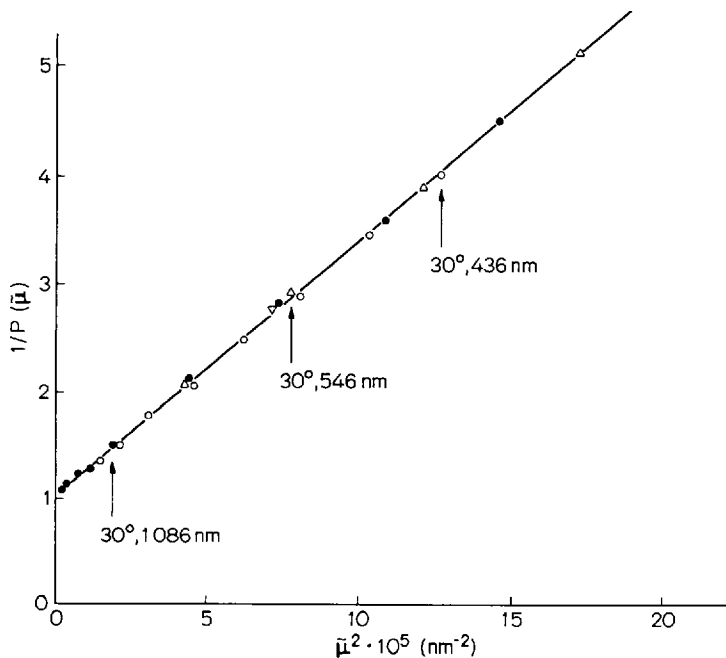


Fig. 35. Reciprocal particle scattering function<sup>60</sup>) as a function of  $\mu^2$  for polystyrene of  $M = 13.8 \times 10^6$ . Different symbols distinguish different LS photometers (Fica – 50 at 436 nm, low angle photometer at 436 nm and near IR photometer of Burmeister and Meyerhoff at 1086 nm)

concentrations be greater than ca.  $1 \times 10^{-3}$  g/ml for LS measurements. Meyerhoff and Burmeister<sup>60</sup> have made a comparative study of the implementation of visible and near IR wavelengths in the determination of such molecular weights. It will be recalled [cf. Eq. (39)] that at infinite dilution the value of  $Kc/R_\theta$  differs from  $1/M$  by a factor  $1/P(\tilde{\mu})$  or, as more usually expressed,  $1/P(\theta)$ . This factor in turn is greater than unity by an amount  $(\tilde{\mu}^2/3)\langle s^2 \rangle$  and hence will be of considerable magnitude for polymers of large dimensions. Nonetheless, even if  $\langle s^2 \rangle$  is large, extrapolation of  $(\tilde{\mu}^2/3)\langle s^2 \rangle$  to zero yields  $1/M$ . The facility for obtaining very low angle data on the

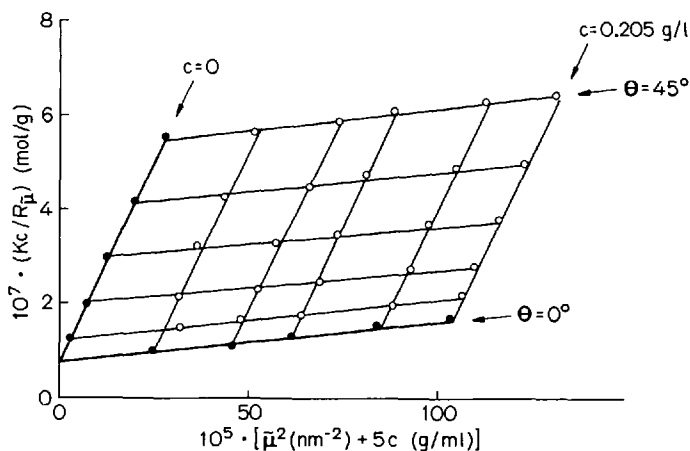


Fig. 36. LS plot<sup>60</sup> in terms of  $\tilde{\mu}$  for sample indicated in Fig. 35. ( $\lambda_0 = 436$  nm)

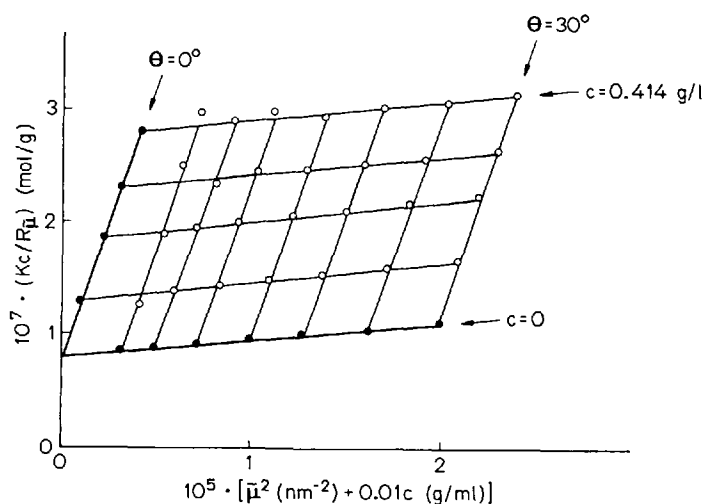


Fig. 37. LS plot<sup>60</sup> in terms of  $\tilde{\mu}$  for sample indicated in Fig. 35. ( $\lambda_0 = 1086$  nm)

instrument is crucial in this respect and so also is the alternative expedient of rendering  $\tilde{\mu}^2$  small with high wavelength incident radiation. Figure 35 illustrates<sup>60)</sup> how  $1/P(\tilde{\mu})$  approaches a value of unity more rapidly for near IR light than for visible wavelengths. The data relate to a solution of a very high molecular weight polystyrene sample having  $\langle s^2 \rangle = 7.02 \times 10^4 \text{ nm}^2$ . The actual Zimm plots for determining  $M$  are shown<sup>60)</sup> in Figs. 36 and 37 for  $\lambda_0 = 436 \text{ nm}$  and  $1086 \text{ nm}$  respectively. A more accurate extrapolation is afforded in the latter situation, since for it a minimal value of only  $3 \times 10^{-6} \text{ nm}^{-2}$  is reached experimentally, for  $\tilde{\mu}^2$  (at  $c = 0$ ) compared with a much larger value of  $30 \times 10^{-6} \text{ nm}^{-2}$  for the same quantity when  $\lambda_0 = 436 \text{ nm}$ . Using near IR incident light, molecular weights have been obtained with minimal uncertainty in extrapolation for PS ( $M = 7 \times 10^6, 13.6 \times 10^6$  and  $39.3 \times 10^6$ ) as well as for cellulose trinitrate<sup>60)</sup> from the alga *Valonia* ( $M = 9 \times 10^6$ ).

An alternative mode<sup>31)</sup> of extrapolating  $1/P(\tilde{\mu})$  to unity is to conduct experiments with light of different wavelength and to extrapolate  $\tilde{\mu}$  to zero at  $\lambda_0 = \infty$ . In this procedure the value of  $\langle s^2 \rangle$  for the sample is constant and  $\theta$  is fixed (e.g. at  $90^\circ$ ) for all experiments. An example<sup>31)</sup> is given in Fig. 38. The resultant value of  $M = 2.8 \times 10^6$  compares well with values lying between  $2.7 \times 10^6$  and  $2.9 \times 10^6$  obtained from six separate determinations *via* Zimm plots in which  $\theta$  is varied and  $\lambda_0$  maintained constant at 365, 436, 488, 546, 578, and 1078 nm.

In contrast to these systems, bacterial suspensions demand the use of near IR incident light as an absolute necessity rather than for preference. Such suspensions require maximum concentrations of the order of only  $3 \times 10^{-6} \text{ g/ml}$ . They scatter light enormously but the relative size parameter exceeds the limits demanded by

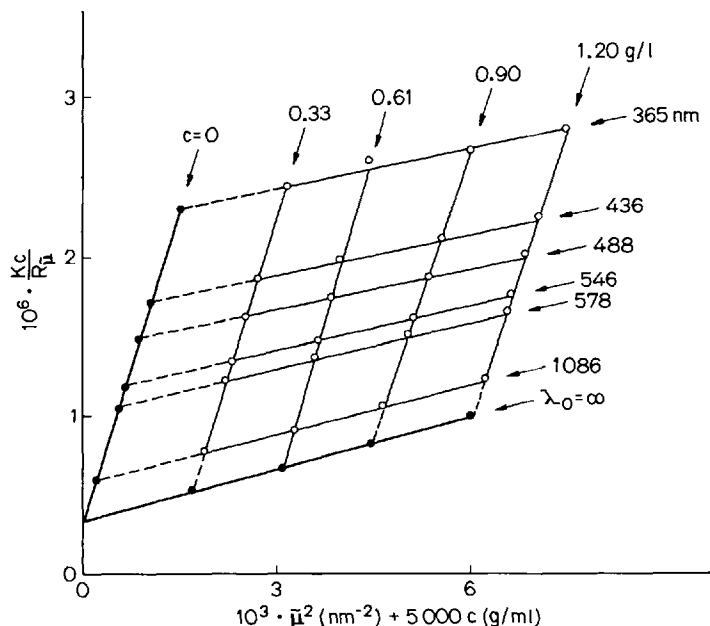


Fig. 38. LS plots<sup>31)</sup> for high molecular weight polystyrene ( $M = 2.8 \times 10^6$ ) at a fixed angle ( $90^\circ$ ) and variable wavelength



Rayleigh-Debye scattering when visible light is used. The angular scattering profile (cf. Fig. 1) exhibits oscillations and precludes the possibility of obtaining a Zimm diagram. Since bacteria are generally neither spherical nor monodisperse, analysis *via* Mie theory is not possible. With the use of near IR incident light<sup>18, 130</sup> the value of  $\lambda_0$  is increased so as to approximately halve the relative size parameter with respect to its value with visible light.

## V. Multicomponent Systems

Many biopolymeric systems such as nucleic acid solutions (except for rare exceptions) always contain additional low molecular weight salts or buffer components. Consequently, they constitute multicomponent or mixed solvent systems. Similar considerations apply to solutions of polyelectrolytes and neutral polymers, since there are often compelling reasons for adding another component. For example, the ionisation of poly-N-n-butyl-4-vinyl pyridinium bromide is suppressed by the addition of KBr to the aqueous solution. Moreover, some polymers do not dissolve molecularly in single solvents, but true molecular solutions can be achieved by using solvent mixtures. The requirement of a certain quality of the solvent medium (*e.g.* thermodynamic interaction with dissolved polymer or a particular refractive index) is attainable much more readily with mixed than with single solvents. The complications in interpreting LS obtained with such multicomponent systems have been reported and reviewed<sup>4, 14, 15, 72</sup>.

### 1. Mixed Solvents

Essentially, the complex behaviour emanates from the fact that the scattering entity no longer consists of the dissolved molecule alone but of this molecule with some molecules of the selectively adsorbed solvent and of the selectively desorbed other solvent. This selective adsorption is quantified by a coefficient  $\gamma_1$  for selective adsorption of solvent-1 (the other constituent of the mixed solvent being solvent-3). This is defined in rigorous thermodynamic terms as the change in molality  $dm_1$  of component-1 caused by changing the polymer (subscript-2) concentration by an amount  $dm_2$  with the chemical potential  $\mu$  of all low molecular weight components remaining constant, viz

$$\gamma_1 = \left( \frac{\partial m_1}{\partial m_2} \right)_{\mu}$$

If  $\gamma_1$  is positive, component-1 is selectively adsorbed on the polymer and if polymer is added to the system, the concentration of component-1 must also be increased, if the activity of component-1 is to remain constant. A helpful schematic illustration has been provided by Kratochvíl<sup>131</sup> and is shown in Fig. 39. The example relates to a binary solvent composition of 1 : 1 for the bulk solvent 1 – solvent 3 mixture.

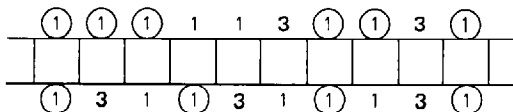


Fig. 39. Selective adsorption to a polymer chain from a bulk solvent medium comprising an equimolar mixture of liquid 1 and liquid 3. Only molecules of liquid 1 (circled) in excess of the equimolar ratio in the solvated shell are part of the selective adsorption complex<sup>131)</sup>

Every segment in the polymer chain is solvated by two solvent molecules. Those molecules of solvents 1 and 3 in the solvated sheath which correspond to the bulk composition of 1 : 1 are disregarded. Only those molecules of solvent 1 in the solvated sheath in excess of this 1 : 1 ratio constitute what may be regarded as the complex with the polymer. In this particular example the value of  $\gamma_1$  is 1 mol of solvent-1 per mol of segment. If the molar volumes of liquid-1 and polymer segment were equal, the coefficient of selective adsorption could also be expressed here as 1 ml of liquid-1 per ml of monomer units.

The coefficient  $\gamma_1$  (or  $\gamma_3$ ) is easy to visualise physically. It is derived readily from an equivalent coefficient  $\lambda'_1$  which is expressed as ml of liquid-1 preferentially adsorbed per g of polymer<sup>72, 132)</sup>:

$$\lambda'_1 = \gamma_1 \bar{V}_1 / M_2 \quad (87)$$

where the partial molar volume  $\bar{V}_1$  of liquid-1 may be approximated to the molar volume  $V_1$ . The true molecular weight of the polymer is  $M_2$ . A comparison of the relevant scattering equations for a polymer in a single and in a binary solvent reveals<sup>72, 132)</sup> that the molecular weight afforded in the latter instance is an apparent value only,  $M_2^*$  viz

$$M_2^* = M_2 \left[ 1 + \lambda'_1 \left( \frac{d\tilde{n}_0}{d\phi_1} \right) / \left( \frac{d\tilde{n}}{dc} \right) \right]^2 \quad (88)$$

In Eq. (88),  $d\tilde{n}_0/d\phi_1$  expresses how the refractive index  $\tilde{n}_0$  of the binary solvent alone varies with its composition expressed as volume fraction  $\phi_1$  of liquid-1. Clearly, if liquids 1 and 3 are iso-refractive or nearly so, then  $M_2^* = M_2$ , that is, a LS experiment will yield the true molecular weight irrespective of the composition of the mixed solvent. This situation is exemplified<sup>133)</sup> by the system polystyrene (2)-ethylacetate (1)-ethanol (3) for which the molecular weight in mixed solvents of different  $\phi_1$  is the same as that obtained in pure ethylacetate (Fig. 40). The values of  $d\tilde{n}_0/d\phi_1$  for the mixed solvents are only of the very small order of ca. 0.01, whilst the values of  $d\tilde{n}/dc$  for the polymer solutions are large (ca. 0.22 ml/g).

It should be noted that  $d\tilde{n}_0/d\phi_1$  is generally not zero and moreover its finite value may be positive or negative. Accordingly, the apparent molecular weight obtained experimentally can be equal to  $M_2$ , less than  $M_2$  or greater than  $M_2$ . Also the binding or selective adsorption coefficient, previously considered to be constant, is now known<sup>132)</sup> to vary with molecular weight, the departure from constancy being manifested by a sharp increase at low M. Although the usual object of these studies is to quantify the selective binding of a particular component, other methods are

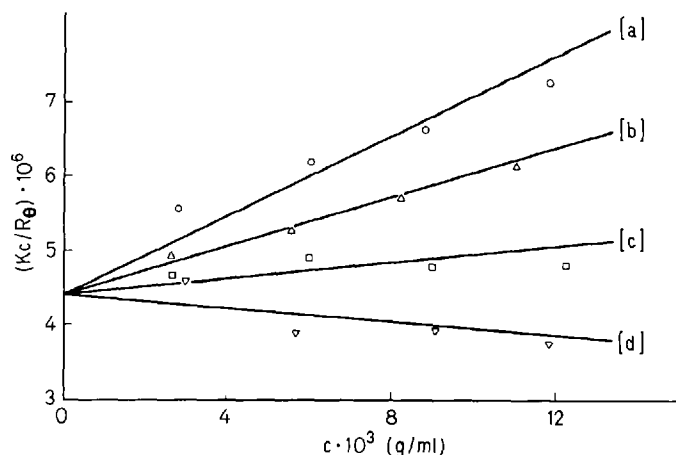


Fig. 40. LS plots for polystyrene in mixed solvents<sup>133)</sup> comprising the following % (vol./vol.) of ethanol in admixture with ethyl acetate: (a) 0, (b) 5.19, (c) 8.24, (d) 10.66

Table 10. Typical values of the selective adsorption coefficient  $\gamma$ , as expressed as the ratio of the apparent ( $M^*$ ) to true ( $M$ ) molecular weight for polymer – mixed solvent systems<sup>131)</sup>

Type of polymer	Specification of system	Typical $M^*/M$
Non-ionic	Medium $\gamma$	1.1–1.3
Non-ionic	Large $\gamma$	3–10
Polyelectrolyte	Equal counterions	1.1–1.3
polyelectrolyte	Different counterions	2–3

available to determine  $\lambda'_1$  such as differential refractometry and densimetry on dialysed and undialysed solutions. Hence the resultant independent value of  $\lambda'_1$  can be combined with  $M_2^*$  in Eq. (87) to yield the true molecular weight  $M_2$ . Full details of these two independent procedures have been reported<sup>134)</sup>. Table 10 due to Kratochvíl<sup>131)</sup> gives a rough indication of the magnitude of selective adsorption effects for different types of systems.

Equation (88) is the expression used commonly for solutions of synthetic polymers, but, where the nature of adsorption and binding is of critical interest, alternative forms exist. These differ mainly in the modes of expressing concentration (e.g. activity, molality, molarity, mass/unit volume). Interrelations among the units and expressions have been presented very clearly by Timasheff and Townend<sup>15)</sup>.

One formulation is

$$\lim_{\theta \rightarrow 0} \left[ K'c_2 \left( \frac{\partial \tilde{n}}{\partial c_2} \right)_{T,p,m_3}^2 / R_\theta \right] = \left[ 1/M_2 (1 + \xi)^2 \right] \left[ 1 + \left( \frac{c_2}{RT} \right) \left( \frac{\partial \mu_2^e}{\partial c_2} \right)_{T,p,m_3} + \left( \frac{\partial \mu_3^e}{\partial c_2} \right)_{T,p,m_3} \left( \frac{\partial m_3}{\partial m_2} \right)_{T,p,\mu_3} + 2. RT (\bar{v}_2)_{T,p,m_2} \right] \quad (89)$$

where

$$\xi = \frac{M_3(1 - c_3\bar{v}_3)_{m_2}}{M_2(1 - c_2\bar{v}_2)_{m_3}} \cdot \left[ \left( \frac{\partial \tilde{n}}{\partial c_3} \right)_{T,p,m_2} / \left( \frac{\partial \tilde{n}}{\partial c_2} \right)_{T,p,m_3} \right] \left( \frac{\partial m_3}{\partial m_2} \right)_{T,p,m_3} \quad (90)$$

$$\left( \frac{\partial m_3}{\partial m_2} \right)_{T,p,\mu_3} = \frac{M_2}{M_3} \left( \frac{\partial g_3}{\partial g_2} \right)_{T,p,\mu_3} = \frac{M_2}{M_3} \frac{(1 - c_2\bar{v}_2)_{\mu_3}}{(1 - c_3\bar{v}_3)_{\mu_2}} \left( \frac{\partial c_3}{\partial c_2} \right)_{T,p,\mu_3}$$

and  $\mu_i$ ,  $\mu_i^e$ ,  $\bar{v}_i$ ,  $m_i$ ,  $M_i$  denote respectively chemical potential, excess chemical potential, partial specific volume, molality and molecular weight of species  $i$ . In Eq. (90) one measures the specific refractive index increment with respect to the concentration of component-2, keeping the molality of component-3 constant. An aqueous solution of a protein as component-2 could have urea, a salt or an added organic liquid as component-3. The expression, just as that leading to Eq. (88), has an important consequence, namely; when light scattering data at  $(\theta = 0)$  are plotted against concentration of protein in the normal manner, the intercept at  $c_2 = 0$  is not  $1/M_2$ , but is the product of this quantity and  $1/(1 + \xi^2)$ , where  $\xi$  is a complicated expression, but essentially measures the interaction of component-3 with the protein. Rather surprisingly, the magnitude and sign of the interaction term turn out to be functions of the concentration units employed. Thus the same system may appear to exhibit preferential adsorption of salt in protein with the molal or g/g scale, but selective desorption when measured on the molar or mol/ml scale.

Figure 41 illustrates the situation for a solution comprising water, bovine serum albumin and 6 M guanidine hydrochloride (GHC1) as components 1, 2 and 3 respectively<sup>15)</sup>. The molecular weight  $M_2^*$  appears as 38 000 if the molarity of GHC1 is kept: identical in solution and solvent, whereas it is 103 000 when the molality of GHC1

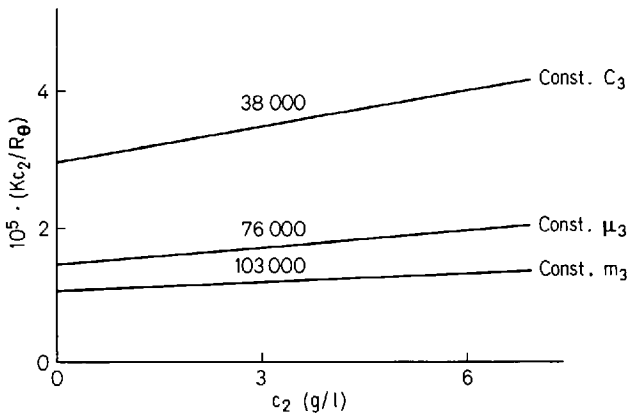


Fig. 41. LS plots for solutions of bovine serum albumin (concentration  $c_2$ ) in aq. 6 M guanidine hydrochloride, obtained at constant molarity  $C_3$ , constant chemical potential  $\mu_3$  and constant molality  $m_3$  of guanidine hydrochloride. The resultant molecular weights yielded for this sample are given above each plot<sup>15)</sup>

### Determination of Molecular Weights by Light Scattering

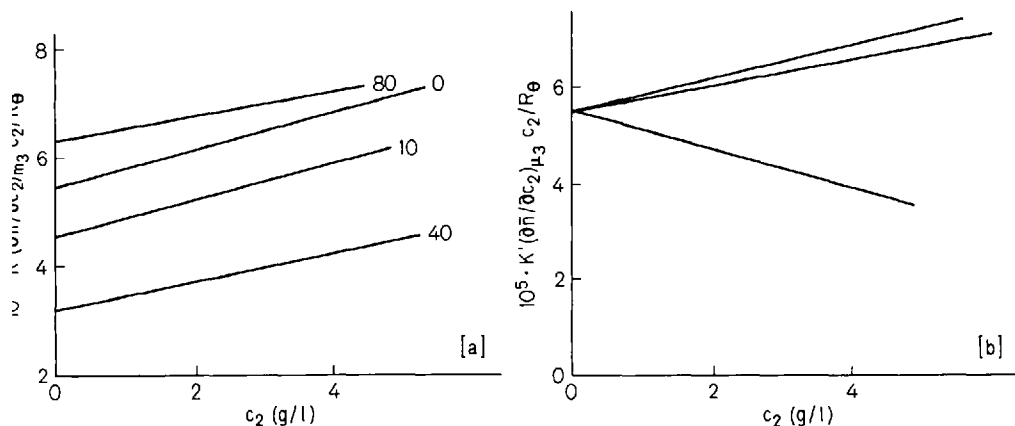


Fig. 42. LS plots for  $\beta$ -lactoglobulin A (concentration  $c_2$ ) dissolved in water/2-chloroethanol mixtures of compositions (% vol./vol. of 2-chloroethanol) indicated in (a). Plots (a) and (b) correspond to constant molality  $m_3$  and constant chemical potential  $\mu_3$  respectively of the organic solvent<sup>135</sup>). The primary data points have been omitted for clarity

is kept constant. Since these molecular weights are respectively less than and greater than the value of 76 000 it is clear from Eq. (89) without detailed analysis that the selective adsorptions will differ in sign and magnitude. The correct molecular weight,  $M_2 = 76\,000$ , is obtained at constant chemical potential of GHC1.

Figures 42 illustrate forcibly how a variety of apparent molecular weights ( $M_2^*$ ) of  $\beta$ -lactoglobulin A is obtained from LS plots in aqueous 2-chloroethanol mixtures of various composition when the molality of the alcohol is kept constant<sup>135</sup>. If the chemical potential of the alcohol is maintained constant, a common intercept yielding the correct molecular weight,  $M_2$ , is obtained for all the solvent mixtures<sup>135</sup>.

The mode of reduction of such systems in pseudo two-component ones is embodied in the following modified expression:

$$\lim_{\theta \rightarrow 0} \left[ K' c_2 \left( \frac{\partial \tilde{n}}{\partial c_2} \right)_{T, \mu_1, \mu_3} / R_\theta \right] = \left( \frac{1}{M_2} \right) \left\{ 1 + \frac{c_2}{RT} \left[ \left( \frac{\partial \mu_2^e}{\partial c_2} \right)_{T, p, \mu_3} + 2RT \bar{v}_2 + 2RT \bar{v}_3 \frac{M_3}{M_2} \left( \frac{\partial m_3}{\partial m_2} \right)_{T, p, \mu_3} \right] \right\} \quad (91)$$

It is fortunate that theory has been extended to take into account selective interactions in multicomponent systems, and it is seen from Eq. (91) (which is the expression used for the plots in Fig. 42b) that the intercept at infinite dilution of protein or other solute does give the reciprocal of its correct molecular weight  $M_2$ . This procedure is a straightforward one whereby one specifies within the constant  $K$  [Eq. (24)] a specific refractive index increment  $(\partial \tilde{n} / \partial c_2)_{T, \mu}$ . The subscript  $\mu$  (a shorter way of writing subscripts  $\mu_1$  and  $\mu_3$ ) signifies that the increments are to be taken at constant chemical potential of all diffusible solutes, that is, the components other than the polymer. This constitutes the osmotic pressure condition whereby only the macromolecule (component-2) is non-diffusible through a semi-permeable membrane. The quantity

$(\partial\tilde{n}/\partial c_2)_{T,\mu}$  is measured as outlined in Section III.2 on solutions which have been allowed to attain dialysis equilibrium. The types of dialyser have been reviewed<sup>40)</sup> and it has been emphasised recently<sup>14)</sup> that it is essential to agitate or mix the polymer solution inside the dialysis bag as well as the mixed solvent outside the bag during the dialysis in order to obtain good results. Reference is especially recommended to authoritative articles on all aspects of the technique<sup>4, 14, 15)</sup>. The procedure for obtaining the correct value of  $M_2$  is not restricted to protein solution of course, and has been employed with synthetic polymers and copolymers.

In certain instances, such as in comparing results involving Na DNA and Cs DNA, it is found preferable<sup>4, 14)</sup> to use equivalent concentrations  $C_u$  (moles of nucleotides or phosphate per litre) instead of weight of polymer per cubic centimetre,  $c_2$ . Equivalent concentration units are invariant to the nature of the counterion of the DNA and, instead of the molecular weight  $M_2$ , it is the number of nucleotides  $Z_2$  per macromolecule which is yielded by LS experiments. If  $M_u$  is the average molecular weight of a paired nucleotide unit in the double helix structure (for example 331 g/mol and 441 g/mol in the Na form and Cs form respectively), then  $M_2 = Z_2 M_u$ . Similarly, the interconversion between the concentration units is  $c_2 = C_u M_u / 10^3$ . The specific refractive index increment is obtained from measurements on solutions of known  $C_u$  and, in the limits of zero angle and zero  $C_u$ , the value of  $Z_2$  is given by:

$$\lim_{\substack{\theta \rightarrow 0 \\ C_u \rightarrow 0}} [K' C_u \cdot 10^3 (\partial\tilde{n}/\partial C_u)_{T,\mu}^2 / R_\theta] = 1/Z_2 \quad (92)$$

The effect of dialysis on the refractive index increment may be illustrated by the following data<sup>14)</sup> for DNA solutions at 25 °C and  $\lambda_0 = 546$  nm:  $d\tilde{n}/dc_2$  in water for NaDNA is 0.179 ml/g; in the presence of 0.2 mol/l NaCl the value of  $(\partial\tilde{n}/\partial c_2)_{T,\mu}$  is 0.168 ml/g.

Sonicated DNA of molecular weight of the order of  $0.5 \times 10^6$  does not present especial difficulties with regard to its molecular weight determination by LS with conventional apparatus. The value of the left hand side of Eq. (92) is only about 10% lower than the value of the quantity under conditions of  $C_u = 0$  and  $\theta = 30^\circ$ . Consequently the necessary extrapolation yielding  $1/Z_2$  is quite short.

However, for high molecular weight samples there is a wide disparity among experimental results; the reasons have been discussed<sup>50)</sup>. Essentially, the difficulties are not unique to this macromolecule and arise from taking readings at insufficiently low angles. (We have referred to this point earlier in Section III.1.) For  $M_2 > ca. 3 \times 10^6$  use of conventional wide angle LS ( $\theta = 30^\circ - 150^\circ$ ) shows there is downward curvature in the scattering envelope below  $\theta = 30^\circ$  resulting in  $M_2$  values which are lower by a factor of at least 2 than those obtained by other methods for high molecular weight DNA samples. Results in the low angle LS range ( $\theta = 10^\circ - 30^\circ$ ) have confirmed the presence of curvature and the magnitude of the error. However, results computed from measurements at  $\theta \geq 10^\circ$  for a monodisperse bacteriophage T7 DNA of  $M_2 = 25 \times 10^6$  were shown to be about 20% too high because of upward curvature in the very low angle region. It is now clear that only very low angle LS data ( $\theta \geq 9^\circ$ ) can be extrapolated linearly to  $\theta = 0$  so as to yield accurate values of  $M_2$ . Table 11 lists<sup>50)</sup> molecular parameters of calf thymus DNA obtained recently

Table 11. Influence of accessible angular range on derived molecular weight and dimensions of Calf-Thymus DNA<sup>50)</sup>

Range of $\theta$ (deg)	$M \times 10^{-6}$ (g/mol)	$(s^2)^{1/2}$ (nm)
6-9	20.0	361
6-24	20.6	486
10-35	23.7	522
30-75	6.38	281

over different angular ranges. The Chromatix instrument offers the almost ultimate relief from extrapolation problems. The plots using this instrument at a fixed angle of  $4.9^\circ$  yield  $M_2 = 25.9 \times 10^6$  for bacteriophage T7 DNA as compared to  $25.5 (\pm 1.0) \times 10^6$  obtained by lengthy sedimentation techniques<sup>136)</sup>. The molecular weights of DNA complexes with a non histone chromosomal protein are found to be of the order of  $100 \times 10^6$ .

## 2. Polyelectrolytes

Polyelectrolytes are long chain molecules bearing ionisable sites. It is not always possible to predict with confidence the extent to which polyelectrolytes behaviour is exhibited. Thus, polyacrylic acid in water is only weakly ionised and in dioxan it behaves as a typical non-electrolyte. It is usual to overcome the complications imposed by ionic interactions by the inclusion of simple salts and LS studies in salt-free solutions are rather rare. The problems have been discussed recently by Kratochvíl<sup>137)</sup>, whilst the review of Nagasawa and Takahashi<sup>138)</sup> constitutes one of the few devoted exclusively to LS from polyelectrolyte solutions. LS from many biopolymers such as proteins is, of course, extremely relevant in this context.

It has been observed by Alexandrowicz<sup>139, 140)</sup> that in salt-free systems the practical osmotic coefficient  $\varphi_p$  rather the molecular weight is actually determined.  $\varphi_p$  is the ratio of the osmotic pressure to the ideal value which would obtain in the absence of electrostatic interactions. The magnitude of  $\varphi_p$  decreases rapidly with increasing charge density. The expression for  $\Pi$  consequently involves  $\varphi_p$  and, since the LS depends on the concentration dependence of  $\Pi$  [cf. Eqs. (34) and (35)], the reduced scattering in terms of  $C_u$ , for example, becomes

$$\lim_{\theta \rightarrow 0} [K' \cdot 10^3 (\partial \tilde{n} / \partial C_u)_{p,T} / R_\theta] = (1/Z_2) (1 + z\varphi_p) \quad (93)$$

where each polymer chain bears  $z$  charges. For highly ionised polyelectrolyte  $z\varphi_p \gg 1$  and the right hand side of Eq. (93) is not  $1/Z_2$  but a quantity much greater than this and the scattering,  $R_\theta$ , is much reduced. This may be seen by comparing the large limiting value of  $Kc/R_\theta$  ( $\approx 10^{-5}$  mol/g) for a polyelectrolyte in a single solvent with the much smaller value ( $\approx 10^{-7}$  mol/g) for the same sample in the

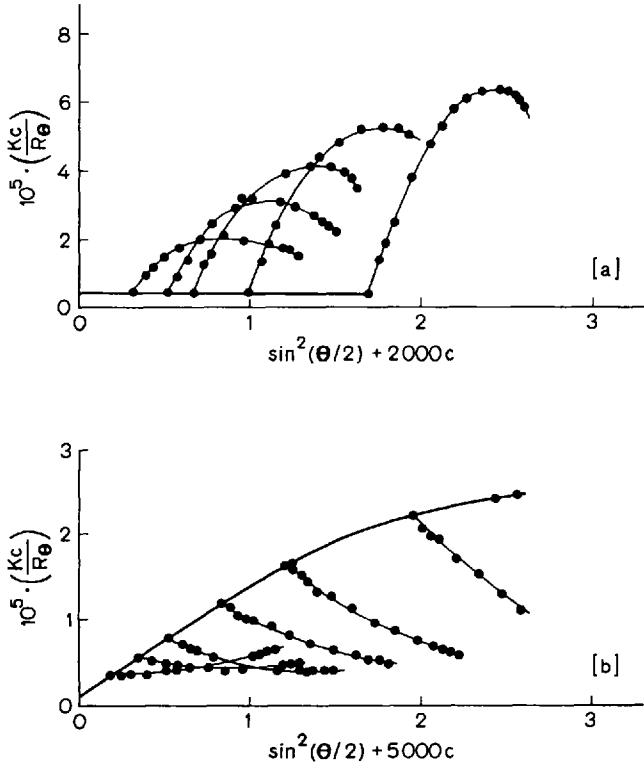


Fig. 43. Zimm diagram<sup>137, 141</sup> for solutions of poly [1 (2-hydroxyethyl pyridinium toluene sulphate methacrylate)] of molecular weight  $1.37 \times 10^6$  in (a) water and (b) methanol. (compare with Fig. 45)

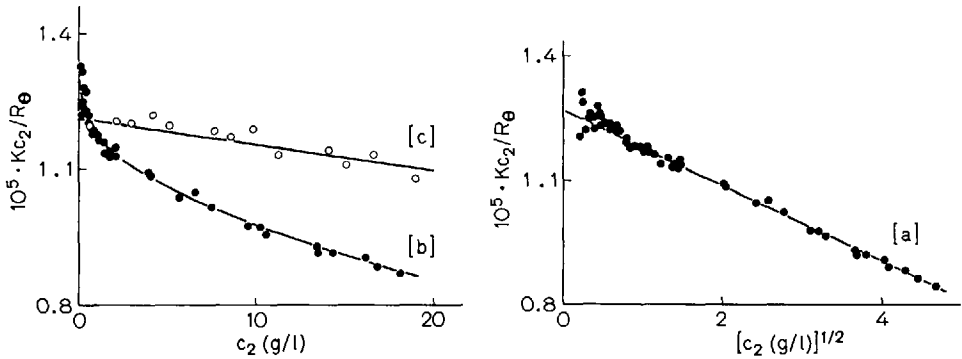


Fig. 44. LS plots<sup>142</sup> for bovine serum albumin in iso-ionic salt free aqueous solution [plot (b)]. Also shown are data (open circles) for solution in 0.001 M NaCl [plot (c)]. Plot (a) is for same data as in (b) plotted against the square root of the bovine serum albumin concentration,  $c_2$ , according to Eq. (94)



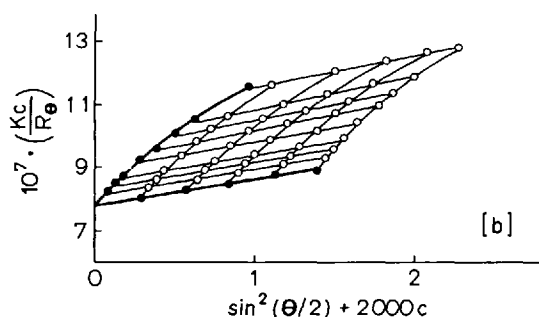
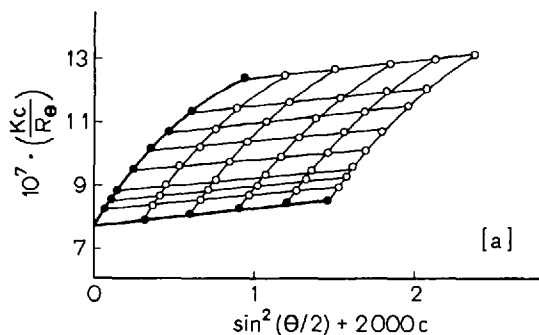


Fig. 45. Zimm diagram<sup>137, 141)</sup> for the polymer in Fig. 43 in (a) 0.5 M aq. KCl and (b) 0.5 M methanolic LiCl. (compare with Fig. 43)

presence of added salt (Fig. 43). The polyelectrolyte effect in a solvent other than the usual one, water, is also evident<sup>137, 141)</sup> from this figure.

In the special case of polymers capable of carrying both positive and negative charges but having a net charge of zero, there will still be species bearing one or two more charges of both signs as a result of charge fluctuations (analogous with density, concentration and polarisability fluctuations). Hence the mean square net charge will not be zero. Application of Debye-Hückel theory leads to

$$\lim_{\theta \rightarrow 0} (Kc_2/R_\theta) = (1/M_2) (1 - \xi c_2^{1/2}), \quad (94)$$

where  $\xi$  is a complex expression involving, *inter alia*, the mean square net charge. Hence the reciprocal reduced scattering extrapolates at infinite dilution of polyelectrolyte to a value of  $1/M_2$  and the slope is negative. Figure 44a relating to ionic salt free aqueous solutions of bovine serum albumen offers a verification<sup>142)</sup> of this equation. The plot in terms of  $c_2$  instead of  $c_2^{1/2}$  is also indicated and the difficulty in obtaining the molecular weight is apparent. The same molecular weight as that yielded<sup>142)</sup> by Eq. (94) is obtained with  $c_2$  as variable, if the system is no longer salt free (Fig. 44b).

Figure 45 should be compared with the distorted plots shown previously<sup>137, 141)</sup> (Fig. 43) for a strongly cationic polyelectrolyte. Normal plots yielding the correct molecular weight are obtained when salt is included; KCl for aqueous solutions and LiCl for methanolic ones in view of the insufficiently great solubility of KCl in

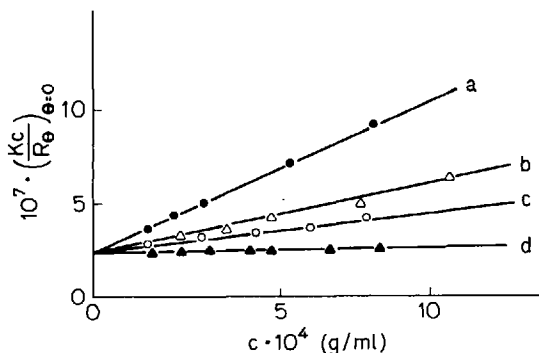


Fig. 46. Determination of molecular weight of poly [1 (2-hydroxyethylpyridinium benzene sulphonate methacrylate)] by extrapolation of  $(Kc/R_\theta)_{\theta=0}$  to zero polymer concentration in aq. KCl of different molarity<sup>141</sup>): (a) 0.01 M, (b) 0.02 M, (c) 0.1 M, (d) 3.0 M. The resultant molecular weight is  $4.3 \times 10^6$

methanol. It is emphasised again that, in the presence of salt, the system becomes a three component one. (When the counterion of a polyelectrolyte is not identical with any of the ions of the added salt, the system must be regarded as a four component one.) Molecular weights are found to be independent of added electrolyte concentration, with the important proviso that the specific refractive index increment at constant chemical potential of diffusible components be measured first and included within the optical constant  $K$ . Figure 46 illustrates<sup>141</sup>) that, although the second virial coefficient [to be denoted strictly as  $(A_2)_\mu$  rather than  $A_2$ ] differs in each case, the plots for different concentration of KCl all extrapolate to the same value for the reciprocal molecular weight<sup>141</sup>). Comparison of these results with those obtained in the presence of KBr and NaF indicates that the molecular weight obtained is also independent of the nature of the added salt. Use of  $(\tilde{dn}/dc_2)_\mu$  for sodium alginate dialysed against aq. NaCl and magnesium alginate dialysed against aq. MgCl<sub>2</sub> yields the same molecular weight<sup>143</sup>) for these two alginates, although the large difference in charge densities has a large effect on  $(A_2)_\mu$ . These recent observations<sup>143</sup>) in conjunction with meticulous attention to sample preparation and clarification by centrifugation resolves the problem associated with earlier work whereby the molecular weight of magnesium alginate in aqueous solutions was reported<sup>144, 145</sup>) to be very much higher than that of the sodium salt of the same material.

Mention should be made of an expedient for evaluating correct molecular weights without resort to equilibrium dialysis or using  $(\tilde{dn}/dc_2)_{T,\mu}$ . It has been used by Vrij and Overbeek<sup>146</sup>) for half neutralised polymethacrylic acid in 0.1 molar solutions of sodium halides. The relevant equation is

$$M_2^* = M_2 [1 - \xi M_3 (\partial \tilde{n} / \partial c_3)_{c_2}]^2 \quad (95)$$

where subscripts 2 and 3 refer to polymer and salt respectively. The constant  $\xi$  is a function of the charge,  $M_2$  and the specific refractive index increment of the polymer solution at constant concentration (not constant chemical potential) of salt. The

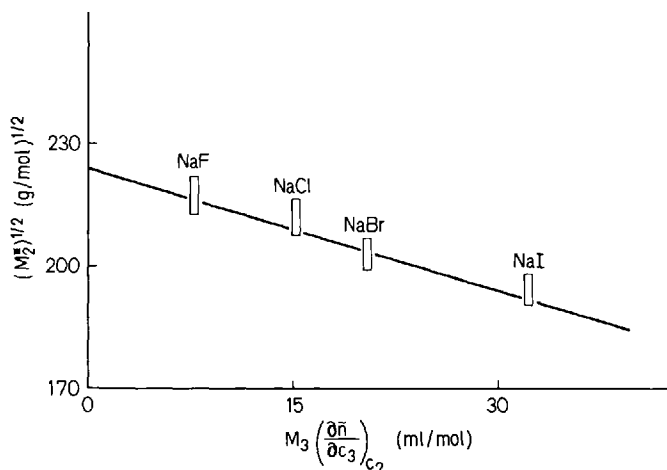


Fig. 47. Square root of apparent molecular weight by LS as a function of molar refractive index increment of salt for sodium polymethacrylic acid in aqueous solution of different sodium halides<sup>146)</sup>

value of  $\xi$  need not be known. Since  $(\partial\tilde{n}/\partial c_3)_{c_2}$  is in units of millilitres per gram, the product  $M_3(\partial\tilde{n}/\partial c_3)_{c_2}$  is the molar specific refractive index (ml/mol) increment of salt at constant concentration of polymer. The square root plot<sup>146)</sup> corresponding to Eq. (95) is given in Fig. 47 for four different sodium halides.  $M_2^*$  is the apparent molecular weight of polymer yielded by experiment and the square root of the true molecular weight ( $M_2$ ) is given by the intercept.

Micellar properties of bile salts such as sodium taurodeoxycholate and sodium glycodeoxycholate have been studied by several techniques including LS<sup>147)</sup>. In very dilute solution (ca.  $10^{-3}$  g/ml) the critical micelle concentration,  $c_{cmc}$ , is located. In dilute solution ( $< ca. 10^{-2}$  g/ml) measurements of LS yield the weight average micellar molecular weight  $\tilde{M}$ . For this purpose the concentration is taken to be the difference between the actual concentration of bile salt used and the value of  $c_{cmc}$ ; similarly the Rayleigh ratio at an angle of  $90^\circ$  is taken as the difference

Table 12. Micellar molecular weights  $\tilde{M}$  of bile salts by LS and other methods<sup>147)</sup> (SE sedimentation equilibrium; SD, sedimentation - diffusion)

Bile Salt	Temp (°C)	Method	$\tilde{M} \times 10^{-3}$
Sodium taurodeoxycholate	--	LS	11.0
Sodium taurodeoxycholate	20	SD, SE	11.9
Sodium taurodeoxycholate	20	SE	11.4
Sodium taurodeoxycholate	36	SE	9.55
Sodium taurodeoxycholate	25	LS	12.0
Sodium glycodeoxycholate	20	SE	8.80
Sodium glycodeoxycholate	36	SE	7.54
Sodium glycodeoxycholate	25	LS	11.5

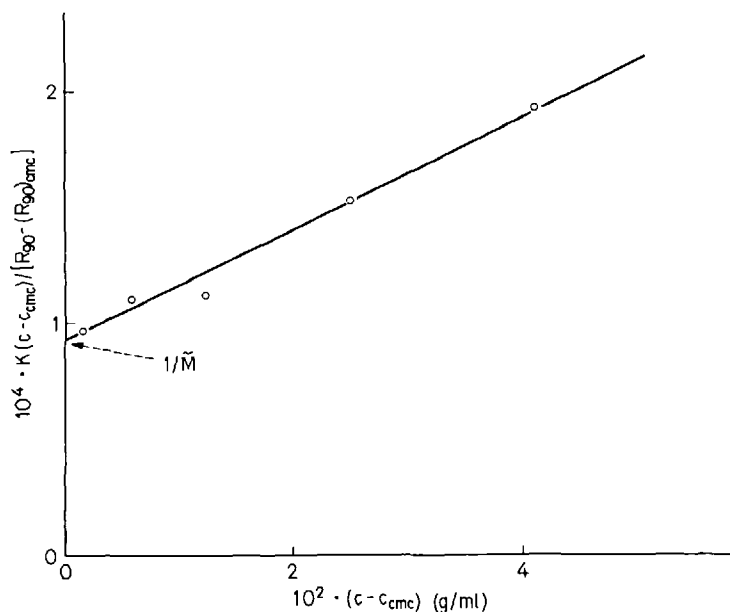


Fig. 48. Plot<sup>147)</sup> according to Eq. (96) for solutions of sodium glycodeoxycholate in 0.15 M aq. NaCl. ( $T = 25^\circ\text{C}$ ,  $\lambda_0 = 436\text{ nm}$ )

between the values of  $R_{90}$  for the solution and the solution at a concentration  $c_{\text{cmc}}$ . The data have been treated successfully according to the theory of charged micelles, which leads to

$$K(c - c_{\text{cmc}})/R_{90} - (R_{90})_{\text{cmc}} = (\xi'/\tilde{M})(1 + \xi''c) \quad (96)$$

Reference should be made to original papers for the significance and use of the involved functions  $\xi'$  and  $\xi''$ . However, the magnitude of  $\xi'$  is usually assumed to be close to unity so that the plot according to Eq. (96) [see Fig. 48] gives  $1/\tilde{M}$  as the intercept<sup>147)</sup>. Some micellar molecular weights obtained by LS and other methods are compared<sup>147)</sup> in Table 12. The estimation *via* LS of the particle weight, size and shape has been reported and reviewed by Tuzar and Kratochvíl<sup>148)</sup>.

### 3. Copolymers and Terpolymers

A copolymer is a macromolecule comprising two chemically distinct types of monomer unit, A and B, whilst a terpolymer is composed of units A, B and C. The analytically determined composition of a copolymer is expressed as the weight fractions  $W_A$  and  $W_B$  of its constituents. For LS studies on a copolymer solution it is necessary to know the value of the specific refractive index increment  $\nu$ , which can be either measured or calculated from:

$$\nu = W_A \nu_A + W_B \nu_B \quad (97)$$

The theory of LS from copolymer solutions was pioneered by Stockmayer *et al.* and later by Bushuk and Benoit, subsequent developments being due to Benoit, Inagaki *et al.* Molecular weight determination constitutes only a part of the most recent review of the field by Benoit and Froelich<sup>149</sup>).

Under stringent conditions of preparation, *e.g. via* controlled anionic polymerization, characterisation of the copolymer poses relatively few problems. The product is uniform with respect to composition and molecular weight<sup>150</sup>). The former means that  $W_A$  is a true measure of the composition of all the molecules and not an average within the range  $(W_A + \delta W_A)$  to  $(W_A - \delta W_A)$ . Measurement or prediction from reaction conditions affords the value of  $W_A$ . Uniformity of molecular weight means that  $M$  should equal  $M_n$ , and here again the molecular weight can be predicted or measured by osmotic pressure, for example<sup>150, 151</sup>). The resultant value should be very close to the molecular weight measured by LS, provided  $\nu$  is sufficiently large; moreover, the value of  $M$  should be independent of the solvent used. Since  $M_n = M$ , the molecular weights of the constituent portions of the copolymer ( $M_A$  and  $M_B$ ) should be given respectively as  $W_A M$  and  $W_B M$ . From LS measurements on copolymer solutions the values of  $M_A$  and  $M_B$  are also yielded. Of the numerous systems studied, most work has been devoted to block copolymers of styrene (A) with either methyl methacrylate (B) or isoprene (B). Some typical results are listed<sup>150</sup>) in Table 13. A slight, but discernible dependence of  $M$  on the nature of the solvent is evident from the data. This will be discussed later.

An alternative and general mode of determining the molecular weight of one constituent is to optically mask the other<sup>152, 153</sup>). Thus, if  $\nu_B = 0$ , then any observed

Table 13. Characteristics of di-block copolymers of styrene (A) – isoprene (B) containing various weight fractions  $W_A$  of styrene<sup>150</sup>)

$W_A \times 100$		Molecular weight $\times 10^{-5}$					
predicted <sup>1)</sup>	found <sup>2)</sup>	$M_{mi}$ <sup>3)</sup>	$\bar{M}_n$ <sup>4)</sup>	M* by LS in toluene	M* by LS in cyclo- hexane	M* by LS in methyl isobutyl ketone	M
25.0	24.7	1.00	1.02	1.29	1.10	1.09	1.07
50.0	52.2	1.00	1.04	1.30	1.14	1.10	1.07
77.8	78.2	1.00	1.03	1.29	1.14	1.12	1.08
25.0	25.5	2.50	2.52	3.00	2.75	2.71	2.62
50.0	48.5	2.50	2.54	2.80	2.70	2.67	2.62
25.0	25.1	5.00	4.99	5.78	5.46	5.42	5.34
50.0	48.7	5.00	5.01	5.64	5.60	5.53	5.41

<sup>1)</sup> From ratio of the weight of styrene to total monomers consumed.

<sup>2)</sup> From uv analysis.

<sup>3)</sup> From ratio of concentrations of monomer to initiator.

<sup>4)</sup> By osmotic pressure.  $M^*$  is apparent weight average mol.wt. yielded directly from LS experiment;  $M$  is true weight average molecular weight obtained from the three values of  $M^*$ .

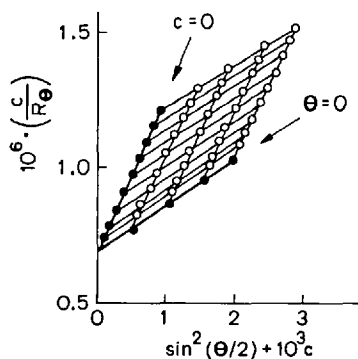


Fig. 49. Zimm plot for a styrene/isoprene block copolymer in methyl isobutyl ketone<sup>153)</sup>

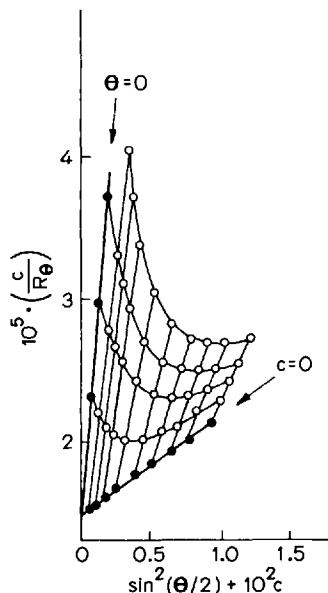


Fig. 50. Zimm plot for same sample as in Fig. 49, but with chlorobenzene as solvent<sup>153)</sup>

scattering will be due to the presence of A only. Rendering the refractive index increment of one portion zero may be accomplished by altering the temperature and/or wavelength, but much more usually by selecting a solvent which is iso-refractive with the portion to be masked. For polystyrene (A) and polymethyl methacrylate (B) in toluene at 70 °C,  $\nu_A$  and  $\nu_B$  are 0.125 and 0.014 ml/g respectively<sup>154)</sup>. Hence for the copolymer, toluene would be almost satisfactory for the purpose of masking the methyl methacrylate portion and thereby obtaining  $M_A$ . At a temperature of 20 °C the system becomes almost perfectly suitable with the same solvent, since the values of  $\nu_A$  and  $\nu_B$  are now 0.110 and 0.001 ( $\approx 0$ ) ml/g. Several solvents which are effectively iso-refractive with polymer portions of a copolymer have been listed<sup>153, 154)</sup>.

In a block copolymer having one portion optically masked the resultant Zimm plots are sometimes spurious. For example, Figs. 49 and 50 both relate to a styrene (A) – isoprene (B) block copolymer<sup>153)</sup>. In the former figure the solvent is one in which  $\nu_A$  and  $\nu_B$  are both large and the plot is normal. In Fig. 50 the solvent is one in which  $\nu_A = 0.083$  ml/g and  $\nu_B$  is effectively zero (actually  $\nu_A = -0.004$  ml/g); the plot is abnormal. Here the observed angular LS envelopes are linear at  $c = 0$  but at low angles they exhibit curvature to an extent which increases with  $c$  and also (although not obvious from the data shown for just this single sample) with  $M$ . For this copolymer a similar effect is observed when the other portion is masked instead, that is, when  $\nu_A = 0$  in bromoform. Other examples have been reported. Until comparatively recently this sort of behaviour was known only for some homopolymers, especially charged ones, in single solvents. For block copolymers in single solvents, reasonable explanation has been advanced on the basis of the loss in scattering power caused by external interference, as known for X-ray scattering from dense groups. Extension to the present situation leads to the formulation of an apparent particle scattering

function  $P^*(\theta)$ , which is related to the normal intramolecular scattering function  $P(\theta)$  via an intermolecular function  $\Phi(\theta)$ :

$$P^*(\theta) = P(\theta) / [1 + (c \mathcal{N} V_{\text{exc}} / M) \Phi(\theta)], \quad (98)$$

where  $V_{\text{exc}}$  is the excluded volume and  $\Phi(\theta)$  is a function of both angle and the excluded mean square radius of gyration,  $\langle s_{\text{exc}}^2 \rangle$ :

$$\Phi(\theta) = 1 - \tilde{\mu}^2 \langle s_{\text{exc}}^2 \rangle / 6 + \dots \quad (99)$$

Appropriate combination of Eqs. (98) and (99) allows the magnitude of  $V_{\text{exc}}$  and  $\langle s_{\text{exc}}^2 \rangle$  to be determined. The amended LS equation is expressible now as

$$Kc/R_\theta = 1/MP^*(\theta) = 1/MP(\theta) + 2A_2c [\Phi(\theta)/P(\theta)] \quad (100)$$

The upward curvature in the scattering envelope due to exceptionally low  $R_\theta$  has been examined theoretically and experimentally, and correlated with the relevant dimensions<sup>153-155</sup>. Essentially, it emanates from the application of normal (as opposed to apparent) LS laws to a system in which only a part actually scatters light. The intermolecular excluded volume, however, which appears within  $P^*(\theta)$  is a function of the size of the whole copolymer molecule, that is, both scattering and non-scattering portions. For normal homopolymers, partial cancellation of the ratio  $\Phi(\theta)/P(\theta)$  produces only a very slight increase in the slope of the angular dependence at higher concentrations. For block copolymers in which B, for example, is masked,  $P(\theta)$  reflects only the size of A and therefore stays closer to unity than expected for a whole copolymer molecule of a larger total size. On the other hand,  $\Phi(\theta)$  is determined by the intermolecular excluded volume of the whole molecule and falls in value below unity more rapidly at high angle and for a large excluded volume cf. Eq. (99). The net effect is an exaggerated decrease in the ratio  $\Phi(\theta)/P(\theta)$  at high angles.

From the strictly practical standpoint, it is encouraging to note that  $\Phi(\theta)$  and  $P(\theta)$  both tend to unity as  $\theta$  tends to zero, so that in the limit of infinite dilution the intercept remains as  $1/M$ . Hence, provided  $\nu_A$  is reasonably large, one can work at low concentration and obtain the molecular weight without too much difficulty. The anomalous behaviour described appears to depend on both types of unit, A and B, being in the same chain and in block form, since no similar effects have been reported for random copolymers or mixtures of two homopolymers. When anomalous behaviour is possible, a larger distortion is expected if the unmasked portion is small relative to the overall dimensions of the whole molecule and also if the deviation of the centre of mass of the unmasked portion from the centre of mass of the whole molecule is large. Thus, if prepared under identical conditions an A-B di-block would give a larger distortion, whilst a B-A-B tri-block a smaller distortion.

Block copolymers of styrene(A)/dimethyl siloxane (B) are even more unusual in the respect that in many solvents  $\nu_A$  and  $\nu_B$  are roughly of similar magnitude, but the former is positive and the latter negative<sup>156</sup>. Hence, depending on the composition  $W_A$  [cf. Eq. (97)], the value of  $\nu$  for the copolymer can be positive, negative

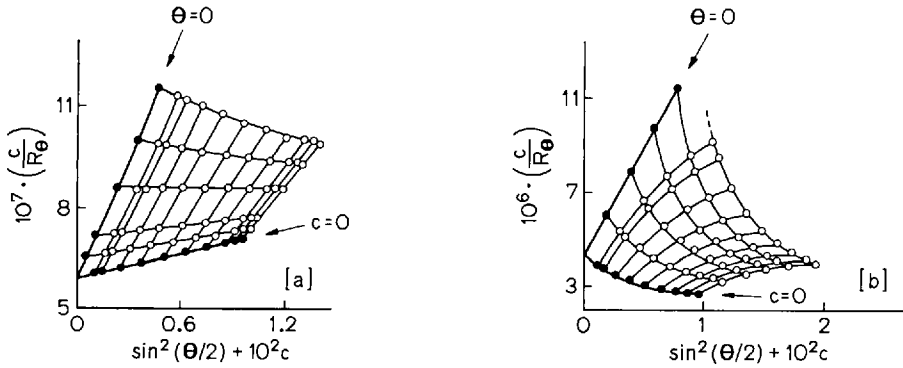


Fig. 51. Zimm plot<sup>156)</sup> for a styrene/dimethylsiloxane block copolymer in (a) cyclohexane and (b) toluene

or zero. This dictates the magnitude of a convenient parameter  $W_A \nu_A / \nu$ , which, as demonstrated theoretically, governs the apparent behaviour of  $\langle s^2 \rangle$  or the slope of  $1/P(\theta)$  at zero concentration. An enigmatic situation can thus arise when using a solvent in which neither  $\nu_A$  nor  $\nu_B$  is zero, whereby the apparent  $\langle s^2 \rangle$  is zero or even negative (see Figs. 51). Such behaviour at infinite dilution is in total accord with predictions hitherto unsubstantiated by experimental results. Reference is recommended to the original papers<sup>149, 156)</sup>, since this behaviour does not introduce any real difficulties in the measurement of the molecular weight.

Most copolymers are heterogeneous in both molecular weight and composition. The latter of these arises from the mechanism of the copolymerisation (particularly at high conversion) and individual copolymer molecules differ slightly in their value of  $W_A$ . Solutions of heterogeneous copolymers constitute multicomponent systems

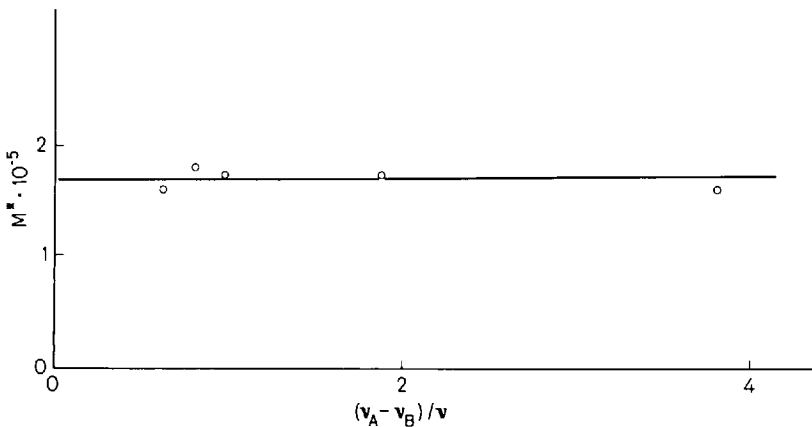


Fig. 52. Demonstration of the constancy of the measured apparent molecular weight  $M^*$  for a block copolymer, which is monodisperse with respect to composition and molecular weight<sup>157)</sup>



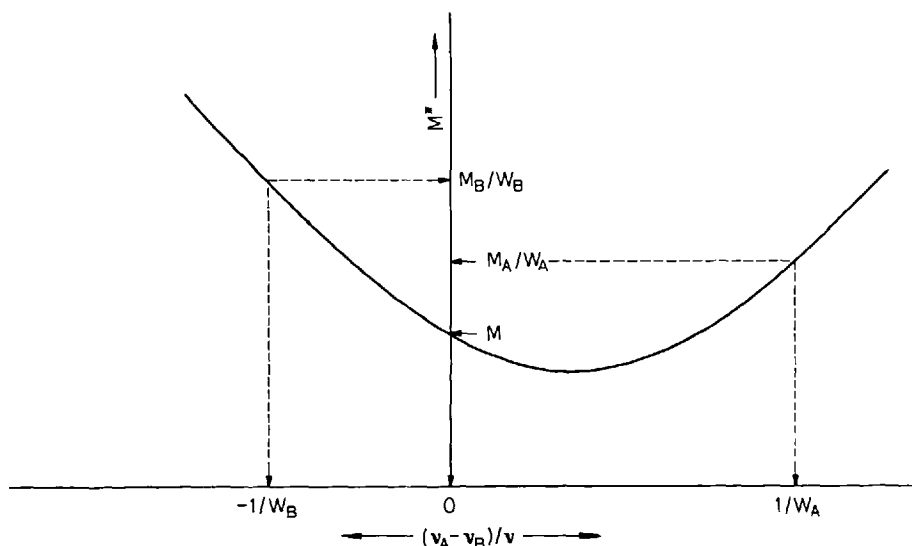


Fig. 53. Parabola according to Eq. (101) showing derivation of molecular weights of copolymer and its constituents<sup>149)</sup>

with respect to the polymer. Since  $W_A$  differs somewhat among the copolymer molecules, so also does  $\nu$ , which is an average value (and the only one, in fact, which is accessible experimentally). The molecular weight of the copolymer using the measured  $\nu$  is only an apparent value  $M^*$  which differs from the true one  $M$  in accord with the following equivalent expressions<sup>149)</sup>:

$$M^* = (\nu_A \nu_B / \nu) M + [\nu_A (\nu_A - \nu_B) / \nu^2] W_A M_A - [\nu_B (\nu_A - \nu_B) / \nu^2] W_B M_B \quad (101)$$

$$M^* = M + 2P [(\nu_A - \nu_B) / \nu] + Q [(\nu_A - \nu_B) / \nu]^2 \quad (102)$$

Changing the solvent to one of different refractive index induces a change in  $(\nu_A - \nu_B) / \nu$ . The form of  $M^*$  as a function of this parameter is parabolic of curvature dictated by the quantities  $P$  and  $Q$ . If these, or more conveniently,  $P/M$  and  $Q/M$  are zero,  $M^*/M$  will always have a value of unity, that is, the true molecular weight  $M$  will always be yielded by LS irrespective of the solvent used (Fig. 52)<sup>157)</sup>. The general form of the parabola is shown schematically<sup>149)</sup> in Fig. 53 and the required molecular weights are afforded by specific co-ordinates of it, viz for abscissae of  $1/W_A$ ,  $0$  and  $-1/W_B$  the corresponding ordinates are  $M_A/W_A$ ,  $M$  and  $M_B/W_B$  respectively. Several approaches have been made to evaluate the heterogeneity parameters  $P$  and  $Q$ . These include solution of simultaneous equations<sup>149)</sup>, recasting data to yield a linear plot<sup>42)</sup> and computer least squares fit of data<sup>158)</sup>.

Since  $P$  and  $Q$  are characteristics of the copolymer sample, they are independent of the nature of the solvent and hence, in principle, a knowledge of their values can yield the correct molecular weight  $M$  from Eq. (102). Many of the reported

Table 14. Refractometric data and apparent LS molecular weight of a styrene (A)/di-n-butyl itaconate (B) copolymer<sup>159</sup> of composition  $W_A = 0.169$ 

Solvent	$\nu_A$ (ml/g)	$\nu_B$ (ml/g)	$\nu$ (ml/g)	$(\nu_A - \nu_B)/\nu$	$M^* \times 10^{-3}$ (g/mol)
Carbon tetrachloride	0.156	0.020	0.043	3.163	144.8
Styrene	0.054	-0.077	-0.055	-2.382	109.3
n-Amyl acetate	0.205	0.074	0.096	1.365	82.3

values of P and Q are now considered to be considerable over-estimates of the truth and the rather stringent conditions necessary for accurate determination of P and Q by LS have been analysed and discussed<sup>131</sup>). On the whole, determination of M *via* the parameters P and Q is not a reliable or recommendable procedure.

The use of simultaneous equations with at least three sets of experimental data can, however, be applied to Eq. (101) or (102) to yield M,  $M_A$  and  $M_B$ . This is especially useful, if the specific co-ordinates of the whole parabola cannot be realised experimentally as is often the case. The data<sup>159</sup>) in Table 14 relate to a random copolymer of styrene (A)/di-n-butyl itaconate (B) in which  $W_A = 0.169$ . Solution of simultaneous equations [Eq. (101)] yields  $M = 67300$ ,  $M_A = 56800$  and  $M_B = 64700$ . The compositional heterogeneity is such that the data conform to the required theoretical relationship<sup>149</sup>):

$$M > W_A M_A + W_B M_B \quad (103)$$

(that is,  $67\,300 > 63\,300$ )

The values of  $(\nu_A - \nu_B)/\nu$  in Table 14 lie between 3.16 and -2.38. Hence, with these data or with the inclusion of additional ones within the range delineated by these extrema, it would be possible to use the parabola also to determine M and  $M_B$ , since the abscissae yielding them are 0 and  $-1/(1-0.169)$ , *i.e.* -1.20 respectively. However, the range of  $(\nu_A - \nu_B)/\nu$  does not extend to a large enough positive value ( $1/0.169 = 5.92$ ) to enable  $M_A$  to be derived in a similar fashion.

On the assumption of some finite compositional heterogeneity, Eq. (101) reveals the following criteria necessary for the most sensitive determination of the relevant molecular weights<sup>152</sup>):

$$\nu_A = \nu_B \text{ and both large: to obtain } M \quad (104)$$

$$\nu_B = 0 \text{ and } \nu_A \text{ large: to obtain } M_A \quad (105)$$

$$\nu_A = 0 \text{ and } \nu_B \text{ large: to obtain } M_B \quad (106)$$

Clearly, if one is using only a single solvent, these three requisites are mutually exclusive; the criteria may well be satisfied with different solvent in each case. Expression (104) means that poly-A and poly-B are iso-refractive and that they have a very different refractive index from that of the solvent. Such systems are comparatively

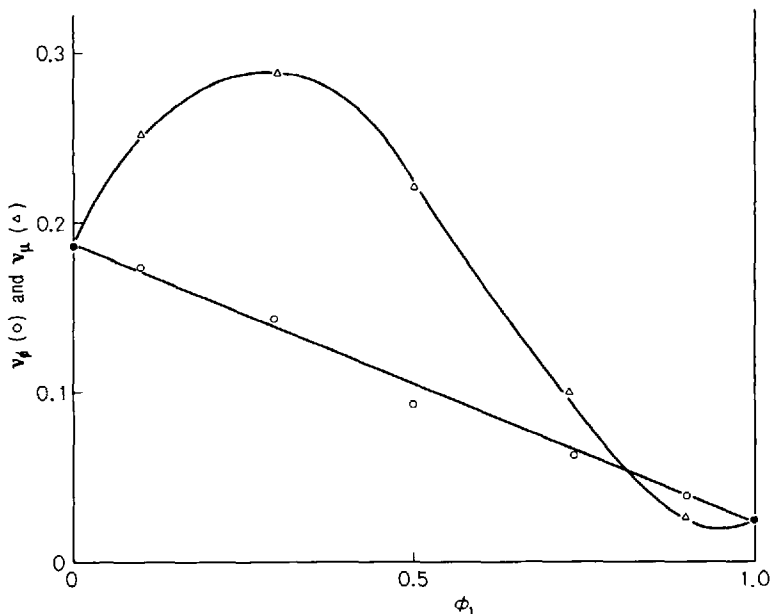


Fig. 54. Specific refractive index increments at constant composition (o) and constant chemical potential ( $\Delta$ ) for solutions of nylon-6 in 2,2,3,3-tetrafluoropropanol/1-chlorophenol binary mixtures,  $\phi_1$  is the volume fraction of 1-chlorophenol and filled circles refer to the two pure single solvents<sup>161)</sup>

rare, although polystyrene and cellulose tricarbnilate approximate to this situation<sup>160)</sup>. When appropriate solvents cannot be found, recourse is made to the far more versatile expedient of using binary solvent mixtures comprising liquids 1 and 3 of variable composition as expressed by the volume fraction  $\phi_1$  of liquid -1. The refractive index of the mixed solvent  $\tilde{n}_0$  depends on  $\phi_1$  and the value of  $\nu$  for the copolymer will therefore be governed also by  $\phi_1$ . The consequent complications due to selective adsorption in mixed solvents have already been discussed and the specific refractive index increments employed must be those at constant chemical potential of mixed solvents. Fortunately, Kratochvíl and co-workers<sup>152)</sup> have demonstrated that Eqs. (101) and (102) as well as criteria (104), (105), and (106) apply equally well with  $\nu_A$ ,  $\nu_B$  and  $\nu$  (or, as they should be more precisely expressed,  $\nu_{\phi A}$ ,  $\nu_{\phi B}$  and  $\nu_{\phi}$ ) replaced by  $\nu_{\mu A}$ ,  $\nu_{\mu B}$ , and  $\nu_{\mu}$  respectively. The difference between the specific increments at constant composition and constant chemical potential can often be quite dramatic, as indicated<sup>161)</sup> in Fig. 54.

Another way of determining the composition of the most appropriate mixed solvent for the particular requirement is to actually conduct LS on a polymer in binary solvents of different composition. Since the intensity of scattered light is proportional to the square of the specific refractive index increment at constant chemical potential, it follows that the square root of the light scattering intensity at a given concentration and angle (say  $90^\circ$ ) will be proportional to  $\nu_{\mu A}$  for poly-A and to  $\nu_{\mu B}$  for poly-B in solution. The sign (positive or negative) of the root

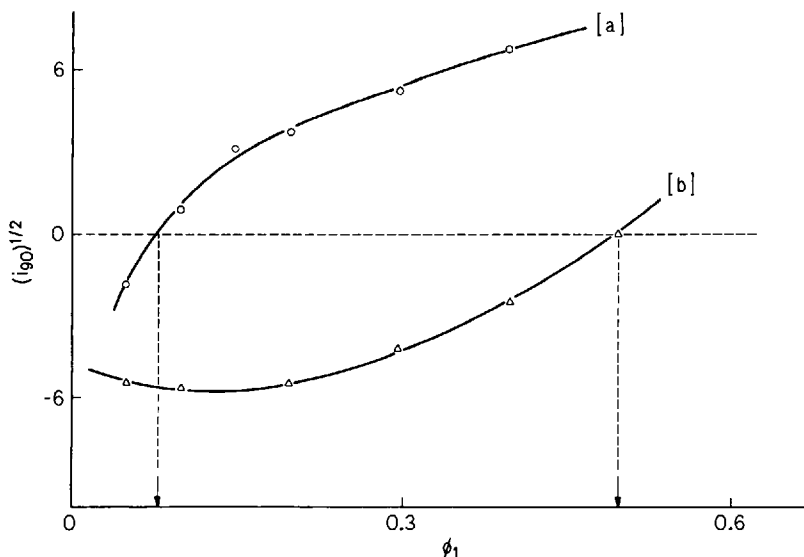


Fig. 55. Dependence of square root of excess LS for solutions of (a) polyethyleneglycol methacrylate and (b) polymethyl methacrylate in mixed solvents comprising 2,2,3,3-tetrafluoropropanol (volume fraction  $\phi_1$ ) and benzyl alcohol. ( $T = 25^\circ\text{C}$ ,  $\lambda_0 = 546\text{ nm}$ ). Broken lines indicate composition of mixed solvent yielding no excess scattering from the polymer in each case<sup>152</sup>)

of the scattered intensity must be inferred by reasoning<sup>152</sup>). Examples are given in Fig. 55 from which it is seen that for a copolymer comprising the two species in question, a binary solvent comprising a low volume fraction of tetrafluoropropanol will optically mask one portion and yield the molecular weight of the other (polymethyl methacrylate); similarly, if the volume fraction of the tetrafluoropropanol is large ( $\approx 0.5$ ), the other portion of the copolymer would be masked and the molecular weight of poly-2-hydroxyethyl methacrylate in the copolymer yielded<sup>152</sup>).

Characterisation of A/B/C terpolymers is still in its infancy, but there are already clear indications that, in a compositionally heterogeneous terpolymer, the determination of molecular weights  $M_A$ ,  $M_B$ ,  $M_C$  and  $M$  may prove an intractable problem in the general case. Apart from some semi-quantitative studies, most effort in this direction has been made by Kambe, Kambe and collaborators<sup>162, 163</sup>), who extended the original approach of Bushuk and Benoit<sup>164</sup>).

The concepts and definitions involved are more numerous and complex than those involved in the derivations of Eqs. (101) and (102). The full treatment of Y. Kambe has not been published but has been kindly made available to the author. Mention will be made here of only very small selected aspects.

- (i) Instead of one parameter  $P$ , there are three  $P_A$ ,  $P_B$  and  $P_C$ ,
- (ii) similarly, parameters  $Q_A$ ,  $Q_B$  and  $Q_C$  are invoked,
- (iii) additional heterogeneity parameters  $R_{AB}$ ,  $R_{BC}$  and  $R_{CA}$  are introduced,
- (iv) deviations in composition of A, B and C from their mean values are required,
- (v) molecular weights of portions ( $M_{AB}$ ,  $M_{BC}$  and  $M_{CA}$ ) are invoked,
- (vi) the molecular weight  $M$  of the terpolymer is defined as

$$M = \sum W_i M_i$$

$$= W_A M_A + W_B M_B + W_C M_C + 2(W_{AB} M_{AB} + W_{BC} M_{BC} + W_{CA} M_{CA}) \quad (107)$$

Unfortunately there is no expression corresponding to Eq. (101) for copolymers in which the measured apparent molecular weight  $M^*$  appears solely as a function of  $M_A$ ,  $M_B$ ,  $M_C$  and the true molecular weight  $M$ . The only available and tractable expression in the following one<sup>162</sup> [Eq. (108)]; in principle it is capable of yielding  $M$  and the values of the five heterogeneity parameters. It does not yield  $M_A$ ,  $M_B$  or  $M_C$ .

$$M^* = M + 2P_A(\nu_A - \nu_C)/\nu + 2P_B(\nu_B - \nu_C)/\nu + Q_A(\nu_A - \nu_C)^2/\nu^2$$

$$+ Q_B(\nu_B - \nu_C)^2/\nu^2 + 2R_{AB}(\nu_A - \nu_C)(\nu_B - \nu_C)/\nu^2 \quad (108)$$

By analogy with Eq. (97), the specific refractive index of a terpolymer is given by the following expression, which has been verified experimentally;

$$\nu = W_A \nu_A + W_B \nu_B + W_C \nu_C \quad (109)$$

The existence of compositional heterogeneity may be evidenced by the dependence of the measured  $\nu$  on the extent of conversion of monomers to terpolymer for a random terpolymer<sup>163</sup> (Fig. 56). Other data on the same diagram demonstrate that composition and  $\nu$  remain sensibly constant with conversion for a partial azeotrope. These observations are corroborated by the LS results in Table 15, which show that for the random terpolymer,  $M^*$  varies between  $2.63 \times 10^5$  and  $4.05 \times 10^5$  (that is, by about 50%) according to the solvent used. In contrast, for the partial

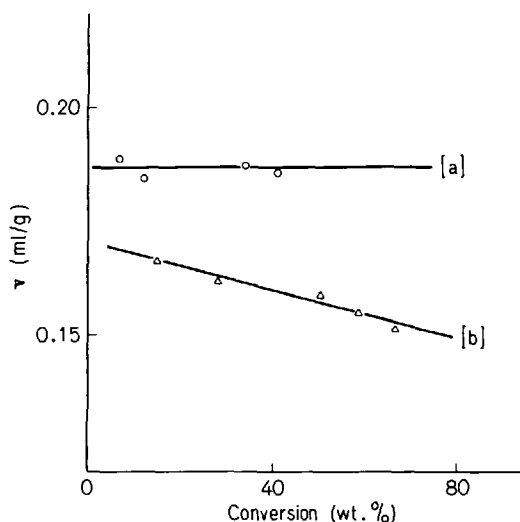


Fig. 56. Dependence of specific refractive index increment on conversion of monomers to polymer for a styrene/acrylonitrile/methyl methacrylate terpolymer in methyl ethyl ketone at 20 °C and 436 nm.: (a) - partial azeotrope, (b) terpolymer with composition distribution<sup>163</sup>

Table 15. Apparent molecular weights ( $M^*$ ) by LS in different solvents for terpolymers comprising acrylonitrile, styrene and methyl methacrylate

Solvent	$M^* \times 10^{-4}$ Partially azeotropic terpolymer	Compositionally heterogeneous terpolymer
Dioxan	45.5	26.3
Acetonitrile	insoluble	29.0
Tetrahydrofuran	47.6	29.1
Methyl ethyl ketone	44.5	30.6
Dimethyl formamide	50.0	40.5
Chloroform	58.8	50.0
Toluene	52.6	insoluble

azeotrope wherein the compositional heterogeneity is low, one anticipates that Eq. (108) should reduce approximately to the form  $M^* = M$  irrespective of solvent (that is, irrespective of the values of  $\nu$ ,  $\nu_A$ ,  $\nu_B$  and  $\nu_C$ ). The data in the table suggest that this is so, since  $M^*$  ranges only from  $4.65 \times 10^5$  to  $5.21 \times 10^5$  (that is, by ca. 12%).

The azeotropic terpolymer, being atypical in general, one is faced with the prospect of solving at least five simultaneous sets of Eq. (108) in order to obtain  $M$ . This manipulation is exact, but the inherent inaccuracies in five different measurements of  $M^*$  are coupled with those involved in measuring the refractive index increments. It is as true for a terpolymer as it is for a copolymer that the difference between specific increments (for example,  $\nu_A - \nu_B$  or  $\nu_B - \nu_C$ ) must be measured for high

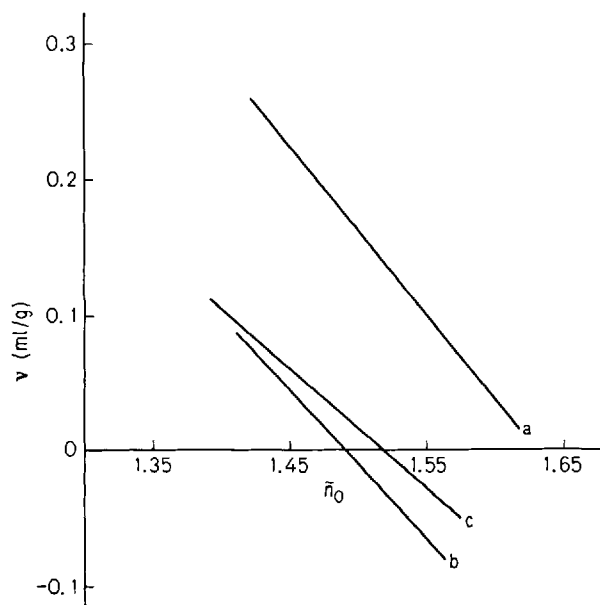


Fig. 57. Gladstone - Dale plots [Eq. (110)] for solutions of (a) polystyrene, (b) poly-n-butyl methacrylate, (c) polymethyl methacrylate<sup>165</sup> ( $\lambda_0 = 436 \text{ nm}$ )

accuracy, since this difference varies slightly with the nature of the solvent. According to the Gladstone-Dale equation.

$$\nu = \bar{\nu}_2 (\tilde{n}_2 - \tilde{n}_0) \quad (110)$$

the specific increment of a homopolymer is a linear function of the refractive index  $\tilde{n}_0$  of the solvent, the slope being  $-\bar{\nu}_2$  where  $\bar{\nu}_2$  is the partial specific volume of the polymer in solution. Actually,  $\bar{\nu}_2$  itself can vary according to the solvent so that in any selected solvent of refractive index  $\tilde{n}_0$  the difference in specific refractive index increments for two polymers,  $\nu_A - \nu_B$ , may be independent of  $\tilde{n}_0$  (as in Fig. 57(a) and (b) relating to solutions of homopolymers A and B) or may change markedly with  $\tilde{n}_0$  [as in Fig. 57(c)]<sup>165</sup>.

The individual values of  $\nu_A$ ,  $\nu_B$  and  $\nu_C$  have been excluded from Table 15 and indeed for this system the value of  $\nu_B$  can only be measured in three solvents due to the insolubility of polyacrylonitrile in the others. For the purpose of calculating  $(\nu_A - \nu_B)/\nu$ , the value would have to be interpolated rather less accurately *via* Eq. (110). In the same order as the solvents listed in Table 15, the values of  $(\nu_A - \nu_C)$  are 0.114, —, 0.117, 0.115, 0.109, —, 0.110, 0.110 and 0.116 ml/g, that is, a variation of only 8% between the largest and smallest values. The only circumstance in which the procedure could be grossly simplified would be that of a terpolymer in which two of the components, say B and C, happen to be iso-refractive. Insertion of  $B \equiv C$  into Eq. (108) thereby reduces the expression to the one for an A/B copolymer [Eq. (101)].

#### 4. Mixtures

We have noted that LS yields the weight average molecular weight  $M$ . If the solution comprises as solute a mixture of two polymers A and B each of identical molecular weight, LS distinguishes between these species only by virtue of their different specific refractive index increments  $\nu_A$  and  $\nu_B$ . Under these conditions a mixture of isorefractive polymers behaves as a single species solute of concentration equal to the sum of the two individual concentrations.

In general not only will  $\nu_A$  and  $\nu_B$  differ, but also the individual molecular weights  $M_A$  and  $M_B$  will not be the same. If these four quantities are obtained first from experiments on the individual polymers then the molecular weight  $M_{AB}$  of the mixture of known composition is calculated directly from

$$M_{AB} = W_A M_A + W_B M_B \quad (111)$$

The equation differs from the corresponding one for a copolymer. It is in fact simply an application of the definition of weight average molecular weight [Eq. (10)]. Provided the magnitude of  $M_{AB}$  can be established for a mixture of known composition and the molecular weight of one of the polymers is known, Eq. (111) can provide the molecular weight of the other polymer if this is unknown.

Table 16. Molecular weights ( $M_A$ ) by LS of polymer A alone and in the presence of polymer B when the latter is optically masked by conditions wherein  $\nu_B = 0$  or  $\nu_{\mu B} = 0$ 

Polymer(s)	$W_A$	$M_A \times 10^{-3}$	Ref.
Polystyrene(A)	1.0	120	
Polystyrene(A) + polymethyl methacrylate	0.5	118	166)
Polystyrene(A) + polybutadiene (B)	0.5	125	
Polymethyl methacrylate(A)	1.0	200	166)
Polymethyl methacrylate(A) + polystyrene(B)	0.5	199	
Polybutadiene(A)	1.0	148	166)
Polybutadiene(A) + Polystyrene(B)	0.5	145	
Nylon-6(A)	1.0	49.7	161)
Nylon-6(A) + Polymethyl acrylate (B)	0.573	47.4	

For meaningful implementation of Eq. (111) it is necessary to use the true molecular weight  $M_{AB}$  and not the apparent value  $M_{AB}^*$  always yielded by a LS experiment, since a mixture constitutes a system of maximum compositional heterogeneity. Equations (101) and (102) for a copolymer apply also to a mixture<sup>152)</sup> provided that for the latter one uses  $M_{AB}^*$  (instead of  $M^*$ ),  $M_{AB}$  (instead of  $M$ ), and the specific refractive index of the mixture in solution  $\nu_{AB}$  (instead of  $\nu$ ). If mixed solvents are used, the specific refractive index increments at constant chemical potential of diffusible solvents are involved. The analogy with copolymers is furthered by optical masking<sup>152, 161)</sup> (usually, but not necessarily, by using mixed solvents) one polymer to obtain the molecular weight of the other. Thus, if the mixed solvent is one in which  $\nu_{\mu B} = 0$ , the molecular weight of polymer A is yielded by

$$M_{AB}^{*2} = (\nu_{\mu A}^2 / \nu_{\mu AB}^2) W_A M_A \quad (112)$$

Examples have been reported for several systems<sup>161, 166)</sup>; some results are listed in Table 16. In summary, polymer mixtures can be treated as copolymers of extreme heterogeneity in chemical composition. Under suitable conditions the techniques used in analysing data of LS from copolymer solutions can be applied to yield with good accuracy the molecular weights of components of the binary polymer mixtures.

The increasing interest in polymer blends has acted as a stimulus not only to the aspects just outlined but also to a study of interactions between polymer A and polymer B in solution as a route to quantifying their thermodynamic compatibility. Hyde<sup>167)</sup> has reviewed the relevant theory whilst Kratochvíl and co-workers<sup>168, 169)</sup> have been responsible for much of the latest experimental studies.

Essentially, separate experiments on each polymer in the same solvent yield  $\nu_A$ ,  $M_A$  and the second virial coefficient  $(A_2)_A$  as well as the corresponding quantities for polymer B. When a mixture of the two polymers in which the composition of the polymers are  $W_A$  and  $W_B$  is dissolved in the same solvent, there are two approaches.



In the first, the ratio  $c_A/c_B$  is kept constant and LS is conducted on solutions of varying total concentration  $c (= c_A + c_B)$ . As for experiments on single polymers, dilution is effected with pure solvent. Theoretical analysis shows that:

$$\lim_{\theta \rightarrow 0} (K'c/R_\theta) = 1/(\nu_A^2 W_A M_A + \nu_B W_B M_B) + \xi' c \quad (113)$$

where  $\xi'$  is a function of  $\nu_A$ ,  $\nu_B$ ,  $W_A$ ,  $W_B$ ,  $M_A$ ,  $M_B$  as well as certain interaction parameters. Although they are of prime importance in a different context, we shall ignore these parameters in view of the emphasis purely on molecular weights. The intercept at  $c = 0$  in the linear plot according to Eq. (113) is seen to be a composite quantity involving both  $M_A$  and  $M_B$ . If, for example, polymer B is isorefractive with the solvent, then  $\nu_B = 0$  and the system is optically masked in part. The intercept becomes  $1/\nu_A^2 W_A M_A$  thus yielding the molecular weights of polymer A as expected and as indicated previously. Similarly, if  $\nu_A = 0$ , the intercept yields the value of  $M_B$ .

The second approach is radically different in the respect that the concentration  $c_B$  is kept constant. Hence the whole solution may be regarded as comprising polymer A as solute and polymer B at a fixed concentration in the liquid as the complex solvent. The Rayleigh ratio  $R'_\theta$  is obtained by measuring the total LS (from polymer A + polymer B + liquid) and subtracting from it the LS due to solvent, that is, the scattering due to polymer B at a concentration  $c_B$  in the liquid. The variable is thus  $c_A$  and the relevant equation<sup>168</sup> is

$$\lim_{\theta \rightarrow 0} (K' \nu_A^2 c_A / R'_\theta) = (1/\xi M_A) + (\xi_1/\xi^2 M_A^2) c_A \quad (114)$$

where  $\xi$  and  $\xi_1$  are both functions of interaction parameters as well as of  $\nu_A$ ,  $\nu_B$ ,  $M_A$ ,  $M_B$ , and  $c_B$ . Under the special circumstance that  $\nu_B = 0$ , the form of  $\xi$  dictates that in the linear plot according to Eq. (114), the intercept at  $c_A = 0$  is simply  $1/M_A$ .

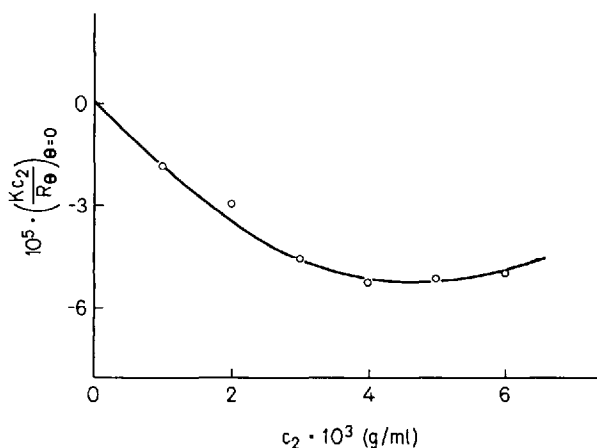


Fig. 58. Concentration dependence of negative LS for solutions of polymethyl methacrylate (concentration  $c_2$ ) dissolved in a solution of polystyrene in dioxan<sup>169</sup>

However, in general, the intercept affords no simply derivable information on molecular weights because of the presence of interaction parameters within  $\xi$ . This system in which one component of the solvent is a polymer and the more common system (Section V.1) in which both components of the binary solvent are low molecular weight compounds form the basis of some novel and interesting comparisons by Kratochvíl and Vorlíček<sup>169</sup>. In both instances the experimental data yield only an apparent molecular weight of the polymer solute, as seen in Eqs. (88) and (114). The ratio of the apparent molecular weight to its true value is denoted in either case by  $\xi$ . The significance of  $\xi$  for a polymer dissolved in a binary liquid mixture has been referred to, whilst if the solute itself contains a polymer,  $\xi$  depends on interaction parameters. Hence in the latter situation the interaction of unlike (and also identical) macromolecules in solution may be regarded as a form of selection adsorption. More precisely, it is selective desorption or exclusion of one polymer from the domains of the other. Selective exclusion of bovine serum albumin<sup>170</sup> by hyaluronic acid, for example, has been demonstrated by LS.

For a mixture of polymers A and B in one liquid the parameter characterising polymer A/polymer B interaction is positive and finite. Without reproducing the complex expression for  $\xi$  (which contains this parameter), it suffices to note the important consequence that addition of polymer A to a solution comprising polymer B at a concentration  $c_B$  in the liquid need not change the intensity of scattered light; in fact it might even decrease it. Recalling that scattered light intensity refers to excess of scattering between solution and solvent, it is apparent that zero or negative scattering is feasible in principle. Figure 58 provides one of the few published examples<sup>169</sup> to date of negative LS and shows the effect of the concentration  $c_A$  of polymethyl methacrylate ( $M_A = 1.66 \times 10^5$ ) on a solvent comprising polystyrene ( $M_B = 1.75 \times 10^5$ ) at a concentration  $c_B = 2 \times 10^{-3}$  g/ml in dioxan.

## VI. Concluding Remarks

The voluminous literature on LS from solutions indicates that the technique is already one worthy of serious consideration for all concerned with macromolecular characterisation. In this review an attempt has been made to emphasise its versatility with respect to the possible number of variables in the system. It is only fair to re-iterate that the manipulations involved should be approached with caution in view of the stringent requirements of absolute cleanliness of equipment and solutions.

Until comparatively recently one of the most crucial limiting factors in the practice of LS was the quantity of monochromatic incident radiation which it is possible to collimate into the cell using conventional light sources. The resultant scattered light intensity is, of course, dependent on this. Hence there is a practical lower limit on the solute concentration which can be successfully studied. The advent of continuous laser light sources goes a long way to freeing this restriction and the minimum concentrations of solutes detectable with the Chromatix instrument have already been quoted in Fig. 9. As a useful rule of thumb, one aims to obtain a scattered light intensity from a solution which is at least twice that of the solvent.

## 1. Comparison of LS with Other Methods

In his recent book Billingham<sup>16)</sup> has discussed the relative merits and disadvantages of some common modes of measuring the molecular weights of polymers. Many of these are equally applicable to ordinary small solutes and oligomers. Indeed, the conventional colligative properties such as lowering of freezing point, elevation of boiling point and vapour pressure osmometry become more accurate the lower the molecular weight of the solute. Membrane osmometry, though admirable in principle at low molecular weight, cannot be used for  $\bar{M}_n < \text{ca. } 15 \times 10^3$  because of possible diffusion of low molecular species present in a polydisperse sample or comprising all of a monodisperse one. Moreover, despite the use of pressure transducers and strain gauges there remains a practical upper limit of ca.  $1 \times 10^6$  for  $\bar{M}_n$  in view of the very small osmotic pressures exerted. Thus, under ideal conditions, a polymer of  $\bar{M}_n = 1 \times 10^6$  and a concentration of 0.01 g/ml in water at room temperature would exert an osmotic height of only ca. 0.25 cm; a realistic uncertainty of  $\pm 0.05$  cm has a drastic impact on the molecular weight derived.

The use of LS as a preferred technique must be assessed in relation to the following factors:

- (a) availability, complexity and cost of equipment
- (b) time demanded by the experiment
- (c) number and type of ancillary experiments necessary for final evaluation of molecular weight
- (d) quantity of solute required; this can be a crucial consideration for certain biopolymers
- (e) feasibility of recovering solute after measurements
- (f) range of molecular weight amenable to determination
- (g) type of molecular weight average yielded.

In addition to these, the polymer scientist may be influenced by the possibility of deriving further information such as chain dimensions from the same LS data as those gained primarily to afford  $M$ . With respect to the third factor above, (c), a determination of  $\nu$  or  $\nu_\mu$  is essential in LS, but the remaining factors place LS in a very favourable position in comparison with other techniques. Such a comparison has been reported<sup>171)</sup> and comprises part of the larger one assembled here in Table 17.

It is illuminating to quote some early results on aqueous sucrose solutions obtained by Maron and Lou<sup>36)</sup>. They demonstrate clearly the complementarity between osmotic pressure and LS. Reference to Eqs. (34) and (35) shows that

$$Kc/R_{90} = (1/\mathcal{R}T) (\partial \Pi / \partial c)_T \quad (115)$$

and in the limit of infinite dilution both sides of Eq. (115) are equal to the reciprocal of the molecular weight. Measured values of  $R_{90}$ , corrected with the Cabannes factor, are plotted versus concentration in Fig. 59. For each value of  $c$  the right hand side of Eq. (115) was computed from published osmotic pressure data on these solutions and the corresponding variation of  $(1/\mathcal{R}T) (\partial \Pi / \partial c)_T$  with  $c$  appears as the full curve<sup>36)</sup>. It is seen that there is excellent agreement between the two sets of data

Table 17. Comparison of different techniques for measuring molecular weight

Method	Advantages	Disadvantages	Typical Accuracy %
Chemical end-group analysis	Absolute; single determination	Destructive, restricted to low mol. wt.	1-2
Analysis of radioactively labelled end-groups	Absolute; single determination; wide range of mol. wt.	Restricted to certain types of polymer; requires knowledge of mode of chain termination	1-2
Vapour pressure osmometry	Requires very small sample size	Several concentrations necessary; restricted to mol. wt. < ca. $2 \times 10^4$ ; calibration constant must be established with solute of known mol. wt.	1-2
Membrane osmometry	Absolute; small sample size; reasonable range of mol. wt. ( $2 \times 10^4 - 1 \times 10^6$ )	Several concentrations necessary	5
Sedimentation equilibrium	Absolute; requires only centrifuge measurements and partial specific volume of solute	Time-consuming measurement and interpretation; somewhat limited mol. wt. range	5
Sedimentation-diffusion	Absolute; fairly fast	Requires 3 separate determinations (diffusion coefficient, sedimentation constant and partial specific volume)	<5
Neutron scattering	Can be used with solid sample	Expensive equipment requires deuteration of sample and calibration with substance of known mol. wt.	2
Low angle X-ray scattering in solution	Non-destructive	Time-consuming	5
Brillouin scattering	Absolute	Requires knowledge of certain physical properties of solvent; several concentrations necessary	2
Light scattering in solution	Fairly fast; wide range of mol. wt.	Must measure $d\tilde{n}/dc$ ; several concentrations necessary; for most (but not all) apparatuses requires calibration and rigorous exclusion of dust	5

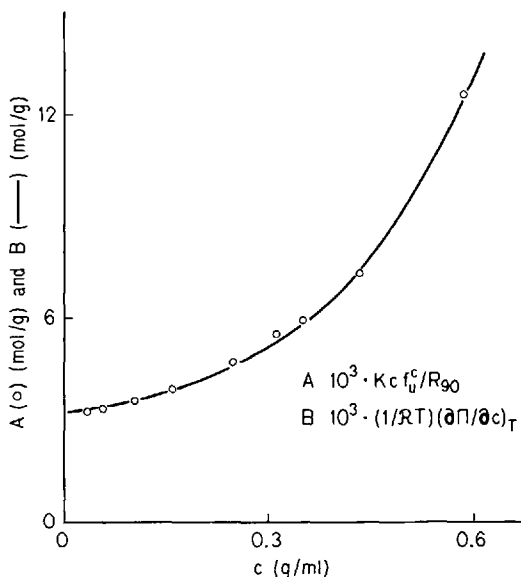


Fig. 59. Agreement between LS data and osmotic pressure data for solutions of sucrose in water<sup>36)</sup> at 25 °C

and that the intercept at  $c = 0$  yields a molecular weight ( $338 \pm 6$ ) which is in good accord with the theoretical one of 342.

Standards suitable for molecular weight comparison by LS have been listed by Dietz and Green<sup>19)</sup>. These comprise mainly pure low molecular weight materials. Periodically, polymer samples have been subjected to “round-robin” characterisation by different techniques (including LS) in different laboratories throughout the world. In the first of these the results were disappointing and the co-ordinators of the second batch of data were also faced with a fairly wide spread of  $M$  values all obtained from a single batch of polymer. A critical examination of procedures adopted led to no obvious single source of such a spread of results. Among the reasons advanced was a possible injudicious selection of the range of concentrations used and uncertainty in extrapolation to infinite dilution<sup>172)</sup>. The most recent survey of this nature was conducted in several Japanese laboratories<sup>173)</sup>. These results were much more self-consistent and also displayed good agreement among the different experimental techniques used. Relevant data are given in Table 18<sup>173)</sup>.

## 2. Errors

The determination of  $M$  by LS involves several experimental procedures, each of which has some error associated with it. A typical breakdown of errors is the following due to Jolly and Campbell<sup>174)</sup> in relation to their value of  $M = 3.1 \times 10^6 \pm 6\%$  for superhelical DNA from bacteriophage  $\phi$  X174: —

- (a) Ludox calibration constant,  $\pm 2\%$
- (b) Concentration measurements,  $\pm 2\%$
- (c) Instrument readings,  $\pm 1\%$
- (d) Value of  $d\tilde{n}/dc$ ,  $\pm 1\%$

Table 18. Values<sup>173)</sup> of (molecular weight  $\times 10^{-4}$ ) for two polystyrene samples: PS – PX prepared by Asahi Dow Chem. Co. Ltd. and PS – IU distributed by Macromolecular Division of I.U.P.A.C. see footnote for further details and explanation of abbreviations

Mol. wt. average.	Method	PS – IU Observed	Reported Calculated		PS – PX Observed	Calculated
$\bar{M}_n$	O.P.	8.0	7.92	–	38.6	38.6
$\bar{M}_n$	D. – 4th	6.5	–	6.5	41.5	–
$\bar{M}_{Dm}$	D. – 2nd	9.7	–	11.7	50.1	50.3
$\bar{M}_{DA}$	D. – Area	16.1	–	18.4	67.5	66.3
$\bar{M}_v$	V.	19.5	20.0	20.5	71.3	71.4
$\bar{M}_s$	S.V.	20.6	–	–	70.8	–
M	L.S.	{ 25.9, 24.3   24.1	23.5	–	83.7, 81.5, 81.6	–
	S.E.	24.5	21.7	24.7	79.5	81.3
	A.	–	–	–	80.3	–
$\bar{M}_z$	S.E.	44.8	39.7	42.9	124	124
$M/\bar{M}_n$	L.S./O.P.	3.09	3.22	3.8	2.11	2.11

- (i) Osmotic pressure measurements in methyl ethyl ketone at 30.2 °C for PS – PX and in toluene at 25.0 °C for PS – IU. The remainder relate to cyclohexane at 35.0 °C, and for L.S. results in triplicate derive from use of two additional temperatures.
- (ii) Osmotic pressure (O.P.) yields number average mol. wt.  $\bar{M}_n$ .
- (iii) Light scattering (L.S.) yielding weight average mol. wt. M. was calibrated with benzene, taking  $R_{90} = 46.5 \times 10^{-6} \text{ cm}^{-1}$  at  $\lambda_0 = 436 \text{ nm}$ .
- (iv) S.E. denotes sedimentation equilibrium yielding M and Z average mol. wt.  $\bar{M}_z$ .
- (v) A. denotes Archibald method.
- (vi) S.V. denotes sedimentation velocity constant yielding mol. wt.  $\bar{M}_s$ .
- (vii) Diffusion coefficient (D.) method yields mol wt.  $\bar{M}_{DA}$  by the area method, mol. wt.  $\bar{M}_{DM}$  by the second moment method and number average mol. wt.  $\bar{M}_n$  by the fourth moment method.
- (viii) Intrinsic viscosity (V.) gives viscosity average mol. wt.  $\bar{M}_v$ .
- (ix) Reported values in table are averages of data obtained in several different laboratories and collated elsewhere in an earlier report.
- (x) Calculated values in table are obtained from established interrelations between mol. wt. and the appropriate experimental quantity at infinite dilution.

The error in (a) is stated to compare favourably with calibration from benzene, since the absolute value of  $R_{90}$  is hardly known to this accuracy. In (b) the concentration of DNA was measured spectrophotometrically *via* the molar phosphorous extinction coefficient of 6415 (with a standard deviation of 2%). The low error in (c) arises from low levels of dust achieved as well as the integration over a period of 10 secs of the readings on a digital output. The specific refractive index increment used in (d) was an experimental one from the literature. In point of fact the assess-

ment of an error of  $\pm 1\%$  for it is a very realistic one, but since the specific increment appears as a squared term, the overall error in  $M$  should actually be assessed as  $\pm 7\%$ .

It is likely that  $\pm 1\%$  in the instrument reading and  $\pm 2\%$  in  $(d\tilde{n}/dc)^2$  cannot be improved on. However, for an absolute photometer, the error in (a) will be effectively zero. Concentration determinations are often specific to the system. For example, alginates in solution<sup>143)</sup> have been determined colorimetrically, calibration being effected on solutions prepared from alginate previously dried for 24 hr. at  $100^\circ\text{C}$ . However, successful calculation of the concentrations in this instance depends markedly on a prior knowledge of the fact that 10% of tightly bound water is present in the dried material<sup>175)</sup>. In simple systems involving non-volatile solvents, with standard procedures for using volumetric glassware and checks on dried aliquots of solution the error in concentration need not be greater than  $\pm 0.5\%$ . Hence under the most favourable circumstances of instrument and polymer/solvent system cognizance of factors (a) – (d) leads to an overall error in  $M$  of  $\pm 3.5\%$ .

It has been shown previously (Section V.3) that the true molecular weight of a copolymer  $M$  is obtainable in general by calculation involving experimental values of the apparent molecular weight  $M^*$  in three solvents differing in refractive index. Simultaneous equations of expressions (101) or (102) are involved. Abbreviating the variable  $(\nu_A - \nu_B)/\nu$  to  $\tilde{\nu}$  and distinguishing the three sets of data by subscripts 1, 2 and 3 yields the following expression for  $M$  after solution of Eq. (102) by determinants

$$M = \frac{M_1^* \tilde{\nu}_2 \tilde{\nu}_3 (\tilde{\nu}_3 - \tilde{\nu}_2) + M_2^* \tilde{\nu}_3 \tilde{\nu}_1 (\tilde{\nu}_1 - \tilde{\nu}_3) + M_3^* \tilde{\nu}_1 \tilde{\nu}_2 (\tilde{\nu}_2 - \tilde{\nu}_1)}{\tilde{\nu}_2 \tilde{\nu}_3 (\tilde{\nu}_3 - \tilde{\nu}_2) + \tilde{\nu}_3 \tilde{\nu}_1 (\tilde{\nu}_1 - \tilde{\nu}_3) + \tilde{\nu}_1 \tilde{\nu}_2 (\tilde{\nu}_2 - \tilde{\nu}_1)} \quad (116)$$

Equation (116) is not readily amenable to assigning a relative error ( $dM/M$ ) to the derived true molecular weight, even if numerical estimates can be afforded to the six different experimental parameters within the expression for  $M$ . It is clear, however, that it is imperative to ensure large (positive or negative) differences between parameters  $\tilde{\nu}$ . [If the constituent homopolymers are isorefractive, then  $\tilde{\nu}_1 = \tilde{\nu}_2 = \tilde{\nu}_3 = 0$  and Eq. (116) seems to imply that  $M$  is indeterminate. Actually the converse is true and  $M$  is always obtained. For such a situation there are simply no variables and  $M_1^* = M_2^* = M_3^* = 0$ ]. In other words, as previously indicated, the true molecular weight is yielded directly from one measurement in one solvent. The value obtained for the molecular weight of the copolymer comprising isorefractive homopolymer units is subject to no more or no less error than that of ca.  $\pm 7\%$  liable in a single determination of  $M$  for a polymer.

In certain multicomponent systems it may be necessary to derive the molecular weight  $x$  from two other measured molecular weights  $y$  and  $z$  together with a knowledge of the composition by weight  $W$  of the polymers. Reference to Eq. (111) provides an example of such a system. Here  $x$ ,  $y$  and  $z$  correspond to the required molecular weight  $M_A$  of polymer A in the mixture, the true molecular weight  $M_{AB}$  measured for the mixture and the known or measured molecular weight  $M_B$  of polymer B in the mixture respectively. The composition  $W$  corresponds to  $W_A$  in Eq. (111). Another example of a system to which Eq. (111) and the symbols  $x$ ,  $y$ ,  $z$  and  $W$  may be applied is copolymer formation by radiation grafting to a pre-formed

substrate of known measured molecular weight prior to grafting. This molecular weight corresponds to  $y$ . A certain weight fraction  $W$  participates in grafting and becomes the backbone (of unknown molecular weight  $x$ ) of the resultant copolymer. That fraction  $(1 - W)$  of the original polymer which remains untouched and does not participate in grafting, may be isolated by extraction and its molecular weight ( $z$ ) measured.

For both examples one derives the required molecular weight  $x$  in terms of measured quantities. Thus, Eq. (111) assumes the form

$$y = Wx + (1 - W)z \quad (117)$$

$$x = (1/W)y - [(1 - W)/W]z \quad (118)$$

If  $\epsilon_x$ ,  $\epsilon_y$  and  $\epsilon_z$  are the respective errors in  $x$ ,  $y$  and  $z$ , then it is readily shown that

$$(\epsilon_x/x)^2 = \{1/[y - (1 - W)z]^2\} [\epsilon_y^2 + (1 - W)\epsilon_z^2] \quad (119)$$

Expressed in terms of relative errors  $r_x (= \epsilon_x/x)$ ,  $r_y (= \epsilon_y/y)$  and  $r_z (= \epsilon_z/z)$ , the relative error in the required molecular weight  $x$  is:

$$r_x^2 = \{1/[y - (1 - W)z]^2\} [y^2 r_y^2 + (1 - W)^2 z^2 r_z^2] \quad (120)$$

A rough estimate of the conditions leading to a small value of  $r_x$  may be made from Eq. (120) by assigning  $r_y = r_z = 0.07$  and then by considering small, moderate and large values of  $y/z$ , each taken in conjunction with  $W = 0.1, 0.5$  and  $0.9$ . The result is what might have been predicted intuitively, viz. (i) for any particular composition  $W$ , the molecular weight  $x$  should be large compared with  $z$  and (ii) for a specified molecular weight combination,  $W$  should be large.

Hence for a mixture of polymers A and B, the molecular weight  $M_A$  can be derived most accurately from the measured quantities  $M_{AB}$  and  $M_B$  if A comprises a large proportion by weight of the mixture. The corresponding condition for a grafting system is an unfortunate one, because it is rarely realisable in practice<sup>176</sup>). The backbone of the copolymer should comprise a large fraction by weight of the original polymer prior to grafting. However, although statistical considerations do dictate that longer chains participate in grafting (and hence  $x$  is large, as required for a small  $r_x$ ), the weight fraction of polymer which is grafted is usually less than 0.1 (most of the polymer remains ungrafted) and thus  $W$  in Eq. (120) does not attain a desirable large value.

## VII. References

- 1) Serdyuk, I. N.: Dokl. Akad. Nauk SSSR 217, 231 (1974)
- 2) Serdyuk, I. N., Grenader, A. K.: FEBS Letters 59, 133 (1975)
- 3) Serdyuk, I. N., Fedorov, B. A.: J. Polym. Sci-Polym. Letts. Ed. 11, 645 (1973)
- 4) Eisenberg, H.: Biological macromolecules and polyelectrolytes in solution. Oxford: Oxford Univ. Press. 1976, Chapt. 4



- 5) McIntyre, D., Gornick F. (eds.): *Light scattering from dilute polymer solutions*. New York: Gordon and Breach 1964
- 6) Huglin, M. B.(ed.): *Light scattering from polymer solutions*. London/New York: Academic Press 1972
- 7) Fechner, B. M., Strazielle, C.: *Makromol. Chem.* 160, 195 (1972)
- 8) Miller, G. A.: *J. Phys. Chem.* 71, 2305 (1967)
- 9) Scholte, Th. G.: *Eur. Polym. J.* 6, 1063 (1970)
- 10) Scholte, Th. G.: *J. Polym. Sci. Pt. A-2*, 9, 1553 (1971)
- 11) Scholte, Th. G.: Report MS 929, Dutch State Mines, Geleen 1971
- 12) Schulz, G. V., Lechner, M.: In Ref.<sup>6)</sup>, Chapt. 12
- 13) Delmas, G., Patterson, D.: *Polymer* 7, 513 (1966)
- 14) Eisenberg, H., in: *Procedures in nucleic acid research*. Cantoni, G. L., Davies, D. R. (eds.). New York: Harper and Row, 1971, Vol. 2, p. 137 et seq.
- 15) Timasheff, S. N., Townend, R., in: *Physical principles and techniques of protein chemistry*. Leach, S. J. (ed.). New York: Academic Press 1970, Part B, p. 147 et seq.
- 16) Billingham, N. C.: *Molar mass measurements in polymer science*. London: Kogan Page 1977, Chapt. 5
- 17) Sicotte, Y., Rinfret, M.: *Trans. Faraday Soc.* 58, 1090 (1962)
- 18) Coles, H. J., Jennings, B. R., Morris, V. J.: *Phys. Med. Biol.* 20, 225 (1975)
- 19) Dietz, R., Green, J. H. S.: *Pure and Appl. Chem.* 48, 243 (1976)
- 20) Oster, G., in: *Techniques of chemistry*. Weissberger, A. (ed.). New York: Wiley 1972, Vol. 1. Part III A, Chapt. 2
- 21) Jennings, B. R.: *Brit. Polym. J.* 1, 252 (1969)
- 22) Flory, P. J.: *Principles of polymer chemistry*. Ithaca N. Y.: Cornell Univ. Press 1953, Chapt. 7
- 23) Morawetz, H.: *Macromolecules in solution*. New York: Wiley 1965
- 24) Tanford, C.: *Physical chemistry of macromolecules*. New York: Wiley 1961
- 25) Tsvetkov, V. N., Eskin, V. E., Frenkel, S. Ya.: *Struktura Makromolekul V Rastvorakh*. Moscow: Nauka 1964
- 26) Kerker, M.: *Scattering of light and other electromagnetic radiation*. New York: Academic Press 1969
- 27) Stacey, K. A.: *Light scattering in physical chemistry*. London: Butterworths 1956
- 28) Deželić, Gj.: *Croat. Chem. Acta* 33, 99 (1961)
- 29) Utiyama, H.: In Ref.<sup>6)</sup>, Chapt. 4
- 30) Kratochvíl, P.: In Ref.<sup>6)</sup>, Chapt. 7
- 31) Meyerhoff, G., Burmeister, A.: *Makromol. Chem.* 175, 3029 (1974)
- 32) Casassa, E. F., Berry, G. C., in: *Polymer molecular weights. Vol. 4 of techniques and methods of polymer evaluation*. Slade, P. E. Jr. and Jenkins, L. T. (eds.); Slade, P. E. Jr. (ed.). New York: Dekker 1975, Chapt. 5
- 33) Rempp, P.: *J. Chim. Phys.* 54, 421 (1957)
- 34) Elias, H.-G., Lys, H.: *Makromol. Chem.* 92, 1 (1966)
- 35) Meyerhoff, G., Moritz, U.: *Makromol. Chem.* 109, 143 (1967)
- 36) Maron, S. M., Lou, R. L. H.: *J. Phys. Chem.* 59, 231 (1955)
- 37) Brice, B. A., Nutting, G. L., Halwer, M. A.: *J. Am. Chem. Soc.* 75, 824 (1953)
- 38) Burchard, W., Cowie, J. M. G.: In Ref.<sup>6)</sup>, Chapt. 17
- 39) Valtasaari, L.: *Tappi* 48, 627 (1965)
- 40) Huglin, M. B.: In Ref.<sup>6)</sup>, Chapt. 6
- 41) Miller, G. A., San Filippo, F. I., Carpenter, D. K.: *Macromolecules* 3, 125 (1970)
- 42) Huglin, M. B.: *Pure & Appl. Chem.* 49, 929 (1977)
- 43) Utiyama, H.: In Ref.<sup>6)</sup>, Chapt. 3
- 44) Utiyama, H., Tsunashima, Y.: *Appl. Optics* 9, 1330 (1970)
- 45) Kratochvíl, J. P.: *J. Coll. Interface Sci.* 21, 498 (1966)
- 46) Kratochvíl, J. P., Oppenheimer, L. E., Shubsa, F. E.: *Kolloid Z. Z. Polymere* 222, 157 (1968)
- 47) Roche, R. S., Tanner, A. G.: *Angew. Makromol. Chem.* 13, 183 (1970)

- 48) Aughey, W. H., Baum, F. J.: *J. Opt. Soc. Amer.* **44**, 883 (1954)
- 49) Livesey, P. J., Billmeyer, F. W., Jr.: *J. Coll. Interface Sci.* **30**, 447 (1969)
- 50) Levine, H. I., Fiel, R. J., Billmeyer, F. W., Jr.: *Biopolymers* **15**, 1267 (1976)
- 51) Utiyama, H., Sugi, N., Kurata, M., Tamura, M.: *Bull. Inst. Chem. Res. Kyoto Univ.* **46**, 198 (1968)
- 52) Doty, P.: *J. Cell. Comp. Physiol* **49**, 22 (Suppl. 1.) (1957)
- 53) Sharp, P., Bloomfield, V.: *Biopolymers* **6**, 1201 (1968)
- 54) Fleischman, J. B.: *J. Mol. Biol.* **2**, 226 (1960)
- 55) Schmid, C. W., Rinehart, F. P., Hearst, J. E.: *Biopolymers* **10**, 883 (1971)
- 56) Butler, J. A. V., Laurence, D. J. R., Robins, A. B., Shooter, K. V.: *Proc. Roy. Soc. Ser. A*, **250**, 1 (1959)
- 57) Hays, J. B., Magar, M. E., Zimm, B. H.: *Biopolymers* **8**, 531 (1969)
- 58) Small angle light scattering photometer bulletin: Nederlandsche Optiek en Instrumentenfabriek, Dr. C. E. Bleeker nv., Thorbeckelaan 3, Zeist, Holland
- 59) Chromatix GmbH, D-6903 Neckargemünd – Dilsberg, Untere Str. 45a, W. Germany
- 60) Burmeister, A., Meyerhoff, G.: *Ber. Bunsen, Gesellschaft für physik. Chem.* **78**, 1366 (1974)
- 61) Tabor, B. E.: In Ref.<sup>6)</sup>, Chapt. 1
- 62) Bernardi, G.: *Makromol. Chem.* **72**, 205 (1964)
- 63) Huglin, M. B., in: *The polymer handbook*. Brandrup, J., Immergut, E. H. (eds.). New York: Wiley 1975, 2nd Edit., Chapt IV – 10
- 64) Coles, H. J., Jennings, B. R., Morris, V. J.: *Phys. Med. Biol.* **20**, 310 (1975)
- 65) Schoenes, F. J.: *Z. Angew. Physik* **28**, 363 (1970)
- 66) Ref.<sup>59)</sup>: Application Note LS – 1
- 67) Washburn, E. W. (ed.): *Internat. Critical Tables*. New York: McGraw Hill 1930
- 68) Mächtle, W., Fischer, H.: *Angew. Makromol. Chem.* **7**, 147 (1969)
- 69) Schultz, A. R.: *J. Am. Chem. Soc.* **76**, 3422 (1954)
- 70) Range of other published values quoted with references in Ref.<sup>66)</sup>
- 71) Kaye, W., Havlik, A. J.: *Appl. Optics* **12**, 541 (1973)
- 72) Strazielle, C.: In Ref.<sup>6)</sup> Chapt. 15
- 73) Krachtohvil, J. P., in: *Characterisation of macromolecular structure*. McIntyre, D. (ed.). Publication 1573, Nat. Acad. Sci., Washington D. C., 59 (1968)
- 74) Jennings, B. R., Plummer, H.: *Brit. J. Appl. Physics (J. Phys. -D)*, Ser. 2, **1**, 1201 (1968)
- 75) Scornaux, J., Van Leemput, R.: *Makromol. Chem.* **177**, 2721 (1976)
- 76) Hermans, J. J., Levinson, S.: *J. Opt. Soc. Amer.* **41**, 460 (1951)
- 77) Miller, G. A., Lee, C. S.: *J. Phys. Chem.* **72**, 4644 (1968)
- 78) Hosseinalizadeh-Khorassani, M.-K., Huglin, M. B.: Univ. of Salford, to be published
- 79) Evans, J. M.: In Ref.<sup>6)</sup>, Chapt. 5
- 80) Wijk van R., Staverman, A. J.: *J. Polm. Sci. Pt. A*, **2**, 1011 (1966)
- 81) Berry, G. C.: *J. Chem. Phys.* **44**, 4550 (1966)
- 82) Evans, J. M., Huglin, M. B., Lindley, J.: *J. Appl. Polym. Sci.* **11**, 2159 (1967)
- 83) Urwin, J. R., Girolamo, M.: *Makromol. Chem.* **142**, 161 (1971)
- 84) Bryce, W. A. J.: *Polymer* **10**, 804 (1969)
- 85) Miller, W., Stepto, R. F. T.: *Eur. Polym J.* **7**, 65 (1971)
- 86) Bullough, R. K.: *J. Polym. Sci.* **46**, 517 (1960)
- 87) Hölle, H. J., Kirste, R. G., Lehnen, B. R., Steinbach, M.: *Progr. Coll. and Polym. Sci.* **58**, 30 (1975)
- 88) Isdale, J. D., Brunton, W. C., Spence, C. M.: NEL Rept. No. 591, Nat. Eng. Labs., Dept. of Industry, East Kilbride, Glasgow 1975
- 89) Ziegler, I., Freund, L., Benoit, H., Kern, W.: *Makromol. Chem.* **37**, 217 (1960)
- 90) Rousset, A., Lochet, R.: *J. Polym. Sci.* **10**, 319 (1953)
- 91) Outer, P., Carr, C. I., Zimm, B. H.: *J. Chem. Phys.* **18**, 830 (1950)
- 92) Carr, C. I., Zimm, B. H.: *J. Chem. Phys.* **18**, 1616 (1950)
- 93) Trap, H. J. L., Hermans, J. J.: *Rec. Trav. Chim. Pays-Bas.* **73**, 167 (1954)
- 94) Brice, B. A., Halwer, M., Speiser, R.: *J. Opt. Soc. Amer.* **40**, 768 (1950)
- 95) Elias, H.-G., Schumacher, R.: *Makromol. Chem.* **76**, 23 (1964)

- 96) Elias, H.-G.: *Chemie-Ing.-Techn.* **33**, 359 (1961)
- 97) Elias, H.-G., Schlumpf, H.: *Makromol. Chem.* **85**, 118 (1965)
- 98) Feist, J., Elias, H.-G.: *Makromol. Chem.* **82**, 78 (1964)
- 99) Fee, J. G., Port, W. S., Whitnauer, L. P.: *J. Polym. Sci.* **33** 95 (1958)
- 100) Levy, G. B., Frank, H. P.: *J. Polym. Sci.* **10**, 371 (1953)
- 101) Adank, G., Elias, H.-G.: *Makromol. Chem.* **102**, 151 (1967)
- 102) Levy, G. B., Frank, H. P.: *J. Polym. Sci.* **17**, 247 (1955)
- 103) Smith, T. E.: Ph. D. Thesis, Georgia Inst. Technol., Atlanta, U.S.A., quoted in Ref.<sup>41)</sup>
- 104) Kratochvíl, P., Bohdanecký, M., Šolc, K., Kolinsky, M., Ryska, M., Lím, D.: *J. Polym. Sci. Pt. C* **23**, 9 (1968)
- 105) Dziejziela, W. M., Huglin, M. B., Richards, R. W.: *Eur. Polym. J.* **11**, 53 (1975)
- 106) Altgelt, K., Schulz, G. V.: *Kunststoffe-Plastics* **5**, 325 (1958)
- 107) Kratochvíl, P.: *J. Polym. Sci. Pt. C* **23**, 143 (1968)
- 108) Kratochvíl, P.: *Coll. Czech. Chem. Commun.* **30**, 1119 (1965)
- 109) Kratochvíl, P.: *Coll. Czech. Chem. Commun.* **29**, 2767 (1964)
- 110) Tuzar, Z., Kratochvíl, P.: *Coll. Czech. Chem. Commun.* **32**, 2255 (1967)
- 111) Tuzar, Z., Kratochvíl, P., Bohdanecký, M.: *J. Polym. Sci. Pt. C* **16**, 633 (1967)
- 112) Abbás, K. B., Porter, R. S.: *J. Polym. Sci. – Polym. Chem. Ed.* **14**, 553 (1976)
- 113) Abbás, K. B., Kirschner, T., Porter, R. S.: *Eur. Polym. J.* **14**, 361 (1978)
- 114) Burchard, W.: *Polymer* **10**, 29 (1969)
- 115) Elias, H.-G.: In Ref.<sup>6)</sup>, Chapt. 9
- 116) Gupta, A. K., Strazielle, C., Marchal, E., Benoit, H.: *Biopolymers* **16**, 1159 (1977)
- 117) Sund, H., Markau, K.: *Intern. J. Polym. Mater.* **4**, 251 (1976)
- 118) Tsimpris, C. W., Mayhan, K. G.: *J. Polym. Sci. – Polym. Phys. Ed.* **11**, 1151 (1973)
- 119) Berry, G. C., Ruman, K. A.: *J. Polym. Sci. A-2* **8**, 2089 (1970)
- 120) Worsfold, D. J., Bywater, S.: *Macromolecules* **5**, 393 (1972)
- 121) Tonelli, A. E., Flory, P. J.: *Macromolecules* **2**, 225 (1969)
- 122) Henley, D.: *Arkiv Kemi* **18**, 327 (1961)
- 123) Vink, H.: *Arkiv Kemi* **14**, 195 (1959)
- 124) Utiyama, H.: *J. Phys. Chem.* **69**, 4138 (1965)
- 125) Utiyama, H., Kurata, M.: *Bull. Inst. Chem. Res. Kyoto Univ.* **42**, 128 (1964)
- 126) Benoit, H., Holtzer, A. M., Doty, P.: *J. Phys. Chem.* **58**, 635 (1954)
- 127) Holtzer, A.: *J. Polym. Sci.* **17**, 432 (1955)
- 128) Fujita, H., Teramoto, A., Okita, K., Yamashita, T., Ikeda, S.: *Biopolymers* **4**, 769 (1966)
- 129) Casassa, E. F.: *J. Am. Chem. Soc.* **78**, 3980 (1956)
- 130) Morris, V. J., Coles, H. J., Jennings, B. R.: *Nature (Lond.)* **249**, 240 (1974)
- 131) Kratochvíl, P.: *J. Polym. Sci., Pt. C* **50**, 487 (1975)
- 132) Dondos, A., Benoit, H.: *Intern. J. Polym. Mater.* **4**, 175 (1976)
- 133) Johnson, R. M.: *Chemica Scripta* **1**, 81 (1971)
- 134) Hert, M., Strazielle, C.: *Makromol. Chem.* **175**, 2149 (1974)
- 135) Inoue, H., Timasheff, S. N.: *J. Am. Chem. Soc.* **90**, 1890 (1968)
- 136) Freifelder, D.: *J. Mol. Biol.* **54**, 567 (1970)
- 137) Kratochvíl, P.: *Faserforsch. und Textiltechnik* **24**, 5 (1973)
- 138) Nagasawa, M., Takahashi, A.: In Ref.<sup>6)</sup>, Chapt. 16
- 139) Alexandrowicz, Z.: *J. Polym. Sci.* **40**, 91 (1959)
- 140) Alexandrowicz, Z.: *J. Polym. Sci.* **43**, 337 (1960)
- 141) Stejskal, J., Beneš, M. J., Kratochvíl, P., Peška, J.: *J. Polym. Sci., – Polym. Phys. Ed.* **12**, 1941 (1974)
- 142) Timasheff, S. N., Dintzis, H. M., Kirkwood, J. G., Coleman, B. D.: *Proc. Nat. Acad. Sci. U.S.A.* **41**, 710 (1955)
- 143) Dingsøyr, E., Smidsrød, O.: *Brit. Polym. J.* **9**, 56 (1977)
- 144) Cooper, R. E., Wassermann, A.: *Nature (Lond.)* **180**, 1072 (1957)
- 145) Buchner, P., Cooper, R. E., Wassermann, A.: *J. Chem. Soc.* **1961**, 3974
- 146) Vrij, A., Overbeek, J. Th. G.: *J. Colloid Sci.* **17**, 570 (1962)
- 147) Kratochvíl, J. P., Dellicolli, H. T.: *Canad. J. Biochem.* **46**, 945 (1968)

- 148) Tuzar, Z., Kratochvíl, P.: *Adv. Coll. and Interface Sci.* 6, 201 (1976)
- 149) Benoit, H., Froelich, D.: In Ref.<sup>6)</sup> Chapt. 11
- 150) Girolamo, M., Urwin, J. R.: *Eur. Polym. J.* 8, 1159 (1972)
- 151) Ho-Duc, N., Prud'homme, J.: *Intern. J. Polym. Mater* 4, 303 (1976)
- 152) Tuzar, Z., Kratochvíl, P., Straková, D.: *Eur. Polym. J.* 6, 1113 (1970)
- 153) Prud'homme, J., Bywater, S.: *Macromolecules* 4, 543 (1971)
- 154) Tanaka, T., Kotaka, T., Inagaki, H.: *Macromolecules* 9, 561 (1976)
- 155) Tanaka, T., Kotaka, T., Inaga, H.: *Macromolecules* 7, 311 (1974)
- 156) Zilliox, J. G., Roovers, J. E. L., Bywater, S.: *Macromolecules* 8, 573 (1975)
- 157) Freyss, D., Rempp, P., Benoit, H.: *J. Polym. Sci. Pt. B*, 217 (1964)
- 158) Spatorico, A. L.: *J. Appl. Polym. Sci.* 18, 1793 (1974)
- 159) Veličković, J. S., Filipović, J. M.: *Bull. Soc. Chim. Beograd.* 35, 459 (1970)
- 160) Guthrie, J. T., Huglin, M. B., Phillips, G. O.: *Polymer* 18, 521 (1977)
- 161) Huglin, M. B., Richards, R. W.: *Polymer* 17, 587 (1976)
- 162) Kambe, H., Kambe, Y., Honda, C.: *Polymer* 14, 460 (1973)
- 163) Kambe, Y., Honda, C.: *Angew. Makromol. Chem.* 25, 163 (1972)
- 164) Bushuk, W., Benoit, H.: *Canad. J. Chem.* 36, 1616 (1958)
- 165) Kambe, Y.: *Angew. Makromol. Chem.* 54, 71 (1976)
- 166) Kratochvíl, P., Sedláček, B., Straková, D., Tuzar, Z.: *Makromol. Chem.* 148, 271 (1971)
- 167) Hyde, A. J.: In Ref.<sup>6)</sup>, Chapt. 10
- 168) Kratochvíl, P., Vorlíček, J., Straková, D., Tuzar, Z.: *J. Polym. Sci. – Polym. Phys. Ed.* 13, 2321 (1975)
- 169) Kratochvíl, P., Vorlíček, J.: *J. Polym. Sci. – Polym. Phys. Ed.* 14, 1561 (1976)
- 170) Ogston, A. G., Preston, B. N.: *J. Biol. Chem.* 241, 17 (1966)
- 171) Cummins, H. Z., Pike, E. R. (eds.): *Photon correlation and light beating spectroscopy.* Proc. NATO A.S.I., Series B: Physics, Vol. 3. New York: Plenum 1974
- 172) Strazielle, C., Benoit, H.: *Pure and Appl. Chem.* 26, 451 (1971)
- 173) Kotera, A., Yamaguchi, N., Yoshizaki, K., Onda, N., Kano, K., Dai, M., Furuya, A., Fukutume, A., Murakami, S.: *Rept. Progr. Polym. Phys. Japan* 18, 1 (1975)
- 174) Jolly, D. J., Campbell, A. M.: *Biochem. J.* 128, 569 (1972)
- 175) Haug, A.: *Rept. No. 30, Norwegian Inst. Seaweed Research, Trondheim* (1964)
- 176) Collins, R., Huglin, M. B., Richards, R. W.: *Eur. Polym. J.* 11, 197 (1975)

Received February 15, 1978, February 27, 1978